Climate and land use change impacts on floods in the Mono River basin of Togo and Benin

Dissertation

zur

Erlangung des Doktorgrades (Dr. rer. nat.)

der

Mathematisch-Naturwissenschaftlichen Fakultät

der

Rheinischen Friedrich-Wilhelms-Universität Bonn

vorgelegt von

Nina Rholan Houngue

aus

Benin

Bonn, 2023

Angefertigt mit Genehmigung der Mathematisch-Naturwissenschaftlichen Fakultät
der Rheinischen Friedrich-Wilhelms-Universität Bonn

Gutachterin: Prof. Dr. Mariele Evers
Gutachter: Prof. Dr. Julian Klaus

Tag der Promotion: 10.05.2023
Erscheinungsjahr: 2023

Preface

This thesis is submitted in partial fulfilment of the requirement for obtaining a PhD degree in Natural Sciences at the University of Bonn, Germany. The research study was conducted at the Department of Geography between October 2019 and December 2022, under the supervision of Prof. Dr. Mariele Evers and Prof. Dr. Julian Klaus. The research was conducted as part of the CLIMAFRI project (Implementation of Climate sensitive Adaptation Strategies to Reduce the Flood Risk in the Catchment Area of the Transboundary Lower Mono River). The research was funded by the German Federal Ministry of Education and Research (Bundesministerium für Bildung unf Forschung BMBF).
This doctoral thesis followed the cumulative dissertation approach, consisting of four manuscripts (Chapters 2 - 5) which have been published in (or submitted to) "Journal of Hydrology-Regional Studies", "Atmosphere", "Sustainability", as well as "Environment, development and sustainability" journals. The following is the list of manuscripts used to compile this dissertation. Additional publications are listed in the publication section.

Hounguè, N. R., Ogbu, K. N., Almoradie, A. D. S., & Evers, M. (2021). Evaluation of the performance of remotely sensed rainfall datasets for flood simulation in the transboundary Mono River catchment, Togo and Benin. *Journal of Hydrology: Regional Studies*, 36. https://doi.org/10.1016/j.ejrh.2021.100875

Houngue, N. R., Almoradie, A. D. S., & Evers, M. (2022). A Multi Criteria Decision Analysis Approach for Regional Climate Model Selection and Future Climate Assessment in the Mono River Basin, Benin and Togo. *Atmosphere*, 13, 1–19. https://doi.org/10.3390/atmos13091471

Houngue, N. R., Almoradie, A. D. S., Thiam, S., Komi, K., Adounkpè, J.G., Begedou, K., & Evers, M. (2023). Climate and land use change impacts on flood hazards in the Mono River Catchment in Benin and Togo. Submitted and under review in *Sustainability*, 13, https://doi.org/10.3390/su15075862

Houngue, N. R., Evers, M., & Almoradie, A. D. S. (2023). Water cooperation in face of climate and land use changes in the transboundary Mono river basin. Submitted and under review in *Environment, development and sustainability*.

Rholan Houngue

Bonn, 2023

Acknowledgement

The completion of this thesis was possible thanks to the support of various people and institutions.

This PhD work was carried out in the framework of the CLIMAFRI project (Implementation of Climate-sensitive Adaptation strategies to Reduce Flood Risk in the transboundary Lower Mono River catchment in Benin and Togo), funded by the German Federal Ministry of Education and Research BMBF.

I am grateful to Prof. Dr. Mariele Evers for her unwavering and tireless support. You have been a great supervisor, advisor and mentor. Thank you for the trust and the multiple opportunities that built my professional skills in academia. Thank you for always been there, and yet allowing me to autonomously develop my potential. I see all your subtle and very motivational encouragements.

I am thankful to Prof. Dr. Julian Klaus for accepting to co-supervise my thesis. Thank you for your availability and promptness to join this journey.

My thanks go to the team of the CLIMAFRI project. Thank you for offering me a multidisciplinary research environment. To the members of the consortium from UNU, ZEF, University of Bayreuth, and Björnsen Consulting Engineers (BCE), I appreciated our interactions and complementarity. Thanks to Dr. Yvonne Walz, Lorina Schudel, Simon Wagner, Yannick Schillinger, Michael Zissener, Dr. Michael Hagenlocher, Dr. Sophie Thiam, Sarah Verleysdonk, Victor Kpokpoya, Prof. Dr. Gesine Schiewer, Gernot Belger, Dr. Sonja Eichentopf, Dr. Nico Schrage, Domenico Tironi, and Dr. Kaj Lippert. We built a family over the years.

Conducting a participatory research work during the Covid pandemic was made easier thanks to the tremendous support of WASCAL staffs in Benin and Togo. I would like to particularly thank Prof. Julien Adounkpè, Prof. Komi Begedou, Dr. Kossi Komi and their team members. Thank you for coordinating, accommodating and jointly moderating our interactions with project stakeholders on the ground. I am grateful to all the stakeholders and institutions that provided valuable input and shared their expert knowledge during the virtual and hybrid workshops of the CLIMAFRI project: ANPC-Benin, ANPC, Togo, Benin Red-Cross, Togo Red-Cross, Caritas-Togo, Caritas Benin, Eau Vive Togo, JVE-Togo, JVE-Benin, PNE-Benin, GIZ Benin, ADELAC, INRAB, ITRA, FNEC, DG-Eau Benin, DRE Togo, Météo Togo, the Ministry of Agriculture of Togo, the Ministry of Environment of Togo, the Ministry of Environment of Benin, CEB/Nangbéto dam Management, the Mono Basin Authority, the Athiémé town hall and Mr. Grace-Felix HOUNAHO. Your support and your availability were highly appreciated.

My sincere gratitude to the current and former members of the Eco-Hydrology and Water Resources Management working group who supported me in multiple ways and encouraged me. Thanks to Dr. Pinar Pamukçu Albers, Dr. Kristian Näschen, Dr. Linda Taft, Dr. Britta Höllermann, Dr. Dennis Schmiege, Dr. Claudia Schepp, Arne Claßen, Maria Horstmann, Elvan Noyan Lehrach, Mark Tuschen and Wiebke Kasner. I am grateful to Dr. Adrian Almoradie for being an excellent

tutor. Thank you for the countless discussions, reflections and advices. Beyond a tutor, you were a teammate throughout the implementation of the CLIMAFRI project. Thank you for being always available through all means, e-mail, Skype, Whatsapp, and anytime. Special thanks to Dr. Joshua Ntajal and Katharina Höreth for making the office a pleasant place and for the friendship that we have developed.

I would also like to thank my colleagues Emmanuel Nkundimana and Alexander Ahring from the Hydrology Working Group. Thank you for the support, the fruitful talks and all the occasions where we shared great ideas.

A warm thank to Simon, Sophie, Victor and Maxime. Thank you for the friendly support beyond academia.

My family has been of a great support from the beginning to the end. Thanks to Mendel, Cessac, Rita and Rhoyale for always being there for me. You paved and enlightened the way for me. To Sèdjro, and the second and wonderful family that you gave me, I am deeply grateful. To my mum Lucie Anago and my dad Raymond Hounguè, be honoured through this thesis.

Summary

Floods are prominent in West Africa and are expected to exacerbate due to global changes, including climate change, land use change, as well as industrial and infrastructure development. It is important to evaluate in advance their patterns and potential impact in order to develop proper response and adaptation strategies. Scenarios and models are thus needed to portray and simulate possible futures. However, these simulations are often affected by the lack of data and uncertainties from models. The aim of this study is to investigate the impacts of future climate and land use change scenarios on floods in the Mono river catchment of Benin and Togo, while assessing the capacity of the two countries to jointly manage these impacts.

The performances of four remotely-sensed precipitation datasets were evaluated, to address the lack of data. These are: the Climate Hazards Group Infrared Precipitation with Station data (CHIRPS), Precipitation Estimation from Remotely Sensed Information using Artificial Neural Networks-Climate Data Record (PERSIANN), Tropical Applications of Meteorology using Satellite data and ground-based observations (TAMSAT), and the Global Precipitation Climatology Centre full daily data (GPCC). The datasets were first assessed at station location, and later used as input to the hydrological model HBV-light (Hydrologiska Byråns Vattenbalansavdelning). The HBV-light model uses areal precipitation of the catchment as input because it is a lumped model. Results indicate that PERSIANN, GPCC and TAMSAT were the best for flood simulation purposes. In addition, it was found that applying the kriging interpolation method to compute the areal precipitation is enough to deal with gaps in observation data, without any need to fill-in the missing values.

This study also explored the use of a Multicriteria Decision Analysis approach to select the best performing Regional Climate Models (RCMs) in the Mono River catchment. The Technique for Order Preferences by Similarity to an Ideal Solution, (TOPSIS), was used to rank 15 RCMs downloaded from the Coordinated Regional Downscaling Experiment (CORDEX) database. This systematic selection process resulted in 6 RCMs. The ensemble of the 6 RCMs was used to assess future climate patterns in the Mono river catchment during 2022-2070 in comparison with the period 1966-2015. The Representative Concentration Pathways (RCP) RCP 4.5 and RCP 8.5 were used as future climate change scenarios. Annual mean temperature showed an increasing trend over the period 1966-2070, whereas annual rainfall depicts high variabilities with no statistically significant trend. The western and north-western parts of the catchment are expected to receive less precipitation in the future, whereas the east central part and the downstream area close to the outlet might experience an increase of annual precipitation. Moreover, the annual cycle of rainfall is expected to be characterised by rainfall intensification and a delayed start of rainy seasons.

The combined impact of these climate projections and land use/land cover change (LULCC) scenarios was assessed using the Soil and Water Assessment Tool (SWAT) for runoff simulation, and the TELEMAC-2D model for flood mapping. The effect of the planned Adjarala dam was also examined. Due to the missing of discharge data for some years, SWAT was not calibrated and

validated over continuous years. The model was calibrated for years 1967-1977, 1990, 1991, 1992 with a Kling-Gupta Efficiency KGE = 0.83, and validated on 1978-1986, 1988, 1989 and 2010 (KGE =0.68). Results show an increase of the magnitude of flood extremes under future climate and land use change scenarios. Events of 10-years return periods during 1987-2010 are expected to become 2-years return period events under the climate and land use change scenarios considered. The planned Adjarala dam showed potentials for extreme peak and flood extent reduction. However, flow duration curves revealed that the discharge of the river during low flow periods may also reduce if the Adjarala dam was built.

In addition, the capacity of Benin and Togo to jointly address the impacts of the projected changes (climate change, LULCC, and the Adjarala dam) was investigated. The transboundary Water Cooperation Quotient (WCQ) was used to assess the current level of water cooperation between the two countries. It was done in a participative way with stakeholders from NGOs, academia and technical sector, as well as decision making and policy implementation institutions. Results indicate existing grounds for transboundary water cooperation (WCQ = 72/100). This finding updates the results published in 2017 by the Strategic Foresight Group (SFG). Mechanisms of data exchange, alternative dispute resolution, and frameworks for joint and sustainable coordination of flood, drought and ecosystems management are still lacking.

This study contributes to a better understanding of how changes in climate and land use would influence floods in the Mono river catchment, and demonstrates the readiness of Benin and Togo to collaboratively manage the impacts. The findings of this thesis serve as basis for adaptation measures identification and the establishment of an active transboundary water cooperation between Benin and Togo, in order to sustainably manage floods in the Mono river catchment.

Zusammenfassung

Hochwasserereignisse sind in Westafrika weit verbreitet, und es wird erwartet, dass sie sich aufgrund globaler Veränderungen wie dem Klimawandel, veränderter Landnutzung sowie fortschreitender Industrialisierung und dem Ausbau der Infrastruktur noch verstärken werden. Es ist wichtig, ihre Muster und potenziellen Auswirkungen im Voraus zu bewerten, um geeignete Reaktions- und Anpassungsstrategien zu entwickeln. Szenarien und Modelle werden daher benötigt, um mögliche Zukunftsszenarien darzustellen und zu simulieren. Diese Simulationen werden jedoch häufig durch den Mangel an Daten und die Unsicherheiten der genutzten Modelle beeinträchtigt. Ziel dieser Studie ist es, die Auswirkungen von Klima- und Landnutzungsänderungen Szenarien für auf Hochwasserereignisse im Einzugsgebiet des Mono in Benin und Togo zu untersuchen und gleichzeitig die Leistungsfähigkeit der Länder zu bewerten, diese Auswirkungen gemeinsam zu bewältigen.

Um dem Mangel an Daten zu begegnen, wurde die Qualität von vier fernerkundlich generierten Niederschlagsdatensätzen bewertet. Dabei handelt es sich um die folgenden Datensätze: CHIRPS (Climate Hazards Group Infrared Precipitation with Station data), PERSIANN (Precipitation Estimation from Remotely Sensed Information using Artificial Neural Networks-Climate Data Record), TAMSAT (Tropical Applications of Meteorology using Satellite data and ground-based observations) und die täglichen Daten des Global Precipitation Climatology Centre (GPCC). Die Datensätze wurden zunächst an den Stationen ausgewertet und später als Eingangsdaten für das hydrologische Modell HBV-light (Hydrologiska Byråns Vattenbalansavdelning) verwendet. Das Modell HBV-light verwendet den Gebietsniederschlag des Einzugsgebiets als Eingangsdaten, da es sich um ein räumlich ungegliedertes Modell handelt. Die Ergebnisse zeigen, dass PERSIANN, GPCC und TAMSAT am besten für Hochwassersimulationen geeignet sind. Darüber hinaus wurde festgestellt, dass die Anwendung der Kriging-Interpolationsmethode zur Berechnung des Gebietsniederschlags ausreicht, um Lücken in den Beobachtungsdaten zu schließen, ohne dass die fehlenden Werte aufgefüllt werden müssen.

Diese Studie untersuchte auch die Verwendung eines multikriteriellen Entscheidungsanalyseansatzes zur Auswahl der leistungsfähigsten regionalen Klimamodelle (RCMs) im Einzugsgebiet des Mono-Flusses. Die TOPSIS-Technik (Technique for Order Preferences by Similarity to an Ideal Solution) wurde eingesetzt, um 15 RCMs aus der CORDEX-Datenbank (Coordinated Regional Downscaling Experiment) zu bewerten. Dieser systematische Auswahlprozess führte zur Auswahl von sechs RCMs. Das Ensemble der sechs RCMs wurde verwendet, um das zukünftige Klimamuster im Einzugsgebiet des Mono-Flusses im Zeitraum 2022-2070 dem Zeitraum 1966-2015 gegenüberzustellen. Die repräsentativen Konzentrationspfade (RCP) RCP 4.5 und RCP 8.5 wurden als Szenarien für den künftigen Klimawandel verwendet. Die Jahresmitteltemperatur zeigte im Zeitraum 1966-2070 eine steigende Tendenz, während der jährliche Niederschlag hohe Schwankungen ohne statistisch signifikanten Trend aufwies. Es wird erwartet, dass die westlichen und nordwestlichen Teile des Einzugsgebiets in Zukunft weniger Niederschlag erhalten werden, während der zentral-östliche

Teil und für das flussabwärts gelegene Gebiet in der Nähe des Gebietsausflusses ein Anstieg der jährlichen Niederschläge erwartet wird. Außerdem wird angenommen, dass der jährliche Niederschlagszyklus durch eine Intensivierung der Niederschläge und einen verzögerten Beginn der Regenzeiten gekennzeichnet sein wird.

Die kombinierten Auswirkungen dieser Klimaprojektionen und Landnutzungs-/ Landoberflächenänderungsszenarien (LULCC) wurden mit dem Soil and Water Assessment Tool (SWAT) für die Abflusssimulation und dem TELEMAC-2D für die Hochwasserkartierung bewertet. Die Auswirkungen des geplanten Adjarala-Damms wurden ebenfalls untersucht. Da für einige Jahre keine Abflussdaten vorlagen, wurde SWAT nicht über kontinuierliche Jahre kalibriert und validiert. Das Modell wurde für die Jahre 1967-1977, 1990, 1991, 1992 mit einer Kling-Gupta-Effizienz KGE = 0,83 kalibriert und für die Jahre 1978-1986, 1988, 1989 und 2010 validiert (KGE =0,68). Die Ergebnisse zeigen eine Zunahme der Magnitude von Hochwasserextremen unter zukünftigen Klima- und Landnutzungsänderungsszenarien. Es wird erwartet, dass Ereignisse mit 10-jährigem Wiederkehrintervall im Zeitraum 1987-2010 unter den betrachteten Klima- und Landnutzungsszenarien zu Ereignissen mit 2-jährigem Wiederkehrintervall werden. Der geplante Adjarala-Damm hat das Potenzial, extreme Hochwasserspitzen und die Ausdehnung von Hochwasser zu reduzieren. Die Dauerkurven zeigen jedoch, dass sich der Abfluss des Flusses während der Niedrigwasserperioden ebenfalls verringern könnte, wenn der Adjarala-Damm gebaut wird.

Darüber hinaus wurde untersucht, inwieweit Benin und Togo in der Lage sind, die Auswirkungen der prognostizierten Veränderungen (Klimawandel, LULCC und Adjarala-Staudamm) gemeinsam zu bewältigen. Der grenzüberschreitende Wasserkooperationsquotient (WCQ) wurde verwendet, um den aktuellen Stand der wasserbezogenen Kooperation zwischen den beiden Ländern zu bewerten. Dies geschah auf partizipative Weise mit Interessenvertreter*innen aus Nichtregierungsorganisationen, der Wissenschaft und dem technischen Sektor sowie mit institutionellen und politischen Entscheidungsträgern. Die Ergebnisse zeigen, dass es eine Basis für eine grenzüberschreitende Wasserkooperation gibt (WCQ = 72/100). Dieses Ergebnis aktualisiert die 2017 von der Strategic Foresight Group (SFG) veröffentlichten Ergebnisse. Mechanismen für den Datenaustausch, alternative Streitschlichtung und Rahmenbedingungen für eine gemeinsame und nachhaltige Koordinierung des Hochwasser-, Dürre- und Ökosystemmanagements fehlen bislang noch.

Diese Studie verbessert das Verständnis der Auswirkungen von Klima- und Landnutzungsänderungen auf Hochwasserereignisse im Einzugsgebiet des Mono-Flusses und zeigt die Bereitschaft von Benin und Togo auf, diesen Auswirkungen gemeinsam zu begegnen. Die Ergebnisse dieser Arbeit dienen als Grundlage für die Identifizierung von Anpassungsmaßnahmen und den Aufbau einer aktiven grenzüberschreitenden Wasserkooperation zwischen Benin und Togo, um Hochwasserereignisse im Einzugsgebiet des Mono-Flusses nachhaltig zu bewältigen.

Table of content

List of Tables

List of figures

List of abbreviations

CHIRPS	Climate Hazards Group Infrared Precipitation with Station data
BC	Base case
BMBF	German Federal Ministry of Education and Research
CEB	Centrale Electrique du Bénin
CLIMAFRI	Implementation of Climate-sensitive Adaptation strategies to Reduce Flood Risk in the transboundary Lower Mono River catchment in Benin and Togo
CLMcom	Climate Limited-area Modelling Community
CMIP	Coupled Model Intercomparison Project
CNEE	Netherlands Commission for Environmental Assessment
CORDEX	Coordinated Regional Downscaling Experiment
CSIRO	Commonwealth Scientific and Industrial Research Organization
DEM	Digital Elevation Model
DGMN	Direction Générale de la Météorologie Nationale
ESGF	Earth System Grid Federation
FAO	Food and Agriculture Organisation of the United Nations
FAR	False Alarm Ratio
FDC	Flow Duration Curve
GCM	General/Global Circulation Models
GPCC	Global Precipitation Climatology Centre full daily data
HBV	Hydrologiska Byråns Vattenbalansavdelning
HQ	Return period
ICHEC	Irish Centre for High-End Computing
IPCC	Intergovernmental Panel on Climate Change
IPSL	Institut Pierre Simon Laplace, France
IUSS	International Union of Soil Sciences
KGE	Kling-Gupta Efficiency
LMR	Lower Mono River
LMRB	Lower Mono River Basin
LU	Land Use
LULC	Land use and land cover
LULCC	land use and land cover change
MBA	Mono Basin Authority
MCDA	Multicriteria Decision Analysis
MODIS	Moderate-Resolution Imaging Spectroradiometer
MOHC	Met Office Hadley Centre
MPI	Max Planck Institute for Meteorology
NGO	Non-Governmental Organisation
NIS	Negative Ideal Solution
NSE	Nash-Sutcliffe efficiency
PBIAS	Percentage of Bias

PERSIANN-CDR	Precipitation Estimation from Remotely Sensed Information using Artificial Neural Networks-Climate Data Record
PIS	Positive Ideal Solution
POD	Probability of Detection
RCM	Regional Climate Model
RCP	Representative Concentration Pathways
REMO	Regional Model
RMSE	Root Mean Square Error
SDG	Sustainable Development Goal
SFG	Strategic Foresight Group
SPI	Standardized Precipitation Index
SWAT	Soil and Water Assessment Tool
TAMSAT	Tropical Applications of Meteorology using Satellite data and ground-based observations
TOPSIS	Technique for Order Preferences by Similarity to an Ideal Solution
UNDP	United Nations Development Programme
UNECE	United Nations Economic Commission for Europe
UNFCCC	United Nations Framework Convention on Climate Change
UNOSAT	United Nations Satellite Centre
WB	Word Bank
WCQ	Water Cooperation Quotient
WMO	World Meteorological Organization
WRB	World Reference Base for Soil Resources

1. Introduction

1.1. Background

Water is at the heart of development and is a key component of all pillars of human security (economic, food, health, political, environmental, personal, and community) (UN, 2021; UNDP, 1994). However, the water cycle in different parts of the world is affected by global changes. From global warming to climate change, through land use change, population growth and industrialisation, the various changes occurring around the world are interlinked and operate in a feedback loop (Hirsch et al., 2017; Sitch et al., 2005). Thus, global warming induces and intensifies climate change, which leads to land use and land cover (LULC) change, which in turn exacerbates global warming. The impact of such changes on the water cycle translates into hydrological hazards such as flood and drought (Alifu et al., 2022; Tabari, 2020), and cause substantial loss and damages. Moreover, their frequency and intensity are expected to increase over the years (Gründemann et al., 2022; Ingram, 2016).

However, changes in extreme flood events are not uniform in all parts of the world (Pfahl et al., 2017; Tabari et al., 2019). Moreover, besides the expectation of dry regions to become drier, they may also receive extremely high precipitation and likewise, usually wet regions may experience drought (Sillmann et al., 2019). Human actions and regional LULC, among other drivers, affect hydrological processes (Mazzoleni et al., 2022; Sofia et al., 2017; Veldkamp et al., 2018). Thus, increases in flood frequency and magnitude were reported in eastern and tropical Africa whereas, decreases are noticed in south-west Africa (Seneviratne et al., 2021). Furthermore, river flood modelling at regional scale embeds more uncertainty due to errors inherent to models and the complexity of processes involved including LULC, water infrastructure and their management (Hirsch et al., 2018; Seneviratne et al., 2021). In addition, regional flood projections based on climate models increase the uncertainty scheme due to biases in regional climate models (RCMs), and in the general circulation models (GCMs) that they are derived from (Arnell & Gosling, 2016; Hattermann et al., 2018; Krysanova et al., 2017). Therefore, local studies supported by quality in-situ data are key to effectively and sustainably manage floods.

Various studies have addressed rainfall pattern and precipitation data gaps management in the Mono river catchment. The works of Amoussou, 2010 revealed rainfall deficits in the 1970s and 1980s and a slight increase in 1988-2000. Rainfall regimes were reported to be latitude-dependent, with a bimodal regime in the south of the catchment and a unimodal pattern in the northern higher latitudes. The authors, as in other studies, reported substantial gaps in precipitation data and the unequal distribution of rain gauges over the Mono catchment. Amoussou, 2010 filled the missing based on surrounding gauges using the double mass method (Brunet-Moret, 1971). Koubodana et al., 2020 also imputed missing values based on neighbouring stations, while Batablinle et al., 2018 filled missing data with similar day averages from previous years. However, these methods employed for precipitation gap filling in the Mono catchment do

not account for the probabilistic aspect of rainfall's spatio-temporal variability. In addition, previous studies, so far, have not explored the possibility of using remotely-sensed precipitation datasets, that have shown good performances in difference parts of the world (Atiah et al., 2020; Brunetti et al., 2021; Fallah et al., 2020; Stampoulis & Anagnostou, 2012; Sun et al., 2017; Xia et al., 2021).

Batablinle et al., 2018 analysed future precipitation indices in the Mono basin based on representative concentration pathways (RCP 4.5 and RCP 8.5), and found that the number of very heavy rainfall days and the number of consecutive dry days will increase until 2100. Variabilities and rainfall irregularity are projected for 2021-2100 (Amoussou et al., 2020; Batablinlè et al., 2019; Lawin et al., 2019). As for temperature, all studies carried out in the catchment agree on its increasing trend until the 2090s (Koubodana et al., 2020; Lawin et al., 2019). The RCMs used in those studies were chosen based on their performance in other countries and mainly based on limited computation time. Climate projections and the subsequent hydrological information in a given region can significantly differ, depending on the climate model used. The findings of Her et al., 2019 highlighted that a careful selection of climate models should be much more prioritized than intense attempts to identify a one-among-many perfect calibration parameters set. A comprehensive evaluation of climate models prior to climate change impact assessment and hydrological studies is therefore recommended to improve future projections and to develop appropriate adaptation measures (Pastén-Zapata et al., 2022; Song et al., 2020).

Runoff and flood related studies in the Mono river catchment were mainly based on rainfall-runoff models including the HBV model (Hydrologiska Byråns Vattenbalansavdelning), IHACRES (Identification of unit Hydrographs and Component flows from Rainfall, Evaporation and Streamflow data), GR4J model (the Génie Rural à 4 paramètres Journaliers) and its monthly variant, the GR2M model. GR4J was concluded as good for the Mono river catchment (Batablinlè et al., 2021; Koubodana et al., 2021), like the GR2M (Amoussou, 2010). IHACRES showed satisfactory results as well in the catchment (Koubodana et al., 2021). Houngue, 2018 used the regional climate model REMO and the HBV model to simulate discharge and reported that the hydrological model performed very well. However, all those models are lumped models that work with relatively simple routines to represent hydrological processes. They do not account for LULCC. Koubodana et al., 2021 addressed that gap and used the SWAT (Soil and Water Assessment Tool) model that allows the integration of LULC maps and soil information. Due to the presence of the Nangbéto hydropower dam, the authors performed one simulation before the commission of the dam in 1987, and another simulation after the dam. The latter yielded poor performances, while the simulation before the dam resulted in good statistics. This is attributable to the substantial gaps in input data during the after-dam period. The authors recommended further calibration works on the model and an assessment of climate change and LULCC impacts for better flood management in the Mono river catchment. Obahoundje et al., 2021 addressed climate change and LULCC impacts using the Water Evaluation and Planning model (WEAP), but from a hydropower generation perspective. The study revealed that, water demands for domestic use, irrigation, livestock and industries in the near future (2020-2050), and on a longer term

(2060-2090), will not be met under the combined effect of climate change, LULCC, and development projects including the planned Adjarala hydropower plant.

Notwithstanding the existing studies in the Mono river catchment, the effect of climate change, LULCC, and the construction of the planned Adjarala dam on floods is still unclear. LULC during 1975-2013 in the Mono river catchment was globally characterised by an expansion of built-up areas and a decrease of forests (Koubodana et al., 2019), that are expected to continue until 2070 (Thiam et al., 2022). Thus, imperviousness will increase and infiltration will decrease, which may exacerbate flooding. Recurrent and devastating flood events are recorded in the Mono river catchment. The most damaging events occurred in 2010, affecting around 686,000 people in Benin and Togo (DREF, 2011; OCHA, 2010), and causing USD 300 million of loss and damages (UNDP, 2010; WB & UNDP, 2011). Furthermore, the transboundary aspect of the Mono river catchment is an essential component of its management especially, regarding flooding, water infrastructure, decision making and conflicts resolution. Transboundary cooperation is necessary for socioeconomic development, for effective adaptation to climate change, and for mutual and equitable sharing of adaptation costs and benefits (Earle et al., 2015; UNECE, 2015b). Nonetheless, cross-border water cooperation has so far not been addressed in the Mono river catchment.

1.2. Aim and research questions

The overall objective of this thesis is to evaluate the impacts of climate and land use changes on floods in the Mono river catchment, while accounting for the transboundary aspect of the basin. The study intends to analyse the response of flood hazards to different scenarios on the one hand, and on the other, to assess how jointly the catchment is managed by riparian in order to respond to potential future changes. The background presented above and the stated objective raise different questions that are addressed in this thesis.

Question 1: What are the alternatives to deal with gaps in precipitation data in the Mono River catchment?

Impact studies like this one mainly require data (quantitative data) to bridge past-to-present information with models simulation. However, observation data, especially precipitation data, which are key input for climate change impact studies, are known to hold substantial gaps in the Mono river catchment. Therefore, the first step in this study was to explore options to deal with gaps. Chapter 2 presents the options that were explored and the one recommended for this study.

Question 2: Which regional climate models best represents the conditions in the Mono River catchment and what is the future climate trend in the basin?

Future climate trend assessments are based on scenario data provided by climate models. Climate models from the CORDEX database are targeted for this study. However, there is a multitude of models available in that database. Selecting good climate models, is essential to well represent the study area. Thus, before undertaking scenarios and trend analyses, a systematic way of

selecting best performing models was investigated. Chapter 3 addresses the selection process and the projected climate trends.

Question 3: What is the impact of climate and land use/land cover changes on the discharge of the Mono River and how does it affect flood hazards in the lower part of the catchment?
Climate change information derived from Question 2 were used together with LULCC scenarios to assess their combined effect on flood. The impact on discharge was first analysed at the station located most downstream of the catchment, and the implication for flood extents was assessed for the area downstream of the Nangbéto dam. The catchment actually hosts a hydropower dam, the Nangbéto dam, and the two countries are planning to build a second one named the Adjarala dam. Thus, the potential effect of the Adjarala dam was also evaluated while addressing this research question. Chapter 4 provides a detailed overview of potential impact of climate change, LULC change and the construction of the Adjarala dam on floods.

Question 4: How jointly is the catchment managed by riparian countries in order to respond to potential future changes?
In addition to the scenario and hazard assessment, the study sought an approach to quantify the level of cooperation between the riparian in order to stand projected changes. A quantitative metric, the Water Cooperation Quotient was used to assess the level of cooperation of the two countries with respect to the Mono catchment that they share together. The assessment was done in a participative way with local stakeholders. The computation process of the Quotient and the results obtained are presented in Chapter 5

1.3. Research framework

This thesis was conducted in the framework of the CIMAFRI (Implementation of Climate-sensitive Adaptation strategies to Reduce Flood Risk in the transboundary Lower Mono River catchment in Benin and Togo) project. The overall aim of the project is to reduce the current and future flood risk through integration of science-based data with information and knowledge from local stakeholders and communities.

The project was structured into 6 work packages (WP) as follow: Data, models and assessment (WP 1), Scenario and adaptation measures development (WP 2), Technical integration of flood risk analyses (WP 3), Stakeholder engagement (WP 4), Capacity building (WP 5), and Implementing adaptation strategies and risk management instruments (WP 6). The research questions addressed in this study are part of WP 1, WP 2, and WP 4. Each work package was led by a specific project partner that coordinates the implementation with other partners. Therefore, partners were complementary and outputs from one serve as input for another. For example, the LULC maps used in this study (Thiam et al., 2022) were provided by partners from the Centre for Development Research (Zentrum für Entwicklungsforschung ZEF), while the flood hazard information presented in this thesis were used by the partners in charge of vulnerability and risk assessment. In addition, the flood maps presented in Chapter 4 were not prepared by the PhD

candidate, even though they are part the publication which served as basis for the content of the chapter.

The project started in April 2019. The implementation happened in the midst of the Covid pandemic which then called for some strategic adaptations. Thus, the following steps were thought over and re-adjusted:

- Fieldwork for river cross-section measurement: the fieldwork was cancelled and the cross-sections were alternately derived with a model and based on expert judgement;
- Physical workshops: workshops were held online to validate flood maps and to compute the Water Cooperation Quotient together with stakeholders.

1.4. The study area

The Mono River Basin is located within latitudes 6.36 °N and 9.39 °N, and longitudes 0.62 °E and 1.99 °E in West Africa (Figure 1). It stretches over 340 km north to south with an area of 23,736.64 km^2. The catchment is transboundary and shared by the Republics of Benin and Togo. 89% of the catchment area is in Togo, while 11% lies on Benin. Moreover, the Mono River catchment covers about 35% of Togo's territory. The Mono River serves as natural border between both countries in the downstream.

The Mono River Basin has two main climatic zones defined by a subequatorial climate for latitudes lower than 7 °N and a tropical climate in the upper part (latitude above 7 °N). Areas of latitude lower than 7 °N experience two rainy seasons every year, whereas above 8 °N, the rainfall regime is unimodal with only one peak (Amoussou, 2010). Within latitudes 70 °N–8 °N, the rainfall regime is halfway between a typical unimodal and bimodal cycle, which is described as a "transitional" regime (Lawin, Hounguè, Biaou, et al., 2019). The mean annual temperature ranges between 26 °C and 28 °C, while an average of 1200 mm precipitation per year is recorded in the catchment. Land use and land cover types in the catchment are predominantly savannah, forest, croplands, settlements and water bodies.

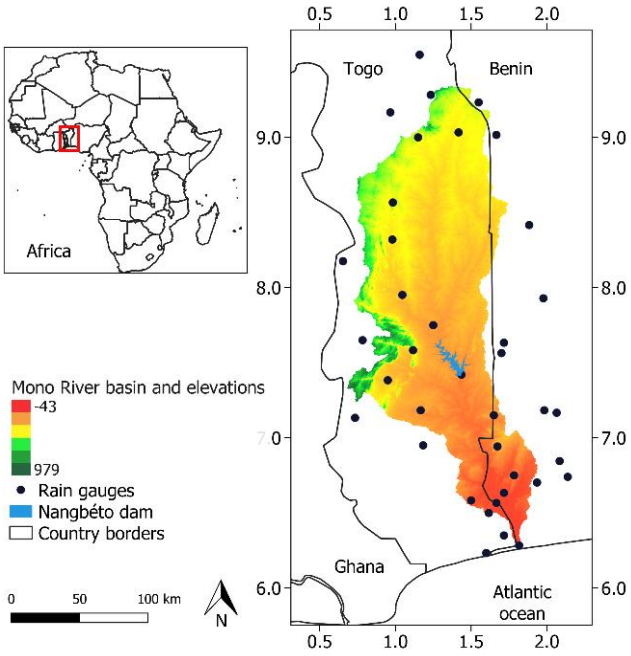

Figure 1.1. Location of the Mono river catchment

The number of inhabitants living in the catchment in 2022 is estimated to 5,266,832 (MBA, 2022). Main economic activities consist of small-scale farming, fishing, small trades, and livestock breeding. The valley of the Mono River contributes to food production in Benin and Togo. The catchment hosts the Nangbéto hydroelectric dam mutually owned by Benin and Togo. The recurrent flood events experienced at the downstream of the Nangbéto dam have become more frequent and intense over the past decades. The downstream of the catchment is characterised by low elevation and flat lands which favour the persistence of flood events in the area.

1.5. Structure of the thesis

The thesis is organised into 6 chapters. Chapter 1 presents the introduction, including the problem statement, the aim and research questions and a description of the study area. Chapter 2 explores the potential of satellite-based rainfall datasets for gaps filling. Chapter 3 presents a systematic approach to select best performing climate models, and the analysis of future climate trends in the Mono river catchment. Chapter 4 focused on the impacts of climate change, land use/land cover change, and the construction of the Adjarala dam on the river discharge and on flood. Chapter 5 addresses the current state of water cooperation between the riparian of the Mono river catchment. Table 1 presents a brief overview of the research questions addressed in Chapter 2-5, the methods used and the key outcomes. Chapter 6 provides a general conclusion to the thesis. References are presented in Chapter 7, list of publications in Chapter 8 and conference contributions in Chapter 9.

Table 1.1. Overview of research questions and key findings

Research question	Methods	Key findings	Main contribution	Publication status
1. What are the alternatives to deal with gaps in precipitation data in the Mono river catchment?	• Evaluation of 4 satellite-based and remotely sensed precipitation datasets; • Evaluation of the Kriging interpolation method; • Statistical and categorical metrics to compare remotely sensed datasets against observed time series; • Analysis of the ability of the assessed datasets to be used as input for hydrological modelling	• All the four datasets assessed reproduced well the seasonal cycle in different parts of the catchment • The datasets performed poorly at daily and annual scale • Filling the missing does not necessarily improve the quality of the data and that may not be needed in the case of the Mono basin if interpolation methods like kriging are applied.	Identification of an efficient way of dealing with gaps in precipitation datasets for flood simulation purposes	Published in *Journal of Hydrology: Regional Studies* doi: 10.1016/j.ejrh.2021.100875
2. Which regional climate models best represents the conditions in the Mono river catchment and what is the future climate trend in the basin?	• Download of 15 RCMs from the CORDEX database; • Ranking of the RCMs to select the best performing ones using the MCDA approach TOPSIS; • Computation of the ensemble of the selected RCMs; • Assessment of rainfall and temperature trends under scenarios RCP 4.5 and RCP 8.5, and during the period 2022-2070	• 6 RCMs were identified as the best ones; • under both climate change scenarios, the annual • temperature has an increasing trend during the period, whereas annual rainfall presents high variability and no statistically significant trend; • Seasonal cycles of rainfall are expected to change with delayed onset of • rainfall, longer dry seasons, and rainfall intensification	Use of a systematic RCM selection procedure and assessment of future climate trends with an ensemble model	Published in *Atmosphere* doi: 10.3390/atmos13091471
3. What is the impact of climate and land use/land cover changes on	• Calibration and validation of the SWAT model; • Discharge simulation over the period 2022-2070 using climate change	• Good calibration and validation results • increase of the magnitude of flood extremes under future climate and land use change scenarios	Assessment of the implication of climate change, LULCC, and the	Published in *Sustainability* doi:

the discharge of the Mono river and how does it affect flood hazards in the lower part of the catchment?	scenarios (RCP 4.5, RCP 8.5) and land use maps from 2030, 2050 and 2070; • Integration of the Adjarala dam in the model to simulate its potential effect; • Discharge magnitude associated with return periods of 2, 5, 10, 50, and 100 years were estimated • Mapping of flood extents corresponding to the return periods using the TELEMAC-2D model	• Events of 10-years return periods during 1987-2010 are expected to become 2-years return period events under the climate and land use change scenarios considered. The planned Adjarala dam showed potentials for extreme peak and flood extent reduction; • The areas flooded by a 10-years return period event under RCP 4.5 will reduce by ~10 km^2 with the Adjarala dam as compared to without the dam	construction of the Adjarala dam for discharge and for extreme flood events	10.3390/su15075862
4. How jointly is the catchment managed by riparian in order to respond to potential future changes?	• Computation of the WCQ by stakeholders in subgroups and all-together in a consensual way; • Comparison of the WCQ by stakeholders with the score published in the report of the Foresight Strategic Group (FSG); • Identification of cooperation aspects that need attention in the Mono catchment and ways to improve the WCQ	• During the subgroup computation, cooperation in terms of data sharing, conflict management, and the management of floods and ecosystems were weighted differently by the groups. All other parameters were weighted equally by all the groups; • The score resulting from stakeholders' computation (whether in subgroups or all-together) implies a stronger cooperation between the two countries than the score obtained in the FSG report • It is recommended to also account for socio-cultural parameters in the computation the Quotient	Assessment of the current state of water cooperation and integration of stakeholders perception	Under review. Submitted to *Environment, development and sustainability*,

2. Evaluation of the performance of remotely sensed rainfall datasets for flood simulation in the transboundary Mono River catchment, Togo and Benin[1]

Abstract

Study region: This study focused on the Mono River Basin in West Africa.

Study focus: The lack of extensive and functional measurement networks for flood monitoring, introduces satellite-based rainfall datasets as an alternative which needs however to be evaluated beforehand. This study investigated the performance of four satellite and gauge-based rainfall products – Climate Hazards Group Infrared Precipitation with Station data (CHIRPS), Precipitation Estimation from Remotely Sensed Information using Artificial Neural Networks-Climate Data Record (PERSIANN), Tropical Applications of Meteorology using Satellite data and ground-based observations (TAMSAT), the Global Precipitation Climatology Centre full daily data (GPCC) – with grid-to-point and hydrologic modelling approaches at different time scales over the Mono basin.

New Hydrological Insights for the Region: With the grid-to-point assessment, results show poor performances at daily and annual scales while the seasonal cycles were well reproduced with Nash-Sutcliffe efficiency (NSE) equal or higher than 0.94, and correlation coefficient above 0.9. All assessed products exhibited high probability of detection (POD) and low false alarm ratio (FAR) at dekadal scale. Based on NSE values of hydrologic modelling, best results were achieved by PERSIANN, followed by GPCC and TAMSAT, but CHIRPS performed worst with negative values. By filling the gaps of gauge data with the satellite-based products, we noticed that filling the missing does not necessarily improve the quality of the data and that may not be needed in the case of the Mono basin if interpolation methods like kriging are applied.

Keywords: Flood; Mono River Basin; Satellite-based rainfall products.

[1] This chapter (2) has been published as: Hounguè, N. R., Ogbu, K. N., Almoradie, A. D. S., & Evers, M. (2021). Evaluation of the performance of remotely sensed rainfall datasets for flood simulation in the transboundary Mono River catchment, Togo and Benin. *Journal of Hydrology: Regional Studies*, 36. https://doi.org/10.1016/j.ejrh.2021.100875

2.1. Introduction

Precipitation datasets are important in climate risks management (Jones & Boer, 2004). Lack of information on precipitation can jeopardize people's livelihood and security. That is particularly true in the context of global warming and climate change whereby high variability and substantial changes are observed in rainfall patterns, along with natural disasters like storm, flood, drought and wildfires, which are expected to increase in magnitude and intensity during the next decades (IPCC, 2014).However in developing countries like those in sub-Saharan Africa, precipitation datasets are characterized by non-existing records or large gaps in time series (Githungo et al., 2016).

In the transboundary Basin of Mono River shared by the republics of Benin and Togo, flood events are recurrent and trigger enormous damages (UNDP, 2010; WB & UNDP, 2011) which are expected to worsen in the future (Amoussou et al., 2020; Batablinlè et al., 2019; Koubodana et al., 2020; Lawin et al., 2019). However, majority of rain gauges (about 20) distributed within the basin, do not have complete time series of at least 30 years, and previous studies use different methods to manage missing data: Pearson correlation with neighbouring station (Koubodana et al., 2020), spatial interpolation with ordinary kriging (Amoussou et al., 2014, 2020; Lawin et al., 2019).

Remotely sensed rainfall products represent a good alternative in dealing with non-existing or incomplete records. Some of the advantages of such data are their relatively fine spatial resolution and consistency of their time series. Remotely sensed data can be retrieved from infrared sensors, microwave sensors or based on weather radars (Hong et al., 2018). A number of studies have been carried out in sub-Saharan Africa at various spatial and time scales, in order to evaluate the performance of satellite-based rainfall product (Le Coz & Van De Giesen, 2020). The increase of such studies supports scientific research and disaster management in areas characterized by sparsely gauged rainfall stations network (Dinku, 2019).

Many studies demonstrated good performances of remotely sensed rainfall products in the fields of hydrology, climatology, agriculture, ecosystem management and basically for natural hazards management (Asadullah et al., 2008; Deblauwe et al., 2016; Dinku et al., 2018; Githungo et al., 2016; Poméon et al., 2017; Romilly & Gebremichael, 2011; Sawunyama & Hughes, 2010). Poméon et al. (Poméon et al., 2017) assessed ten satellite and reanalysis precipitation datasets in six basins in West-Africa and concluded that CMORPH CRT, PERSIANN CDR, TAMSAT, CHIRPS, TMPA 3B42, RFE 2.0, GPCC, and TMPA 3B42 RT provide satisfactory results, whereas CMORPH RAW and CFSR performed poorly. Dembélé and Zwart (Dembélé & Zwart, 2016) evaluated seven satellite-based precipitation products (ARC 2.0, CHIRPS, PERSIANN-CDR, RFE 2.0, TAMSAT, TRMM and TARCAT) over Burkina Faso, at annual, monthly, decadal and daily scales. These authors found out that all evaluated products, except TARCAT, performed well at monthly and annual scale, and showed poor results at daily scale. Larbi et al. (Larbi et al., 2018) evaluated the performance of CHIRPS data at reproducing trend and extremes in the Vea Catchment in Ghana and noticed the satellite-based data has high seasonal agreement with station data. Ogbu et al. (Ogbu et al., 2020)

analysed CHIRPS, PERSIANN-CDR and TAMSAT over Nigeria and found that CHIRPS is more in line with observations in all climatic zones while the performance of PERSIANN and TAMSAT are season and location specific.

The results of these previous studies have shown the good performances of CHIRPS, PERSIANN-CDR and TAMSAT and GPCC at representing regional and local climate, and their suitability for hydrological purposes in different regions in western Africa. Moreover, these products provide long time series datasets, of at least 30 years, to support long term analysis of the climate. Thus, this study aims at assessing three satellite-based (CHIRPS, PERSIANN-CDR, TAMSAT) and one gauge-based (GPCC) rainfall products in the Mono River basin to support gaps handling in precipitation datasets and more specifically for flood management purposes. Therefore, the ability of the selected products was assessed at daily, dekadal, seasonal and annual scales using continuous and categorical statistics.

2.2. Materials and methods

2.2.1. Study area

The Mono River catchment is a transboundary catchment shared by two West-African countries, the Republics of Benin and Togo (Figure 2.1). It covers an area of 23,592.56 km^2 and is located between latitudes 6.36 ◦N and 9.39 ◦N, and longitudes 0.62 ◦E and 1.99 ◦E.

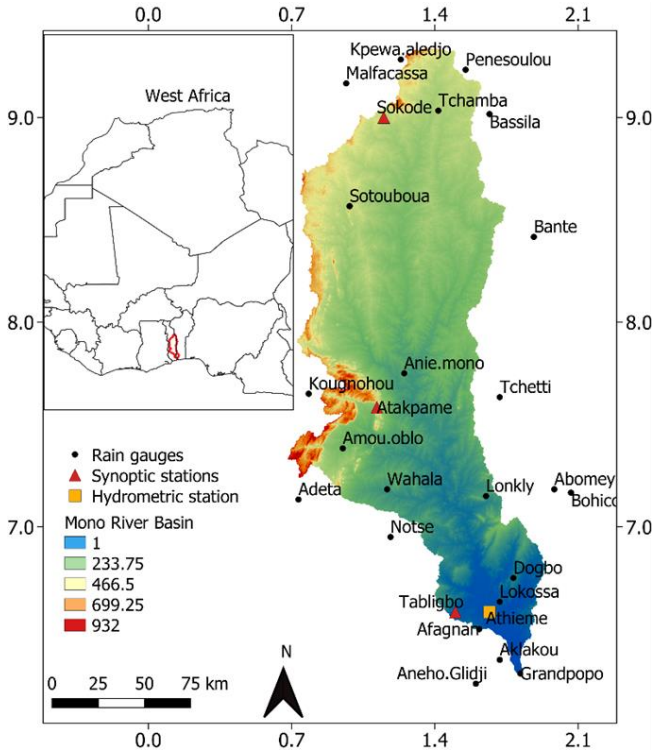

Figure 2.1. Location of the Mono river catchment

The catchment is characterized by a subequatorial climate with a bimodal rainfall cycle, two rainy seasons and two dry seasons, in the southern part (latitude inferior to 7 ◦N) and a tropical climate zone with unimodal rainfall season, one rainy and one dry season, in the central and northern parts of the basin (latitude greater than 7 ◦N) (Amoussou, 2010; E. Lawin, Hounguè, Biaou, et al., 2019). However, between 7◦N and 8 ◦N rainfall regime is *"*transitional*"*, the peak is recorded in July and is relatively maintained till September. In a typical subequatorial area of the basin, two peaks are recorded in June and October, while the peak rainfall is reached in August in tropical areas. Average annual rainfall ranges from 1000 mm per year in the south to about 1200 mm per year in the north.

2.2.2. Data

Rainfall data from 28 rain gauges were collected inside and near the Mono River catchment. The catchment disposes of three (3) synoptic stations that provide complete rainfall time series and temperature over at least 30 years to allow a long term analysis. These stations are located in Tabligbo in the south, Atakpamé in the central part and Sokodé in the northern part of the catchment. Further details about their location are provided in Table 1. Rainfall, temperature, and discharge data used in this study were collected from national meteorological services of Togo (Météo Togo) and Benin (Direction de la Météorologie National).

The three synoptic stations presented in Table 2.1 were used for the grid-to-point analysis due to the completeness of their time series.

Four rainfall datasets were assessed in this study: the Climate Hazards Group Infrared Precipitation with Station data version v2.0(CHIRPS), Precipitation Estimation from Remotely Sensed Information using Artificial Neural Networks-Climate Data Record (PERSIANN-CDR), Tropical Applications of Meteorology using Satellite data and ground-based observations (TAMSAT)and the Global Precipitation Climatology Centre full daily data (GPCC-FDDv1). The first three are satellite based whereas the latter is gauge based.

Table 2.1. Rain gauges from synoptic stations

Station name	Longitude (°)	Latitude (°)	Elevation (m)
Tabligbo	1.50	6.58	40
Atakpamé	1.12	7.58	400
Sokodé	1.15	9	387

The Climate Hazards Group Infrared Precipitation with Station data version 2.0 (Funk et al., 2014), (CHIRPS), is a gridded rainfall time series developed by the U.S. Geological Survey (USGS) Earth Resources Observation and Science (EROS) Centre and the Climate Hazard Group of University of California, Santa Barbara (UCSB) for seasonal drought monitoring. It merges in situ observations and other data input sources such as the monthly precipitation climatology (CHPClim), the quasi-global geostationary thermal infrared satellite observations from the Climate Prediction Centre (CPC) and from National Climatic Data Centre (NCDC), the Tropical Rainfall Measuring Mission

(TRMM) 3B42, and the atmospheric model rainfall fields from the NOAA Climate Forecast System, version 2 (CFSv2).

The precipitation Estimation from Remotely Sensed Information using Artificial Neural Networks-Climate Data Record, hereafter referred to as PERSIANN, uses gridded infrared data from the GridSat-B1 satellite and the National Centres for Environmental Prediction (NCEP) stage IV hourly precipitation data as input data, which are further adjusted with the version 2.2 of the monthly product of the Global Precipitation Climatology Project (GPCP 2.2) (Ashouri et al., 2015; Gehne et al., 2016). TAMSAT was developed for Africa by the University of Reading based on thermal infrared imagery from the Meteosat satellite (Maidment et al., 2014; Tarnavsky et al., 2014). It also uses gauge observations and has a fine resolution of 0.0375◦, approximately 4 km.

The Global Precipitation Climatology Centre Full Data Daily version.2018 (Ziese et al., 2018) , hereafter GPCC, is a gauge-based gridded precipitation dataset developed by the Deutscher Wetterdienst with data provided by national meteorological and hydrological services, global and regional data collections as well as the Global Telecommunication System (GTS) of the World Meteorological Organisation (WMO). It is based on more than 35,000 station gauges per month and uses the SPHEREMAP scheme for interpolation (Schneider et al., 2018). The GPCC dataset have a relatively coarse spatial resolution of 1°. The characteristics of the satellite and gauge products used in this study are shown in Table 2.2.

Table 2.2. Selected satellite-based precipitation products

Rainfall product	Spatial resolution	Spatial coverage	Temporal coverage	Temporal resolution
CHIRPS	0.05° x 0.05°	50N-50S	1981 to present	Daily
PERSIANN	0.25° x 0.25°	60N-60S	1983 to present	Daily
TAMSAT	0.0375° x 0.0375°	Africa	1983 to present	Daily
GPCC	1° x 1°	90°N - 90°S	1982-2016	Daily

The four products were selected based on previous studies (Dembélé & Zwart, 2016; Ogbu et al., 2020; Poméon et al., 2017) that demonstrated satisfactory results over West-Africa. Furthermore, GPCC which is typically not a satellite product, is also of interest in this study because of its common use as reference precipitation dataset and because of its good performance in other studies (Adeyewa & Nakamura, 2003; Poméon et al., 2017; Ziese et al., 2018).

To harmonize the time span of the various datasets and based on the available gauge data, the period 1983-2012 was considered as study period. The products were downloaded and extracted at station grid point and evaluated against gauge rainfall time series. Rainfall estimates from a satellite product at a given station point, is the value of rainfall in the grid in which that station falls.

2.2.3. Grid-to-point evaluation

In the grid-to-point approach, satellite products were evaluated against observed time series by assessing the mean annual rainfall, the annual variability and daily variability using continuous and categorical statistics.

The mean annual rainfall is the monthly rainfall values averaged over 30 years study period. It gives an overview of the annual rainfall cycle in a given location.

The annual variability of the products was checked using the total annual rainfall, the standardized precipitation index (SPI) and, trend analysis based on Mann-Kendall test (Mann, 1945) and Sens' slope estimator (Theil, 1950) at 95% confidence interval.

The SPI quantifies precipitation deficit at different time scales from 1 to 24 months. Precipitation amounts are cumulated for the selected time period and fitted to a normal distribution. Further details about SPI are well documented by McKee et al. (Mckee et al., 1993) and by Edwards and McKee (Edwards & Mckee, 1997). In this study the 12-months SPI is computed to characterize hydrologically dry and wet years based on scale in Table 2.3. (WMO, 2012).

Table 2.3. SPI values and interpretation scale

SPI	Drought and wetness characterization
> or = 2	Extremely wet
1.5 to 1.99	Very wet
1 to 1.49	Moderately wet
-0.99 to 0.99	Near normal
-1 to -1.49	Moderately dry
-1.5 to -1.99	Severely dry
< or = -2	Extremely dry

Moreover, four continuous statistics were used: the Pearson correlation coefficient, the Nash-Sutcliffe efficiency NSE (Nash & Sutcliffe, 1970), the root mean square error RMSE, and the percentage of bias (PBIAS). They were applied to the mean annual rainfall, total annual rainfall and daily rainfall time series.

The Pearson correlation coefficient, r, is used to quantify the linear relationship between observed and rainfall estimates. it varies from -1 to 1, a negative r corresponds to a negative relationship and a positive value denotes a positive correlation.

$$r = \frac{\sum_{i=1}^{n}(O_i-\bar{O})(S_i-\bar{S})}{\sqrt{\sum_{i=1}^{n}(O_i-\bar{O})^2}\sqrt{\sum_{i=1}^{n}(S_i-\bar{S})^2}} \quad (1)$$

where O_i and S_i are respectively observed and simulated values at time i, $\bar{O}$ and $\bar{S}$ are respectively the mean rain gauge and model values, and n the sample size

NSE is used to assess how well the satellite-based or gauge-based products predict the observed station gauge time series. It ranges from minus infinity to one, with one indicating a perfect match between observed and estimated rainfall.

$$NSE = 1 - \frac{\sum_{i=1}^{n}(O_i - S_i)^2}{\sum_{i=1}^{n}(O_i - \bar{O})^2} \quad (2)$$

RMSE is a measure of how spread the predicted values are around the 1:1 line of best fit. It varies between 0 and infinity.

$$RMSE = \sqrt{\frac{1}{n}\sum_{i=1}^{n}(S_i - O_i)^2} \quad (3)$$

As for the PBIAS, it indicates how the simulated values under or overestimate the observed ones.

$$PBIAS = \frac{\sum_{i=1}^{n} S_i - O_i}{\sum_{i=1}^{n} O_i} \quad (4)$$

A positive PBIAS indicates an overestimation while a negative value corresponds to underestimation, with 0 being the optimal value.

To facilitate comparison with the observed time series, the Pearson correlation coefficient and RMSE are presented on a Taylor diagram alongside the standard deviation. Taylor diagram (Taylor, 2001) is a graphical representation of r, RMSE and standard deviation basically designed for evaluating model performance against observation. The X and Y axes are standard deviation. The observed is represented by an isoline of standard deviation, and a dot on the x axis which corresponds to r = 1 and RMSE = 0. Models' RMSE are normalized –divided by observed standard deviation, and represented by isolines.

Furthermore, based on a contingency table, two categorical metrics were also used to evaluate the rainfall detection ability of the selected products. These are the probability of detection (POD) which represents the likelihood of satellite products to detect a rainfall event, and the false alarm ratio (FAR) which describes the fraction of predicted rainfall event that did not actually happen (Sofiati & Nurlatifah, 2019; Stanski et al., 1989). As this assessment is being conducted for flood management purposes, POD and FAR were computed at daily and dekadal (10 days) scale to evaluate how effectively the satellite products can capture rainfall events in a short time period. Every month comprises three dekads, day 1 to day 10 for the first dekad, day 11 to 20 for the second dekad and day 21 to day 28 or 30 or 31 for the third dekad depending on the month and year.

Furthermore, a generalized extreme value (GEV) distribution was used to evaluate the performance of the remotely sensed rainfall products for representing extreme rainfall values and their return periods. GEV is a combination of three probability distribution types: Gumbel characterized by shape = 0, Frechet corresponding to shape >0 and Weibull characterized by shape <0 (Jenkinson, 1955; von Mises, 1936). It was applied to annual daily maxima of rainfall

predicted by satellite products using the generalized maximum likelihood estimation (GMLE). The return levels associated with return periods of 2, 5, 10, 50 and 100 years were compared against those of observed time series.

2.2.4. Hydrologic modeling

A hydrologic assessment was performed in addition to the grid-to-point evaluation using HBV-light (Hydrologiska Byråns Vattenbalansavdelning) model (Seibert, 2000; Seibert & Vis, 2012). HBV-light is a conceptual rainfall-runoff model widely used for runoff modelling, flood forecasting and climate change impact assessment (Cloke et al., 2012; Grillakis et al., 2010; Kebede et al., 2014; Koutsouris et al., 2017; Shiwakoti, 2017). It has already been applied in various basins of Benin with good results (Badou et al., 2018; Bormann & Diekkrüger, 2003; Gado, 2019; U. Charlene Gaba, 2015). The model is simple and requires only rainfall, temperature and evapotranspiration as input data. HBV comprises four components: the snow routine, the soil routine the response routine and the routing routine (Figure 2.2).

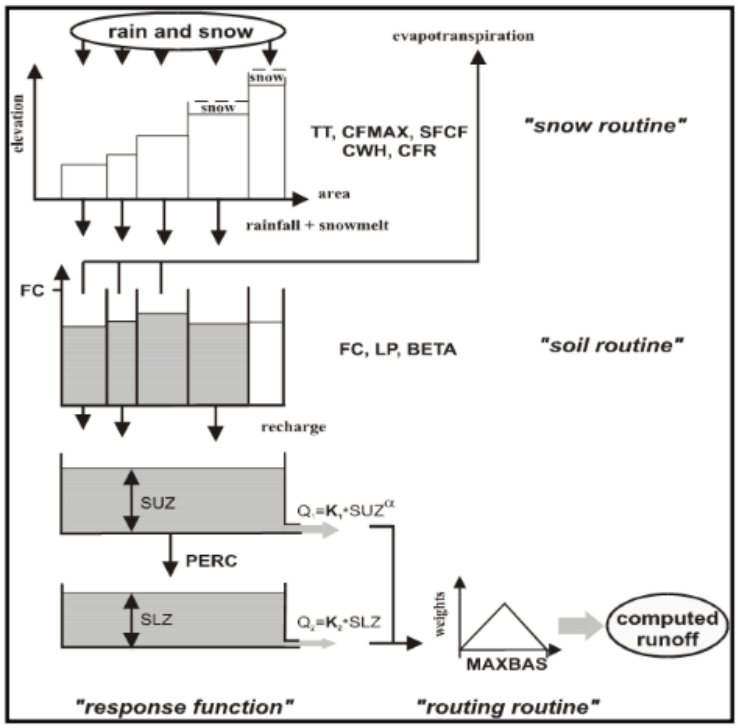

Figure 2.2. General structure of HBV model (Seibert, 2000)

Only the last three components and their parameters described in Table 2.4 were considered since snow routine is not meaningful for the study area. In the soil routing, actual water storage is used to compute groundwater recharge and actual evaporation, while the response and routing routines use respectively three linear reservoir equations and a triangular weighting function to simulate runoff (Seibert & Beven, 2009). Further details about the HBV model are provided by Bergström, 1992; Seibert and Beven, 2009; Seibert and Vis, 2012.

Table 2.4. HBV parameters and default ranges

Routine	Parameter	Description	Minimum	Maximum	Unit
Soil moisture routine	FC	Maximum soil moisture storage	100	550	mm
	LP	Soil moisture threshold for reduction of evaporation	0.3	1	mm
	BETA	Shape coefficient	1	5	
Response routine	PERC	Maximum flow from upper to lower groundwater box	0	4	$mm.d^{-1}$
	UZL	Threshold parameter for K0 outflow	0	70	
	K_0	Recession coefficient	0.1	0.5	d^{-1}
	K_1	Recession coefficient	0.01	0.2	d^{-1}
	K_2	Recession coefficient	5.10^{-5}	0.1	d^{-1}
Routing routine	MAXBAS	Routing, length of weighting function	1	2.5	

The automatic Genetic Algorithm and Powell (GAP) optimisation tool (Seibert, 2000) embedded in the model was used for calibration. With the GAP algorithm, optimized parameters are generated and randomly recombined before being fine-tuned using Powell's quadratically convergent method (Seibert & Vis, 2012). Calibration with HBV is basically manual and consists of varying parameter ranges with a try and error technique until a good model efficiency is achieved for the catchment. Thereafter, that set of parameters can be applied to various input datasets e.g., for validation, data quality control or scenario development. Since we are evaluating datasets performances in this study, they should be compared on the same ground, which implies that we must not run a dataset with the parameters derived from calibration performed with another dataset. Therefore, to avoid a biased comparison, the model was automatically calibrated for each satellite based product with 10,000 GAP runs and using the default parameter ranges which were reported to be realistic especially for catchments in West Africa (Poméon et al., 2017).

The model was calibrated on the period 1986-2000 and validated on 2002-2010 with a three years warm-up period 1983-1985.

Since HBV-light is a lumped model which needs areal precipitation as input, daily average rainfall was computed using ordinary kriging method (Matheron, 1963) for interpolation. The kriging approach applied in this study consisted of computing a variogram with the corresponding characteristics (nugget, sill and range) for each year separately. The advantage of that approach is that it accounts for inter-annual variability of the dataset as opposite to the common kriging application whereby a single variogram is used for the entire time series. More details about the method are available in (Lawin, 2007; Lawin, Hounguè, Biaou, et al., 2019).

Since the final goal of this study is to evaluate the capability of remotely sensed products to deal with missing in gauge data, and because gauge data when they exist are preferable to remotely sensed ones, we filled-in the gaps of available rain gauges (Figure 2.1) with satellite-based products and used the recomposed gauge-satellite dataset as input for hydrologic modelling. Thus, a total of 8 models were created: 4 with satellite based sensed products and 4 with gauge-satellite combinations.

2.3. Results and Discussion

2.3.1. Grid to point evaluation

This section presents the results of the various analyses performed with the grid-to-point assessment.

2.3.1.1. Annual cycle

For the three selected rain gauges, all the products fairly reproduced the annual rainfall cycle and its seasons (Figure 2.3).

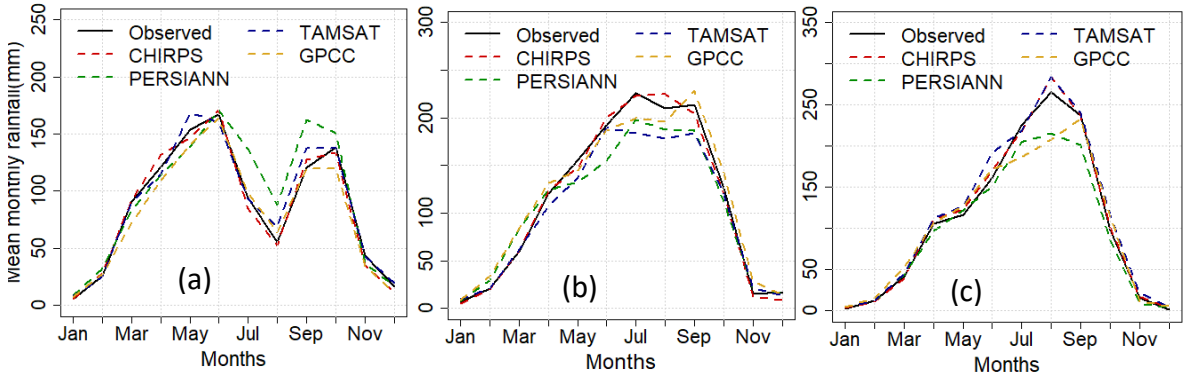

Figure 2.3. Annual cycle of rainfall at Tabligbo (a), Atakpamé (b) and Sokodé (c)

At Tabligbo, PERSIANN presents higher rainfall values after the first peak and the second peak occurred one month earlier than the gauged; as for TAMSAT, it has the first peak occurring in May instead of June. At Atakpamé, the peak is underestimated by TAMSAT and PERSIANN, and it occurs two months later with GPCC, whereas CHIRPS has one-month delay of the peak. As underlined by Lawin et al. (Lawin et al., 2019), the annual cycle in the central part of Mono basin (where Atakpamé gauge belongs) is characterized by a “transitory” cycle which is not clearly bimodal neither strictly unimodal, and none of the four products assessed in this study fairly represent that pattern along with the peak rainfall amount. At Sokodé, the peak is underestimated by PERSIANN and GPCC and for the latter the peak happens in September instead of August. Overall, CHIRPS reproduced best the annual cycles.

This is further supported by results as shown in the Taylor diagrams (Figure 2.4) as well as statistics of NSE and PBIAS values in Table 2.5.

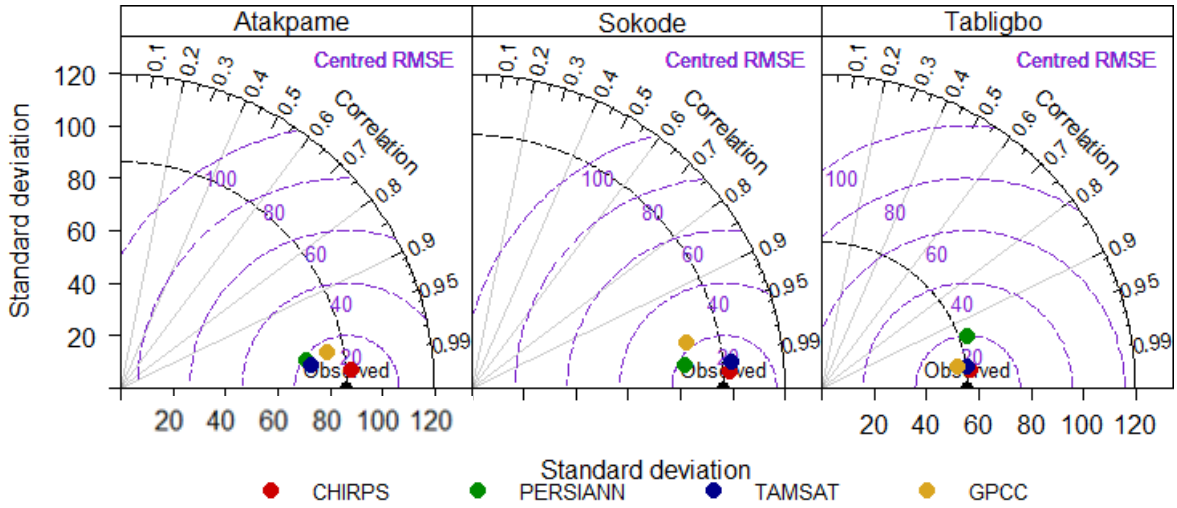

Figure 2.4. Taylor diagram of mean monthly rainfall

Table 2.5. NSE and PBIAS statistics of mean monthly rainfall

Station	Statistics	CHIRPS	PERSIANN	TAMSAT	GPCC
Tabligbo	NSE	**0.99**	**0.85**	**0.98**	**0.97**
	PBIAS	-1	10.6	3.3	-6
Atakpamé	NSE	**0.99**	**0.94**	**0.95**	**0.97**
	PBIAS	-1	-8.1	-9.9	2.6
Sokodé	NSE	**0.99**	**0.96**	**0.98**	**0.95**
	PBIAS	2.9	-10.1	7.7	-3.5

At Tabligbo, CHIRPS has the highest NSE value and the lowest bias. It is followed by TAMSAT, GPCC and PERSIANN. At Atakpamé, the best product after CHIRPS is GPCC, followed by TAMSAT and PERSIANN which have almost same results. In Sokodé, TAMSAT shows the second best NSE results after CHIRPS. All the products show very high correlation with observed data (r>0.9) for the three stations. However, PERSIANN time series globally displayed the lowest NSE, highest bias and highest error except at Sokodé where it has slightly outperformed GPCC.

2.3.1.2. Return period

The return levels of daily maximum rainfall associated with 2, 5, 10, 50 and 100 years return period are presented on Figure 2.5. The return levels simulated by the products are overall underestimated compared to observed, except for 50 and 100 years return period of GPCC at Tabligbo. TAMSAT predicted the lowest daily extreme values and highly underrated them,

therefore, it cannot be commended for flood management purposes in order to reduce unforeseen risks.

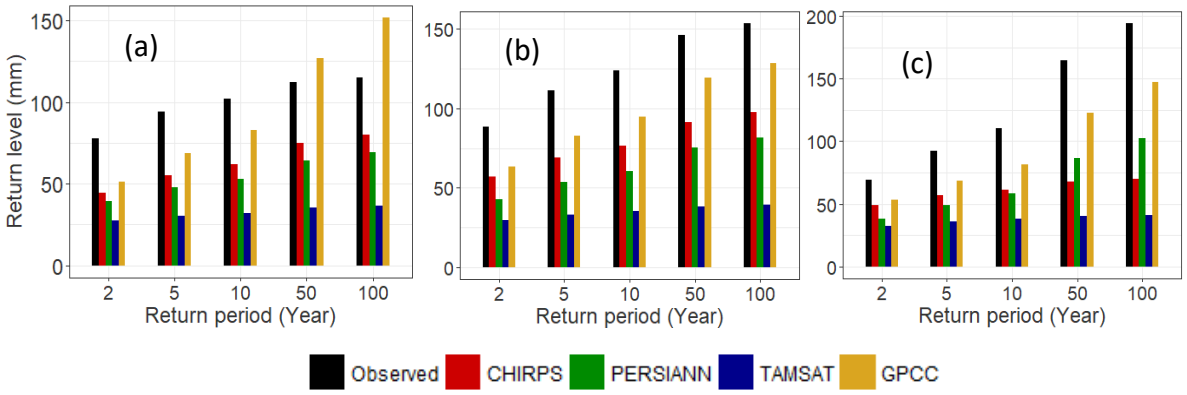

Figure 2.5. 2, 5, 10, 50 and 100 years return levels at Tabligbo (a), Atakpamé (b) and Sokodé (c)

The results of CHIRPS and PERSIANN also underestimated the return levels of extreme daily maximum precipitation, and that made them not very suitable for flood monitoring activities. The closest values to gauges' data are noted with GPCC. However, the recurrence of the rarest events, above 10 years return period, must be regarded with caution because of the short length of the evaluation period.

2.3.1.3. Trend analysis of annual rainfall

The Z statistics and p-value of Mann-Kendall trend assessment and Sen's slope values for gauge time series and the satellite-based products are summarized in Table 2.6. Significant trends are indicated by bold p-values. The positive Z statistics noted for observed time series at all three gauges indicates increasing trends which are however not significant at 95% confidence since p-values are greater than 0.05 (or alternatively Z values are lower than 1.96).

Table 2.6. Mann-Kendall statistics and Sen's slope

Station	Statistics	Observed	CHIRPS	PERSIANN	TAMSAT	GPCC
Tabligbo	Z	1	1.96	1.07	3.18	1.82
	p-value	0.32	**0.05**	0.28	**0.001**	0.07
	Sen's slope	4.25	7.1	4.41	12.46	5.46
Atakpamé	Z	0.79	1.18	0.54	3.12	0.11
	p-value	0.43	0.24	0.59	**0.002**	0.91
	Sen's slope	3.72	6.34	2.87	9.78	0.95
Sokodé	Z	0.80	1.14	1.43	4.21	0.18
	p-value	0.42	0.25	0.15	**2.55×10^{-5}**	0.86
	Sen's slope	3.16	4.43	6.28	12.73	0.84

Over the three stations, TAMSAT time series exhibit significant increasing trends and the magnitude of increase as indicated by slope values are in average three time those of gauge data.

In the opposite, the other products showed agreement with the observed trends, except CHIRPS at Tabligbo where p-value = 0.05. At Tabligbo, PERSIANN and GPCC stand out as the best products while at Atakpamé, PERSIANN, and CHIRPS are the best two. At Sokodé, CHIRPS and PERSIANN have the closest statistics to observed ones, followed by GPCC that showed an insignificant increasing trend as gauge data but with lower slope.

2.3.1.4. Standardized Precipitation Index (SPI)

Figure 2.6 presents the 12-months SPI computed for observed time series and satellite products, as well as their correlation coefficient. At Tabligbo (Figure 2.6-a), SPI from all the four satellite products CHIRPS, PERSIANN, TAMSAT and GPCC have high correlation with the indexes from the observed time series. GPCC has the highest correlation 0.81, followed by CHIRPS 0.78, PERSIANN 0.68 and TAMSAT 0.62. At Atakpamé (Figure 2.6-b), CHIRPS showed the best correlation and it is followed by TAMSAT, GPCC and PERSIANN respectively. As for the station of Sokodé in the northern part of the basin (Figure 2.6-c), GPCC has the lowest correlation r=0.35 and CHIRPS the best correlation r=0.57. The satellite products showed average to low performance at detecting dry and wet years as well as the value of the SPI at Sokodé. SPI values from observed time series at Tabligbo station indicate that years 1995, 1996, 1999 and 2010 were wet (SPI ≥ 1). All satellite products at Tabligbo found 2010 wet as well; in addition, 1999 was detected by CHIRPS, PERSIANN and GPCC. However, years 1995 and 1996 were found wet by none of the products. The satellite time series predicted each two wet years over four, except TAMSAT which detected only one. At Atakpamé SPI from the station dataset indicate 1988, 1999, 2007, 2008 and 2009 as wet years. However, no product detected 1988 and 2009; 1999 was found by CHIRPS, PERSIANN and TAMSAT; 2007 was detected only by CHIRPS; and 2008 only by TAMSAT. Over the five actual wet years, CHIRPS and TAMSAT detected two each, PERSIANN one and GPCC none. At Sokodé, out of the four wet years 1988, 1991, 2003 and 2005 from observed, 2003 was equally detected by all the satellite products assessed in this study. Year 1991 was identified as wet by CHIRPS and TAMSAT whereas, 2003 and 2005 was detected by no product. CHIRPS and PERSIANN correctly predicted two wet years over 4, while TAMSAT and GPCC found one each.

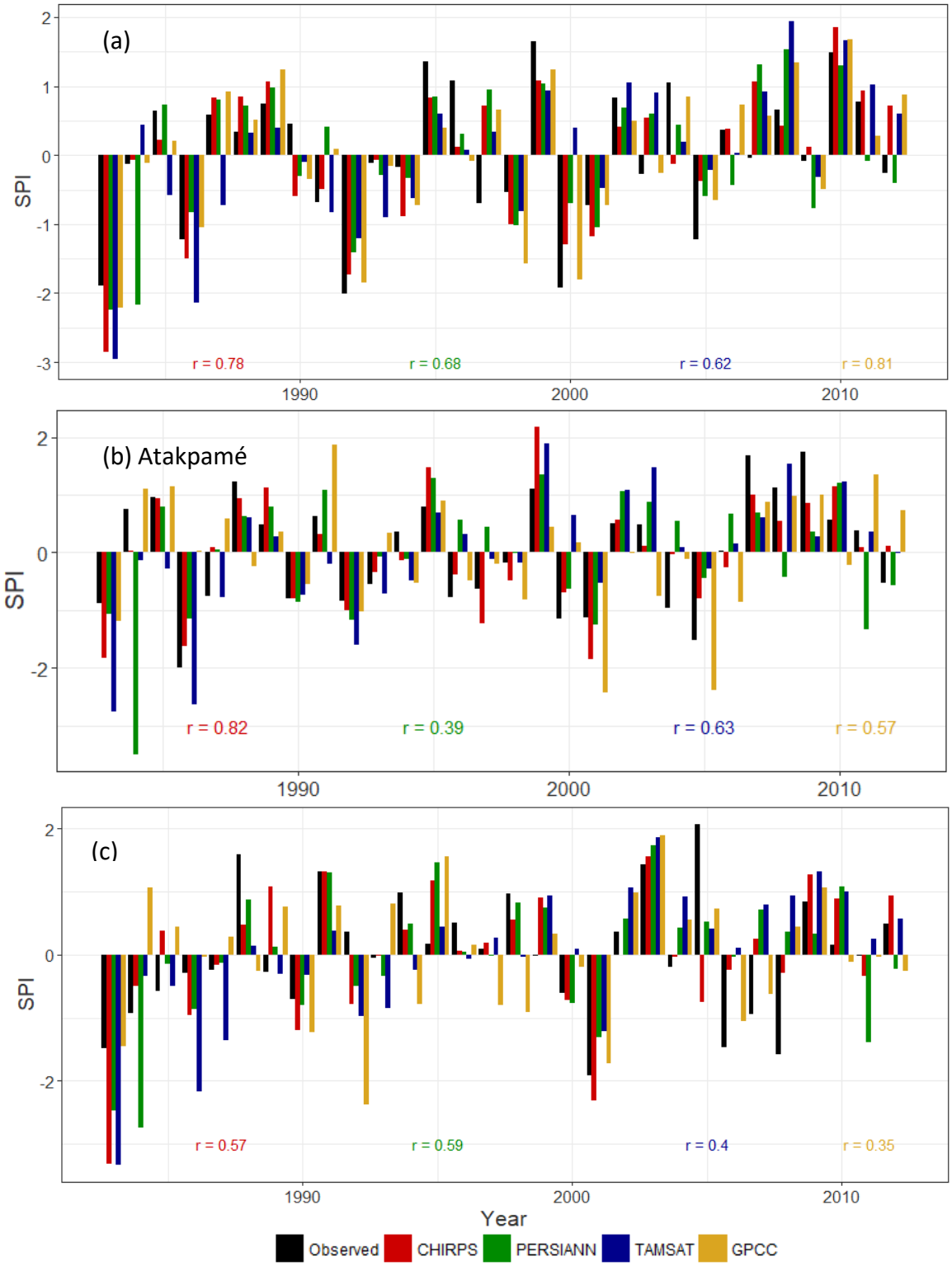

Figure 2.6. Standardized Precipitation Index and correlation with observed at Tabligbo (a), Atakpamé (b) and Sokodé (c)

2.3.1.5. Performance at daily scale

The statistics as presented in Table 2.7 show poor performances at daily scale. A part from GPCC at Tabligbo which scored an NSE of 0.59 all other products have their NSE lower than 0.3. At Tabligbo, GPCC appears to be the closest to observed, with the highest correlation coefficient, 0.77 (Figure 2.7), and the smallest error. At Atakpamé and Sokodé, TAMSAT has the highest Nash-Sutcliffe efficiency value and showed the best correlation coefficient, 0.52, for the two gauges. The significance of the correlations was tested at 95% confidence interval and they are all significant with p-value = 0. Furthermore, for all the three gauges, GPCC has the closest standard deviation to the observed and the lowest PBIAS statistics after CHIRPS data which showed the poorest NSE at daily scale. A part from GPCC at Tabligbo, the outputs of all other products do not match observed ones based on the statistics and cannot be recommended for flood simulation at daily scale without further corrections. Such poor performances at daily scale were also found in Burkina-Faso by (Dembélé & Zwart, 2016).

Table 2.7. NSE and PBIAS statistics of daily rainfall

Station	Statistics	CHIRPS	PERSIANN	TAMSAT	GPCC
Tabligbo	NSE	0.01	0.1	0.24	**0.59**
	PBIAS	-1	13.9	8.2	-6
Atakpamé	NSE	0.01	0.15	0.27	0.17
	PBIAS	-1	-5.1	-6.5	2.6
Sokodé	NSE	-0.03	0.04	0.24	0.15
	PBIAS	2.9	-7.7	12.2	-3.5

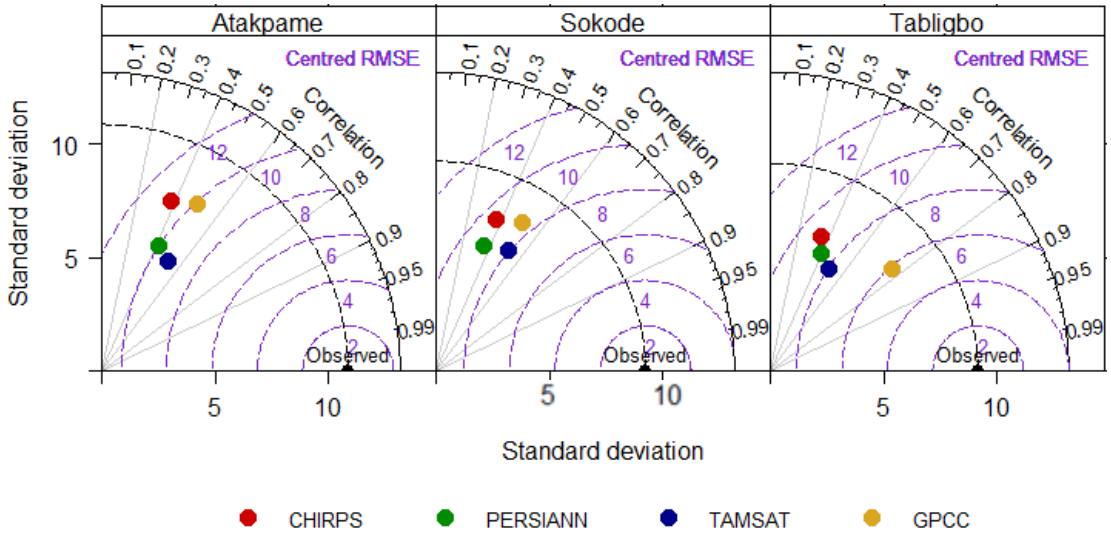

Figure 2.7. Taylor diagram of daily rainfall

2.3.1.6. Performance at annual scale

At Tabligbo, the statistics showed that CHIRPS performs better than other products with the highest NSE, the lowest bias and r=0.77. It is followed by GPCC, NSE=0.49 and r=0.8. Overall, the Pearson correlation between observation and the satellite products at Tabligbo is good, greater than 0.6 for the four products. However, TAMSAT and PERSIANN displayed very low NSE values (Table 2.8). At Atakpamé, once again, CHIRPS has the best statistics: the highest NSE=0.65, the highest correlation r=0.81, the lowest PBIAS 1% underestimation and the lowest RMSE=148. GPCC comes second with NSE = 0.31. As for TAMSAT and PERSIANN, their NSE values are very low: 0.09 and -0.09 respectively. The statistics at Sokodé showed that none of the four products was able to fairly simulate rainfall pattern at that gauge (Table 2.8, Figure 2.8).

Overall, the range of error is relatively high at annual scale with RMSE values above 100mm/year. That is opposite to the findings of Larbi et al., 2018 and Dembélé and Zwart, 2016 who reported good performance of satellite based products at annual scale respectively in Ghana and Burkina-Faso.

Table 2.8. NSE and PBIAS statistics of annual rainfall

Station	Statistics	CHIRPS	PERSIANN	TAMSAT	GPCC
Tabligbo	NSE	**0.58**	-0.02	0.13	0.49
	PBIAS	-1	10.6	3.3	-6
Atakpamé	NSE	**0.65**	-0.09	0.09	0.31
	PBIAS	-1	-8.1	-9.9	2.6
Sokodé	NSE	0.03	-0.56	-0.76	-0.19
	PBIAS	2.9	-10.1	7.7	-3.5

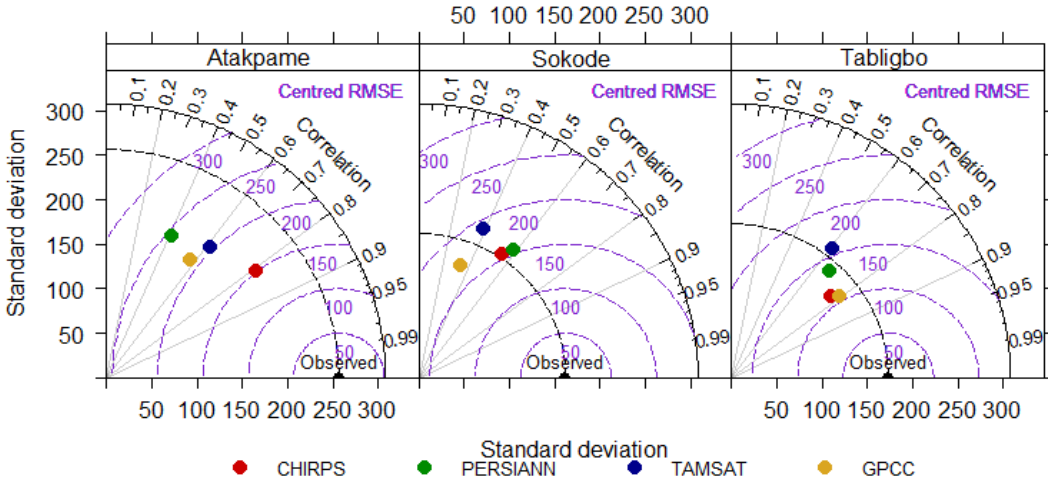

Figure 2.8. Taylor diagram of annual rainfall

The performance of satellite products to detect rainfall events was assessed at daily and dekadal (10-days) scales. Table 2.9 and Table 2.10 present the probability of detection (POD) and the false alarm ratio (FAR) of each product.

Table 2.9. POD and FAR of satellite products at daily scale

Station	Metric	CHIRPS	PERSIANN	TAMSAT	GPCC
Tabligbo	POD	0.55	0.89	0.85	0.98
	FAR	0.47	0.62	0.49	0.54
Atakpamé	POD	0.61	0.91	0.87	0.99
	FAR	0.44	0.55	0.42	0.52
Sokodé	POD	0.65	0.88	0.91	0.99
	FAR	0.34	0.51	0.37	0.46

At daily and for the three gauge points, the highest FAR were recorded by PERSIANN and the lowest by CHIRPS. GPCC has the highest POD, almost 1, which can be explained by the fact that GPCC uses gauge station as input. In addition, CHIRPS presented the lowest POD values which make it less suitable for flood monitoring purposes at such a fine scale as daily.

Table 2.10. POD and FAR of satellite products at dekadal scale

Station	Metric	CHIRPS	PERSIANN	TAMSAT	GPCC
Tabligbo	POD	0.91	1	0.98	1
	FAR	0.12	0.18	0.12	0.13
Atakpamé	POD	0.98	1	0.99	1
	FAR	0.14	0.19	0.14	0.17
Sokodé	POD	0.99	1	0.99	1
	FAR	0.14	0.22	0.14	0.19

All products performed very well at dekadal scale with 0.9 to 1 POD. The detection of rainfall within a 10-day time span is almost 100% and the prediction false alarm ratios are low, making the products more reliable for flood monitoring and predictions.

2.3.2. Spatial analysis and hydrologic modelling

2.3.2.1. Spatial distribution

Mean annual rainfall from the four datasets range from 938 to 2008 mm. The spatial distribution depicted by Figure 2.9 shows similarities between GPCC and PERSIANN with annual precipitation amount below 1500m and the lowest amounts being recorded in the south near the outlet.

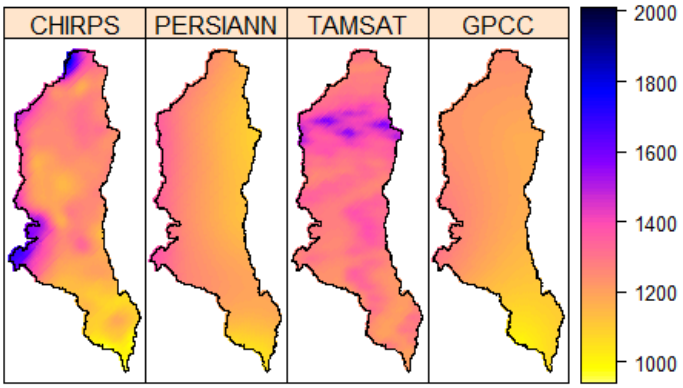

Figure 2.9. Spatial distribution of satellite based products in the Mono basin

This is in line with previous studies (Amoussou, 2010; Koubodana et al., 2020) which reported simular characteritics in the distribution of annual rainfall in the Mono river Basin, and around 1000mm/year close to the outlet (Amoussou et al., 2020). The north-south gradient is explained by the orographic effect of high latitudes between 400 and 930 m in the north (Amoussou, 2010). Although CHIRPS captures relatively well the distibution in the south, it presents however higher values with up to 2000 mm/year in the rest of the basin. As for TAMSAT, the distribution of rainfall is not properly captured and annual rainfall amounts seem to be overestimated all over the basin.

2.3.2.2. Hydrological modelling

The results of calibration and validation are depicted respectively by Figure 2.10 and Figure 2.11. Based on NSE values presented in Table 2.11, the simulation with PERSIANN showed the best agreement with observed discharge during both calibration and validation periods; followed by GPCC and TAMSAT. It was noticed that TAMSAT overestimated the peaks and that is in line with the overestimation earlier highlighted by the spatial map.

As for CHIRPS, it performed worst with negative NSE values, high base flow and very low peak flow. This can be explained by the low POD reported for CHIRPS at daily scale. A low POD implies that a high number of rainfall events are not accounted for, which in turn will lead to rainfall trends and amount not being well captured. As for the high base flow noticed with CHIRPS, it may be related to the values of its false alarm ratio, especially when the 'false' rainfall events are simulated during the dry season. Overall, these results confirm again that CHIRPS is not an appropriate dataset for flood monitoring purposes in the Mono River Basin and also that a fine resolution data does not necessarily imply a higher performance.

Furthermore, by filling in the gaps of stations' time series with satellite data, we noticed that all the combinations of gauge-satellite performed almost the same as if model efficiency does not depend on which product is used to fill-in the gaps. Recalling the very poor performance of CHIRPS in simulating the hydrograph and the good result from PERSIANN in the first hand, and having the combinations gauge-CHIRPS and gauge-PERSIANN performing almost identically on the other hand, indicates that filling-in the gaps does not guarantee improvement of the data quality and

may not be necessary in the case of the Mono basin when a strong interpolation method like kriging is used.

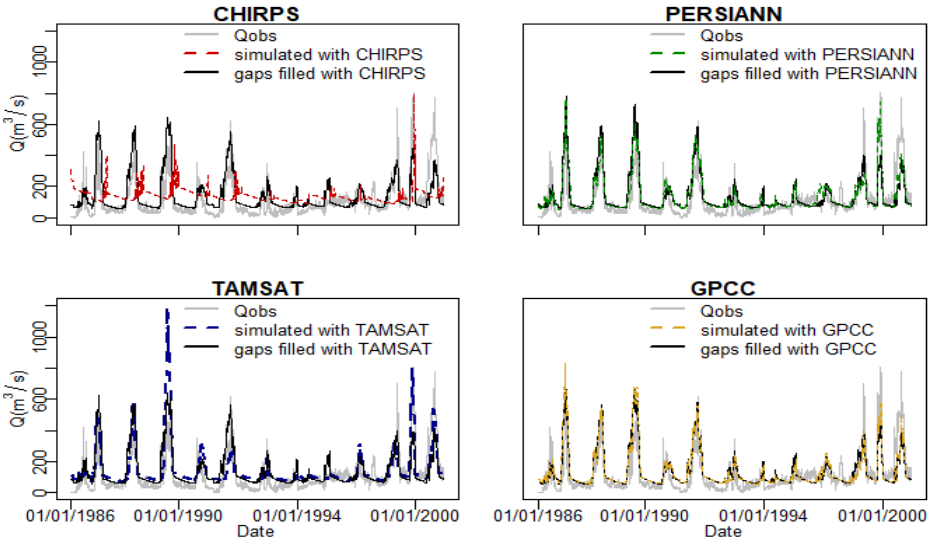

Figure 2.10. Hydrographs in calibration 1986-2000

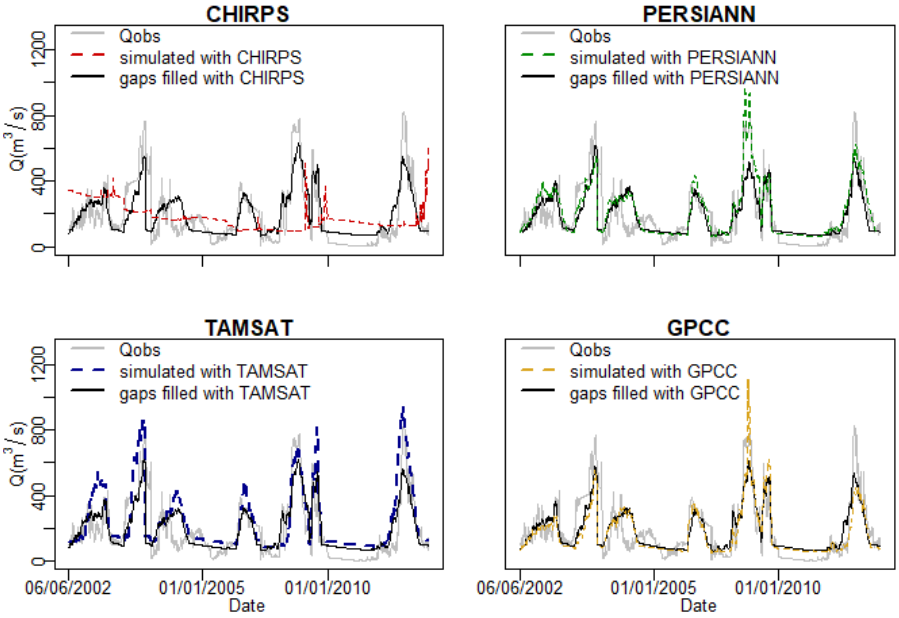

Figure 2.11. Hydrographs in validation 2002-2010

Table 2.11. Nash Sutcliff efficiency of hydrologic modelling

	Satellite based products				Gauge-satellite data			
	CHIRPS	PERSIANN	TAMSAT	GPCC	CHIRPS	PERSIANN	TAMSAT	GPCC
Calibration	-0.088	0.64	0.5	0.61	0.58	0.55	0.58	0.59
validation	-0.22	0.67	0.42	0.57	0.67	0.64	0.69	0.66

2.4. Conclusion

Precipitation data are essential for hydrological risks management especially for flood protection purposes in the context of global climate change. The interest for satellite-based rainfall datasets has grown over recent years because of their practicability in solving issues related to the lack of reliable, consistent and long measured records. However, their performance can vary with location and seasons, which makes it important to evaluate them at local scale. In this study we assessed the performance of CHIRPS, PERSIANN, TAMSAT and GPCC using hydrologic modelling and grid-to-point analyses at three synoptic stations in the Mono River basin. The grid to point analyses conducted over the period 1983-2012 revealed that the four products performed well in reproducing the characteristics of annual cycles at Tabligbo, Atakpamé and Sokodé, but the peaks at Atakpamé were not well captured. Good results were also exhibited at dekadal scale for all the products across the three stations, with low false alarm ratio and almost 100% rainfall detection probabilities. Overall, the products performed poorly at daily and annual scales. Based on the grid to point evaluation it was noticed that the performance of the products varies with temporal scales. Based on Nash Sutcliff efficiency with the hydrologic modelling assessment, the best performance was achieved by PERSIANN, followed by GPCC and TAMSAT. CHIRPS showed very poor results and is not appropriate for flood monitoring in the Mono River Basin. Furthermore, despite the gaps in rain gauge data, attempt to fill them may not be necessary in the case of the Mono Basin if an interpolation method like kriging is used. Further research works could address the correction of the satellite based rainfall products at local scale using gauge data or Artificial Neural Network.

3. A Multi Criteria Decision Analysis Approach for Regional Climate Model Selection and Future Climate Assessment in the Mono River Basin, Benin and Togo[2]

Abstract

Regional climate models (RCMs) are key in the current context of global warming and they are increasingly used to support decision-making and to identify adaptation measures in response to climate change. However, considering the wide range of available RCMs, it is important to identify the most suitable ones prior to climate impact studies, especially at small scales like catchments. In this study, a multi-criteria decision analysis approach, namely the technique for order preferences by similarity to an ideal solution (TOPSIS) was applied to select the best performing RCMs in the Mono river basin of Benin and Togo (West Africa). The TOPSIS method was used to systematically rank 15 RCMs accessed from the coordinated regional downscaling experiment (CORDEX) database. 6 RCMs were finally selected and averaged into an ensemble to assess the future climate in the Mono river basin until 2070 compared to the period 1966-2015. Two climate change scenarios, RCP 4.5 and RCP 8.5, were considered. The results show that under both climate change scenarios, the annual temperature has an increasing trend during the period 1966-2070 whereas annual rainfall for the next 50 years presents high variability and no statistically significant trend. Furthermore, seasonal cycles of rainfall are expected to change in the different parts of the catchment with delayed onset of rainfall, longer dry seasons, and rainfall intensification. In response to the projected changes, impact studies and risk assessments need to be carried out to evaluate potential implications for human security in the Mono river basin and to provide adequate adaptation measures.

Keywords: Multi-criteria decision analysis; TOPSIS; climate change; RCP scenarios; Mono River basin; Benin; Togo

[2] This chapter (3) was originally published as: Houngue, N. R., Almoradie, A. D. S., & Evers, M. (2022). A Multi Criteria Decision Analysis Approach for Regional Climate Model Selection and Future Climate Assessment in the Mono River Basin, Benin and Togo. *Atmosphere*, 13. https://doi.org/10.3390/ atmos13091471

3.1. Introduction

Oceans, lands, and the atmosphere have become warmer over the last five decades due to human activities (Rosenzweig et al., 2007). As a result, changes in the pattern of climate variables and associated consequences such as the rise of mean sea level, ocean acidification, changes in precipitation pattern, and increase in temperature are observed (IPCC, 2021a). Climate models, whether global circulation models (GCM) or regional climate models (RCM) are increasingly used to analyse past and future patterns of climate at the global, regional, or local scale. The Intergovernmental Panel on Climate Change (IPCC) bases its assessment reports on scenarios and climate model information disseminated on the Earth System Grid Federation (ESGF) portals. In that regard, a large number of model data are available for the African region within the Coordinated Regional Downscaling Experiment (CORDEX) under the fifth coupled model intercomparison project (CMIP 5).

Due to the coarse resolution and biases embedded in climate models –both GCMs and RCMs, it is recommended to downscale or bias-correct them before usage in impact studies especially at small scales like catchment scale (Wang et al., 2015). Among other sources, biases in climate models arise from model parameterization, imperfect conceptualisation, boundary conditions, spatial resolution and averaging over grids (Mishra et al., 2014; Yip et al., 2011). Statistical methods are commonly used for bias correction purposes in regional and local climate studies, as opposed to dynamical downscaling methods which require substantial computational resources (Maraun et al., 2010; Wang et al., 2015). Bias correction approaches are built on the assumption that biases remain the same over time, from past to future. The correction consists of comparing model historical data against observations to estimate biases that are afterward removed from future datasets (Chen et al., 2021). There is a wide range of bias correction methods that have proven their suitability with respect to different climate variables and depending on the study area. For instance, quantile mapping methods use cumulative distribution functions (CDFs) of observation and historical model data to construct a transfer function used in turn to correct model outputs (Sarr et al., 2015). The delta change method adds up the difference between observation and model data to adjust biases. It is based on the assumption that changes in climate data are location-specific and occur only over large distances (Beyer et al., 2020; CCAFS, 2014). However, due to its simple transfer function, this method does not capture changes in extreme events (Gunavathi & Selvasidhu, 2021). The linear scaling method corrects the mean of future data by adjusting the long-term monthly mean of model data to that of the observation (Crochemore et al., 2016; Luo et al., 2018).

In West Africa, data excerpted from the CORDEX database have demonstrated overall good performance in simulating climate in the region. A wide range of local studies based on CORDEX datasets has been carried out in the region over the recent years with satisfactory results. Akinsanola et.al., 2015 (Akinsanola et al., 2015) evaluated the capability of three RCMs, namely REMO, RCA4, and CCLM in simulating West-African summer monsoon precipitation and concluded that the first two models simulate rainfall adequately in the region. Likewise, 10 RCMs

analysed by Gbobaniyi et.al, 2014 (Gbobaniyi et al., 2014) were reported to have acceptable performances in reproducing the spatial distribution of rainfall and temperature over the region. Akinsanola and Ogunjobi, 2017 (Akinsanola & Ogunjobi, 2017) assessed the performance of RCA4, CRCM5, CCLM, REGCM3, PRECIS, HIRHAM and REMO against TRMM and CRU rainfall datasets and concluded that they fairly represent the mean annual cycle of rainfall and the interannual variations despite some seasonal and region-specific biases.

Likewise, in the Mono river basin located in West Africa, future climate assessment studies were carried out during the past years using various GCMs and RCMs for trend assessment (Batablinle et al., 2018; Batablinlè et al., 2019; Djan'na Koubodana et al., 2020; E. Lawin, Hounguè, Biaou, et al., 2019), extremes analysis (Amoussou et al., 2020; E. Lawin, Lamboni, et al., 2019) and climate change impact studies (Houngue, 2018). However, none of those studies explicitly exposed the selection process of the climate model used. Models were basically selected with reference to other studies where they were reported to be of good performance, or based on data processing constraints, and barely on the basis of a systematic selection. As reported by Browne and Sylla 2012 (Akinsanola & Ogunjobi, 2017), the performance of a model within a geographical region like West-Africa could vary depending on the location under consideration.

Therefore, the novelty of this study is to carry out a systematic selection of best performing RCMs in the Mono River Basin that will be used afterwards to analyse future climate pattern. In that vein, Lutz et al., 2016 (Lutz et al., 2016) have used a three-step process to select best performing GCMs in the Indus, Ganges and Brahmaputra river basins. The authors first filtered the GCMs based on their ability to represent changes in mean temperature and rainfall; next, the first selection is refined based on performance vis-à-vis four climate extreme indices; and finally, the second list is trimmed down based on model's ability to capture annual cycles. Therefore, this approach basically consists of selecting best performing models based on predefined criteria, which are evaluated individually. Refaey et al., 2019 (Refaey et al., 2019) furthered that approach by using 5 statistical metrics with 4 multi-criteria decision analysis (MCDA) techniques to simultaneously evaluate all selected criteria in the Wadi El-Natrun catchment in Egypt. Recently, there has been an increasing interest for MCDA techniques for climate models selection (Homsi et al., 2020; Raju & Kumar, 2015; Shiru et al., 2019).

Our approach in this paper consists of using a MCDA method to rank RCMs in the Mono river basin based on statistical and categorical metrics. Furthermore, the RCMs are bias-corrected and ensemble-averaged to assess future climate changes or variation in the next 50 years.

3.2. Materials and Methods

3.2.1. Study area

The Mono River basin is located within latitudes 6.36°N and 9.39°N, and longitudes 0.62°E and 1.99°E in West-Africa (Figure 3.1.a). It stretches over 340 km North to South with an area of 23,592.56 km^2. The catchment is transboundary and shared by the Republics of Benin and Togo. The Mono River basin has two main climatic zones defined by a subequatorial climate for latitudes lower than 7 °N and a tropical climate in the upper part (latitude above 7 °N). Areas of latitude lower than 7 °N experience two rainy seasons every year whereas, above 8 °N, the rainfall regime is unimodal with only one peak (Amoussou, 2010). Within latitudes 7 °N - 8 °N, the rainfall regime is halfway between a typical unimodal and bimodal cycle, which is described as “transitional” regime (Lawin et al., 2019b).These three rainfall-based climatic zones are further referred to in this study as: south (latitudes < 7 °N), centre (7 °N < latitude < 8 °N) and north (latitudes > 8 °N). The lower part of the basin is prone to recurrent flood events which trigger economic losses and deaths in both countries. An average of 1000 mm precipitation per year is recorded in the south and 1200 mm in the northern part.

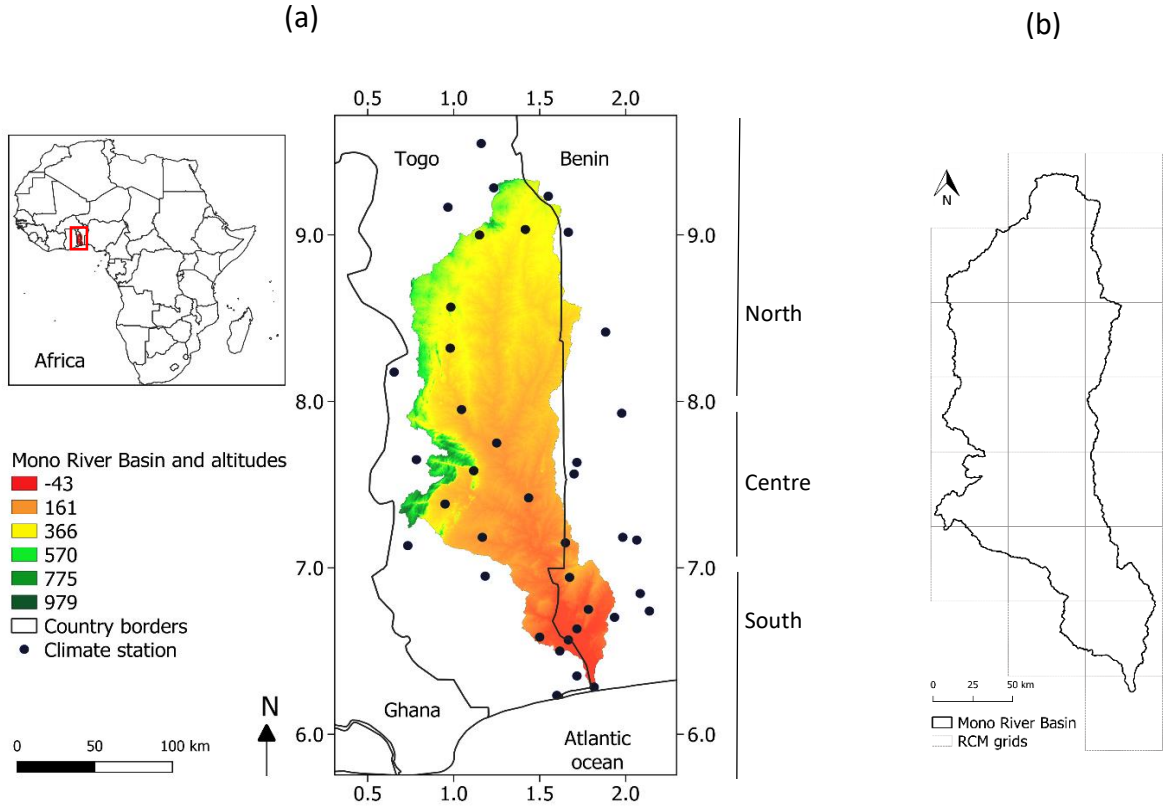

Figure 3.1. Location of (a) the Mono River Basin and (b) RCM grids

3.2.2. Data

All the RCMs available for the Africa Domain in the CORDEX database and which provide complete time series of rainfall and mean air temperature for RCP4.5 and RCP 8.5 until 2070 are considered in this study. The list is made of 4 RCMs driven by 8 GCMs. These are in total 15 RCMs that were downloaded from the Earth System Grid Federation (ESGF) node at the German Climate Computing Centre (DKRZ) https://esgf-data.dkrz.de/projects/esgf-dkrz/, accessed on 05.03.2020. Table 3.1 presents the RCMs used as well as their driving GCM and the designation under which the RCM is subsequently referred to in this study.

Table 3.1. List of RCMs used and details

GCM		RCM		GCM-RCM designation
Name	**Developed by**	**Name**	**Institute**	
CNRM-CERFACS-CNRM-CM5	Centre National de Recherches Météorologiques, Centre, France (CNRM)	CCLM4-8-17	Climate Limited-area Modelling Community (CLMcom)	CNRM-CCLM4
ICHEC-EC-EARTH	Irish Centre for High-End Computing (ICHEC)			ICHEC-CCLM4
MOHC-HadGEM2-ES	Met Office Hadley Centre, UK (MOHC)			MOHC-CCLM4
MPI-M-MPI-ESM-LR	Max Planck Institute for Meteorology, Germany (MPI)			MPI-CCLM4
ICHEC-EC-EARTH	ICHEC	RACMO22T	Royal Netherlands Meteorological Institute (KNMI)	ICHEC-RACMO22T
MOHC-HadGEM2-ES	MOHC			MOHC-RACMO22T
CCCma-CanESM2	Canadian Centre for Climate Modelling and Analysis	RCA4	Swedish Meteorological and Hydrological Institute (SMHI)	CCCma-RCA4
CNRM-CERFACS-CNRM-CM5	CNRM			CNRM-RCA4
CSIRO-QCCCE-CSIRO-Mk3-6-0	Commonwealth Scientific and Industrial Research Organization, Australia (CSIRO)			CSIRO-RCA4
IPSL-IPSL-CM5A-MR	Institut Pierre Simon Laplace, France (IPSL)			IPSL-RCA4
MIROC-MIROC5	The University of Tokyo, National Institute for Environmental Studies, and Japan Agency for Marine-Earth Science and Technology, Japan			MIROC-RCA4
MOHC-HadGEM2-ES	MOHC			MOHC-RCA4
MPI-M-MPI-ESM-LR	MPI			MPI-RCA4
ICHEC-EC-EARTH	ICHEC	REMO2009	Helmholtz-Zentrum Geesthacht, Climate Service Center, Max Planck Institute for Meteorology (MPI-CSC)	ICHEC-REMO
MPI-M-MPI-ESM-LR	MPI			MPI-REMO

The RCM data have a spatial resolution of 0.44° x 0.44°, about 50 km x 50 km. Figure 3.1.b presents the distribution of the RCM grids over the catchment. A grid-to-point extraction of the data was performed at location of observation stations in order to facilitate the bias correction process afterwards. In-situ data were collected from 38 stations within and around the Mono river basin (Figure 3.1.a).

For observation data, the mean temperature is given by the average of minimum and maximum temperature collected from met services whereas, for RCMs, the mean air surface temperature (named "tas" in the CORDEX database) was downloaded. Observation data cover the period 1966-2015 while 2021-2070 is considered as future period. The overlapping period between observations and model predictions for the past is 1966-2005.

3.2.3. Ranking and selection of RCMs

The selection of RCMs to be used for future climate assessment was based on the TOPSIS method, technique for order preferences by similarity to an ideal solution (Hwang and Yoon, 1981). TOPSIS is a multi-criteria decision-making approach for sorting alternatives based on a compromise solution. The best alternative is identified as the closest to the positive ideal solution and the farthest from the negative ideal solution. The TOPSIS method is widely used for ranking alternatives and for decision making in water resources management, early warning systems, participatory flood risk management, social learning and consensus achievement among stakeholders (Almoradie et al., 2015; Evers et al., 2018; Yilmaz & Harmancioglu, 2010; Zeyaeyan et al., 2017). It has been increasingly used in the last decade in the field of climatology to select among different datasets (Homsi et al., 2020; Lutz et al., 2016; Raju & Kumar, 2015; Refaey et al., 2019; Senent-Aparicio et al., 2017; Shiru et al., 2019). The backbone of the TOPSIS method is the existence of many alternatives that are ordered based on criteria.

Considering a set of alternatives A_k , $k = 1, \dots, n$, a set of criteria $C_j, j = 1, \dots, m$, x_{kj} the performance ratings of alternative k to criteria j, and w_j the weight attributed to each criteria, the TOPSIS approach consist of the following steps:

Considering a set of alternatives A_k , $k = 1, \dots, n$, a set of criteria $C_j, j = 1, \dots, m$, x_{kj} the performance ratings of alternative k to criteria j, and w_j the weight attributed to each criteria, the TOPSIS approach consist of the following steps:

- Normalization of performance ratings

For criteria to maximise, also called benefit criteria (the larger, the better), the normalized rating r_{kj} is given by:

$$r_{kj}(x) = \frac{x_{kj} - x_j^-}{x_j^* - x_j^-}, \qquad k=1,\dots, n \ ; j=1,\dots, m \tag{3.1}$$

where x_j^* is the aspired/desired level of criteria j and x_j^- its the worst level.

For criteria to minimise or cost criteria (the smaller, the better), the normalized rating is given by:

$$r_{kj}(x) = \frac{x_j^- - x_{kj}}{x_j^- - x_j^*} \qquad (3.2)$$

- Calculation of weighted normalized ratings, $v_{kj}(x)$

$$v_{kj}(x) = w_j r_{kj}(x), \quad k=1,\dots, n \; ; j=1,\dots, m \qquad (3.3)$$

- Derivation of positive ideal solution (PIS) and negative ideal solution (NIS)

Since there is no good and bad alternative, PIS and NIS represent respectively the most preferable and the less desired set of criteria one wish to achieve. PIS and NIS are given by:

$$PIS = \left\{\left(\max_k v_{kj}\,(x) \mid j \in J_1\right), \left(\min_k v_{kj}(x) \mid j \in J_2\right), k = 1, \dots, n\right\} \qquad (3.4)$$

$$NIS = \left\{\left(\min_k v_{kj}\,(x) \mid j \in J_1\right), \left(\max_k v_{kj}(x) \mid j \in J_2\right), k = 1, \dots, n\right\} \qquad (3.5)$$

where J_1 and J_2 are the benefit and cost elements respectively.

- Estimation of separation from the PIS and the NIS.

The separation from the PIS, D_k^+ , and from the NIS, D_k^- can be estimated as Euclidean distance with equations 6 and 7

$$D_k^+ = \sqrt{\sum_{j=1}^{m}\left[v_{kj}(x) - v_j^+(x)\right]^2}, k = 1, \dots, n \qquad (3.6)$$

$$D_k^- = \sqrt{\sum_{j=1}^{m}\left[v_{kj}(x) - v_j^-(x)\right]^2}, k = 1, \dots, n \qquad (3.7)$$

- Derivation of similarities to the PIS

The similarities to the PIS are computed as:

$$C_k^+ = \frac{D_k^-}{D_k^+ + D_k^-} \quad , k = 1, \dots, n \qquad (3.8)$$

- Ordering of alternatives according to the similarities to PIS in a decreasing order.

Finally, the alternatives can be ranked from most preferred to less preferred by ordering C_k^+ in decreasing order.

In this study, daily rainfall and temperature from RCMs are the alternatives and the criteria consist of a set of statistical metrics. These metrics are the Nash–Sutcliffe efficiency (NSE), the coefficient of determination R^2, and two categorical metrics: the probability of detection (POD) and the false alarm ratio (FAR). POD and FAR are specifically applied to rainfall. POD represents the likelihood for RCMs to detect a rainfall event, and the false alarm ratio (FAR) describes the fraction of predicted rainfall event that did not actually happen (Sofiati & Nurlatifah, 2019).

$$NSE = 1 - \frac{\sum_{i=1}^{n}(O_i - S_i)^2}{\sum_{i=1}^{n}(O_i - \bar{O})^2} \qquad (3.9)$$

$$R^2 = \left(\frac{\sum_{i=1}^{n}(O_i - \bar{O})(S_i - \bar{S})}{\sqrt{\sum_{i=1}^{n}(O_i - \bar{O})^2}\sqrt{\sum_{i=1}^{n}(S_i - \bar{S})^2}} \right)^2 \qquad (3.10)$$

where O_i and S_i are respectively observed and model values at time *i*, $\bar{O}$ and $\bar{S}$ are respectively the mean observed and model values, and *n* the sample size.

$$POD = \frac{hits}{hits + misses} \qquad (3.11)$$

$$FAR = \frac{false\ alarms}{hits + false\ alarms} \qquad (3.12)$$

where *hits* is number of rainfall events that are effectively predicted by the RCM, *misses* is the number of observed rainfall events that were not predicted by the RCM, and *false alarms* is the events predicted by RCMs but did not actually occur.

More details on these metrics are provided by Moriasi et al., 2007. All four criteria were weighted equally with weight 0.25 for rainfall, whereas NSE and R^2 were weighted each 0.5 for temperature.

The ranking approach with TOPSIS was applied to both precipitation and temperature datasets at each station location to determine the performance of each RCM in different parts of the catchment. A heatmap was used to visualise at how many locations a given RCM ranked $k^{th}, k = 1, \dots n$. As this study uses 15 RCMs, the heatmap has a 15 by 15 dimension.

The overall performance of each RCM respective to the whole catchment (not at individual station locations) was determined based on their occurrence frequency at different locations. Following the method of Homsi et.al (Homsi et al., 2020), a score is computed using the ranks of RCMs at individual locations and their frequency of occurrence. If a RCM got rank $1,2,3, \dots, n_z$ respectively at $l_1, l_2, l_3, \dots l_z$ locations, the score of that RCM is given by $\sum_z \left(\frac{l_z}{n_z}\right)$. Therefore, the higher the occurrence frequency of a RCM as well as its rank at individual location, the more weight it is assigned and therefore, the higher its overall rank compared to the other RCMs. For instance, if a RCM got rank 1 at p locations, rank 2 at q locations ,…, rank 15 at s locations, then its overall score in the catchment is given by: $\frac{p}{1} + \frac{q}{2} + \cdots + \frac{s}{15}$.

Finally, the most suitable models for making an ensemble are defined as those falling in the upper 50th percentile of all RCMs, for both precipitation and temperature (Homsi et al., 2020; Khan et al., 2018).

3.2.4. Bias correction

To bias-correct the RCMs, the quantile mapping approach, also called the quantile–quantile method or distribution mapping was applied for precipitation and temperature datasets. The quantile mapping was used considering its good results in different climatic zones all over the world (Boé et al., 2007; Das et al., 2022; Luo et al., 2018; Mendez et al., 2020; Pierce et al., 2015; Putra et al., 2020; Soriano et al., 2019; Teutschbein & Seibert, 2012), and in other West African catchments similar to the Mono River Basin (Kwawuvi et al., 2022; Lawin et al., 2019; N'Tcha M'Po et al., 2016; Sarr et al., 2015). Furthermore, previous studies in the Mono River Basin have reported good performances with the quantile method (Batablinle et al., 2018; Djan'na Koubodana et al., 2020; Lawin et al., 2019b). Quantile mapping methods use cumulative distribution functions (CDFs) of observation and historical model data to construct a transfer function used in turn to correct model outputs (Sarr et al., 2015). Generally, in the application of the quantile mapping method, the Gamma distribution (Equation (13)) is used for precipitation and the Gaussian for temperature (Equation (14)) (Teutschbein & Seibert, 2012). We have

$$f_\gamma\left(x_{\alpha,\beta}\right) = x^{\alpha-1} \cdot \frac{1}{\beta^\alpha \cdot \gamma(\alpha)} \cdot e^{\frac{-x}{\beta}} \; ; \; x \geq 0; \; \alpha, \beta > 0, \tag{3.13}$$

where α is the shape parameter and β the scale parameter, and

$$f_N\left(x_{\mu,\sigma^2}\right) = x^{\alpha-1} \cdot \frac{1}{\sigma.\sqrt{2\pi}} \cdot e^{\frac{-(x-\mu)^2}{2\sigma^2}} \; ; \; x \in R, \tag{3.14}$$

with μ and σ the location and scale parameters respectively.

3.2.5. Future Climate Trend Assessment

To visualise the spatial distribution over past and future periods, the kriging interpolation method (Lawin et al., 2019b) was used. The past period is defined as 1966–2015 and the future as 2021–2070. The percentage of change (Equation (15)) was computed to estimate future changes with respect to the past. We have

$$P_V = \frac{V_{proj} - V_{obs}}{V_{obs}} \times 100, \tag{3.15}$$

where, P_V is the percentage of change, V_{proj} is the average value of variable V for the future period, and V_{obs} the average value during observation period.

In addition, the Mann–Kendall test (Mann, 1945) at 95% confidence interval was used to analyze trends in annual rainfall accumulation and mean annual temperature. A positive Z value from the Mann–Kendall test corresponds to an increasing trend (a negative value to a decreasing trend) and a value lower than 1.96 indicates that the trend is statistically not significant. Sens' slope was also computed to estimate magnitudes of increase or decrease.

3.3. Results and discussion

3.3.1. Ranking and Selection of RCMs

3.3.1.1. TOPSIS Results: Best RCM per Location

The TOPSIS analysis provided a ranking of RCMs at the different locations considered across the catchment. Based on the TOPSIS scores presented in Appendix I and Appendix II, the RCMs which ranked first were derived and mapped as shown on Figure 3.2. The spatial distribution of rank 1 RCMs for temperature shows a pattern whereby MPI-CCLM4 predominantly performed best in the south, MPI-REMO in the centre, and CSIRO-RCA4 in the north. As for rainfall, there is no spatial pattern. However, MPI-RCA4 is the most present all over the catchment from north to south. Similar results with spatial pattern were reported by Homsi et.al. (Homsi et al., 2020). The authors noticed a spatial pattern dominated by three GCMs for rainfall, whereas temperature displayed a different distribution of five new GCMs mixed with only one from the bests of rainfall. Spatial patterns in best performing models were also found by Shiru et.al. (Shiru et al., 2019) in Nigeria.

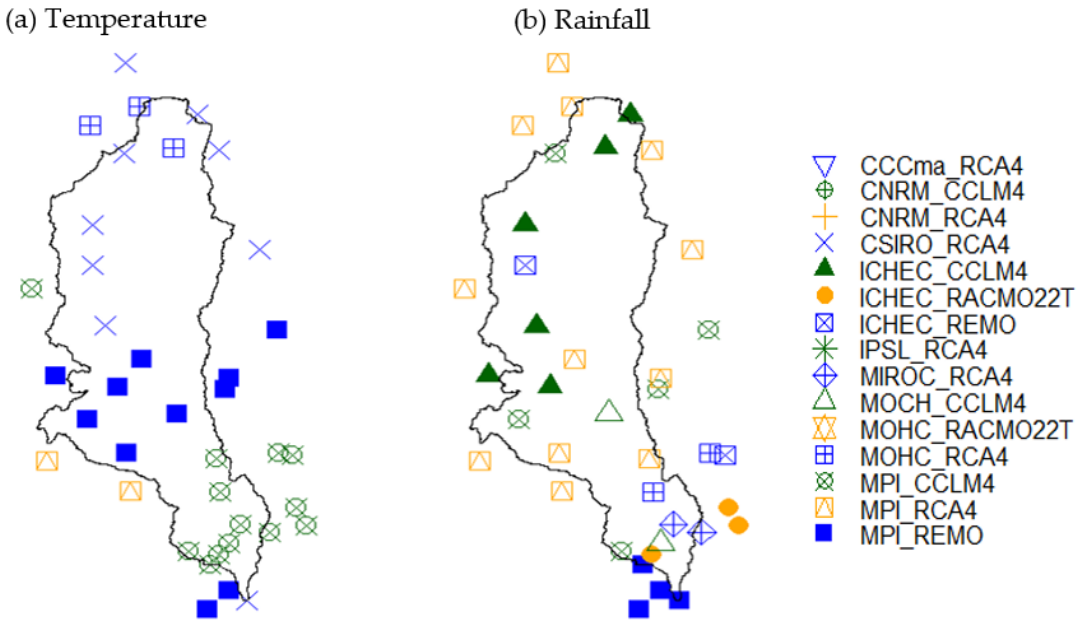

Figure 3.2. Distribution of rank 1 RCMs for (a) temperature and (b) rainfall.

An RCM holding the first position in a certain location does not make it a suitable model at catchment scale because it may perform poorly elsewhere in the study area (Deepthi et al., 2020). Information on the first ranking RCM at an individual location can actually be useful for local studies in different parts of the catchment. Moreover, it points out the fact that RCMs perform differently depending on the climate variable and from one location to another. For example, MPI-CCLM4 ranked first in most areas of the southern part for temperature but came first only at one location for rainfall. Nonetheless, the model performed relatively well, occupying rank 2 at 13 locations (Figure 3.3-b).

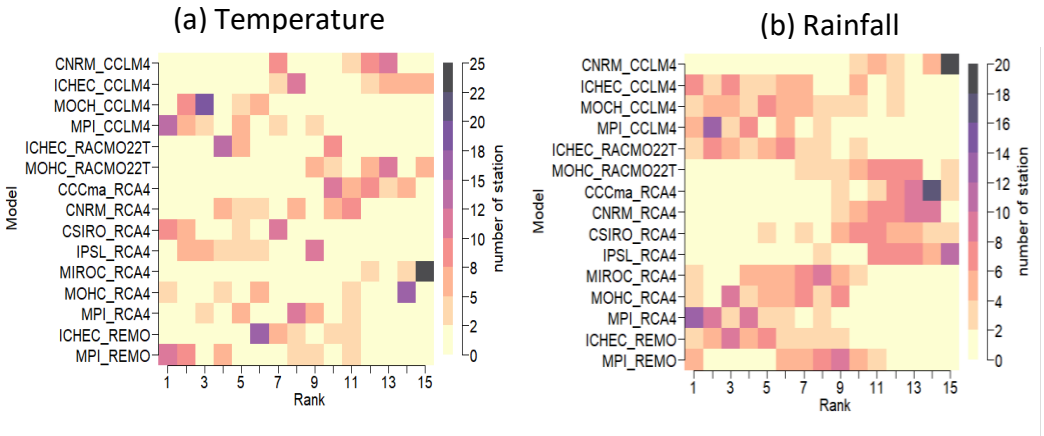

Figure 3.3. Ranks of RCMs all over the study area.

Figure 3.3-a,b are heatmaps displaying the number of times (at how many locations) a given RCM occupied a certain rank. The darker the colour of a cell, the higher the number of stations where an RCM occupies the rank corresponding to the cell. For instance, for temperature (Figure 3.3-a), MIROC-RCA4 occupied rank 15 at 25 stations of 38. Likewise, Figure 3.3-b shows that CNRM-CCLM4 occupied rank 15 at 20 locations over the 38 stations considered, and similarly, CCCma-RCA4 and IPSL-RCA4 occupied only rank 8 onward, making these three RCMs the ones with lowest performances for rainfall.

3.3.1.2. RCMs Selection

Table 2.2 presents the overall ranking of RCMs for rainfall and temperature in the Mono catchment. RCMs perform differently vis-à-vis the two variables, e.g., MPI-RCA4 ranked first for rainfall and has rank 6 for temperature. Finally, to make the ensemble of models to be used for future climate assessment, only RCMs whose ranks simultaneously fall within the range 1–8 for both temperature and rainfall are selected. These are six RCMs, highlighted in bold in Table 2: MPI-RCA4, MPI-CCLM4, ICHEC-RACMO22T, MOHC-CCLM4, MOHC-RCA4, and MPI-REMO. All three RCMs driven by the MPI global model are part of the final list. In fact, good performances of the MPI GCM have been reported in other catchments in Benin and Togo (Badou et al., 2018; Kwawuvi et al., 2022; Lawin, Hounguè, M'Po, et al., 2019) and in the Mono River Basin (Amoussou et al., 2020; Lawin, Hounguè, Biaou, et al., 2019). Because boundary conditions of RCMs are provided by their driving GCMs (Gbode et al., 2021), the high ranking of MPI-driven RCMs indicates that those RCMs may better represent local climate in the Mono catchment.

Table 3.2. Overall ranking of RCMs for rainfall and temperature

Rank	Rainfall		Temperature	
	Model	Score	Model	Score
1	**MPI-RCA4**	20.23	**MPI-CCLM4**	19.99
2	**MPI-CCLM4**	15.59	**MPI-REMO**	18.21
3	ICHEC-CCLM4	12.40	CSIRO-RCA4	16.03
4	**ICHEC-RACMO22T**	11.39	**MOHC-CCLM4**	12.6
5	ICHEC-REMO	11	IPSL-RCA4	8.68
6	**MOHC-CCLM4**	9.67	**MPI-RCA4**	8.06
7	**MOHC-RCA4**	9.02	**MOHC-RCA4**	7.18
8	**MPI-REMO**	8.73	**ICHEC-RACMO22T**	6.95
9	MIROC-RCA4	7.89	CNRM-RCA4	5.79
10	CSIRO-RCA4	3.96	ICHEC-REMO	5.09
11	MOHC-RACMO22T	3.77	ICHEC-CCLM4	4.05
12	CNRM-RCA4	3.41	CNRM-CCLM4	3.94
13	IPSL-RCA4	3.08	CCCma-RCA4	3.54
14	CCCma-RCA4	2.97	MOHC-RACMO22T	3.20
15	CNRM-CCLM4	2.94	MIROC-RCA4	2.76

However, an RCM driven by a certain GCM that performs well does not guarantee good results of the GCM–RCM model because biases in models arise from both RCM and the driving GCM (Amoussou et al., 2020). Furthermore, all four types of RCM in the initial list of models considered in this study (RCA4, CCLM4, RACMO22T, and REMO) are actually represented in the final list of shortlisted models. Because models' performances are region- and variable-specific, composing the average ensemble with models that performed well for the two climate variables under consideration and over the entire catchment, increases the opportunity to capture actual climate patterns in the study area. In fact, model ensembles improve on individual models performances and even outperform them (Gbobaniyi et al., 2014; Kwawuvi et al., 2022).

3.3.2. Assessment of Future Climate

The evaluation of future climate state is based on the mean ensemble of the six best performing RCMs identified above. The mean of those RCMs was computed for temperature and for rainfall to make the ensemble for each variable. The evaluation was conducted through visualisation of variables' spatial distribution, quantification of relative changes, and annual trend assessment.

3.3.2.1. Temperature

Figure 3.4 presents the spatial distribution of average annual temperature for the observation period 1966–2015, and for the future period 2021–2070 under climate scenarios RCP 4.5 and RCP 8.5. An increase of temperature is expected all over the catchment, but more specifically in the northern part and in the downstream area (south) (Figure 3.4-b,c). However, RCP 8.5 projects warmer conditions than RCP 4.5.

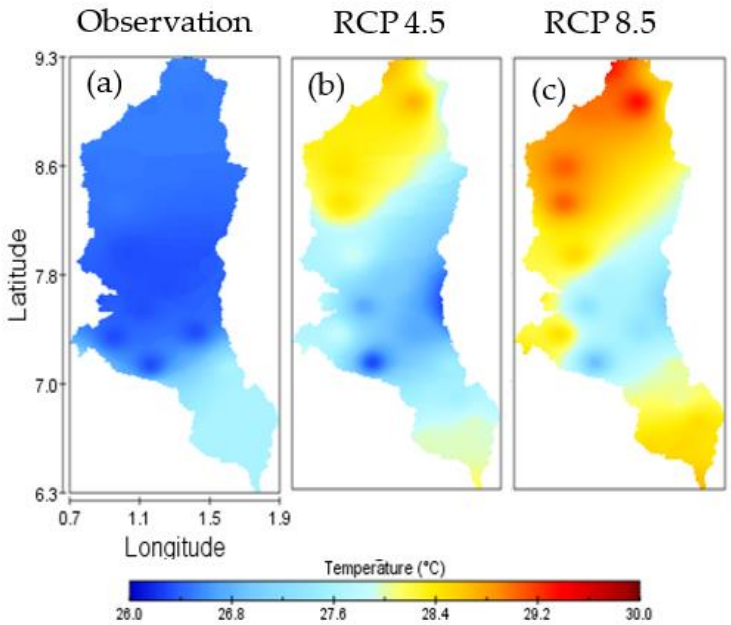

Figure 3.4. Spatial distribution of mean annual temperature for the past 1966–2015, and for future scenarios 2021–2070

The increase in temperature is also depicted by the annual trend 1966–2070 as shown in Figure 3.5.

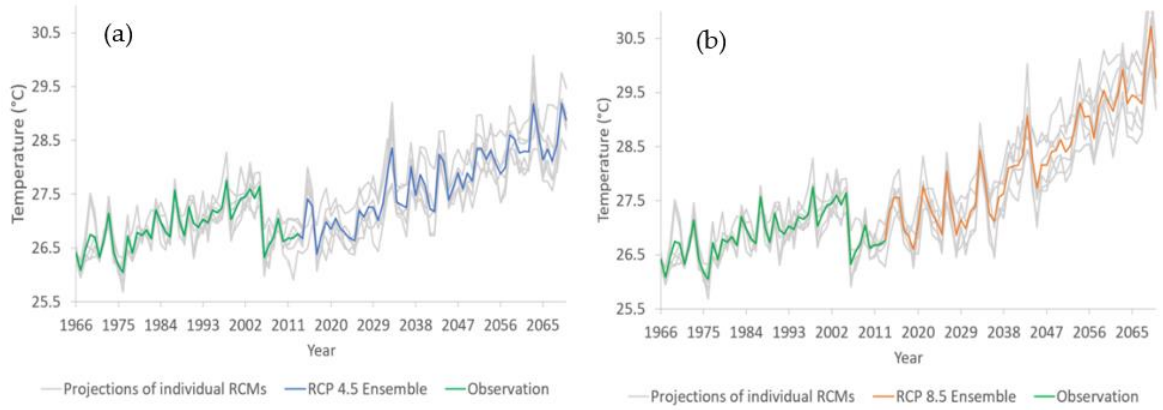

Figure 3.5. Trend of annual temperature 1966–2070 (a) RCP 4.5 and (b) RCP 8.5

From an average annual temperature of 26.9 °C during the period 1966–2015, it is expected to reach 27.8 °C under RCP 4.5 and 28.4 °C for RCP 8.5. Thus, the increase of average annual temperature over the Mono catchment during the period 2021–2070 is estimated to be 1 °C and 1.5 °C under the medium and high pathway scenarios used in this study. This is supported by the Mann–Kendall test and Sens' slope results presented in Table 3.3.

Table 3.3. Results of Mann–Kendall and Sens' slope tests on annual temperature.

Scenario	Z Statistics	*p*-Value	Sens' Slope
RCP 4.5	6.67	0.00	0.04
RCP 8.5	7.81	0.00	0.06

The results are in line with the graphical observation and confirm that the trend in future temperature is statistically significant with 95% confidence. Moreover, the Sens' slope values indicate that annual temperature will increase by 0.04 °C every year based on the scenario RCP 4.5 and 0.06 °C according to projections by RCP 8.5. Overall, there is an agreement of both scenarios on the trend of temperature in the Mono catchment for the future period 2021–2070. Regardless of the models used, previous studies in the Mono catchment have also reported an increase of temperature at horizon 2050 up to 2100 (Djan'na Koubodana et al., 2020; Lawin, Hounguè, Biaou, et al., 2019; Lawin, Lamboni, Manirakiza, et al., 2019). Similar trends are also found across Africa (Bokhari et al., 2018; Macadam et al., 2020; Niang et al., 2014) and are in line with global patterns predicted by the IPCC (IPCC, 2018).

3.3.2.2. Rainfall

Figure 3.6 shows the changes in annual rainfall distribution over the Mono river catchment from 1966–2015 to 2021–2070. Figure 3.6-b,c display similar changes for both RCP 4.5 and RCP 8.5.

The western and north-western parts of the catchment are expected to receive less precipitation in the future, whereas the east central part and the downstream area close to the outlet might experience an increase of annual precipitation. The central part is a mountainous region; thus, the increase may be due to local orographic terrain (Amoussou et al., 2020). As for the downstream area, it is located near the coast where evaporation and cloud formation above the Atlantic ocean may induce the increase of precipitations (Gbode et al., 2021; Lee et al., 2020).

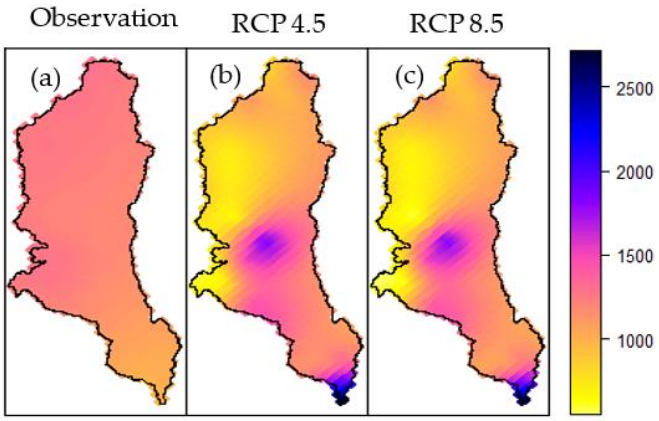

Figure 3.6. Spatial distribution of mean annual rainfall for the past 1966–2015 and future scenarios 2021–2070

However, as reported by Lischeid et.al. (Lischeid et al., 2021), trend analysis in climate change studies may be affected by artefacts in local data. The authors analysed trends of water level and groundwater head data in Northeast Germany and found that the apparent inconsistent trends observed could be attributed to low-pass filtering of the groundwater recharge signal. As reported in the fourth assessment report of the IPCC, artefacts in the models' data are addressed for instance with low-pass filters but may still persist at local scale (IPCC, 2007).

Overall, average annual rainfall over the Mono catchment depicts high interannual variabilities as shown in Figure 3.7.

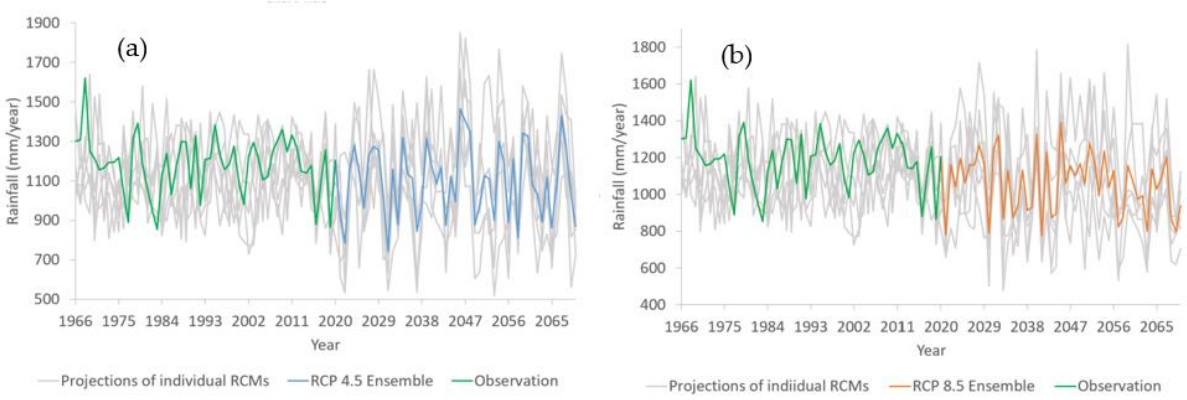

Figure 3.7. Trend of annual rainfall 1966–2070 (a) RCP 4.5 and (b) RCP 8.5

Based on the climate change scenarios, the average total rainfall per year for the future period will be 1091 mm for RCP 4.5 and 1053 mm for RCP 8.5. With both scenarios, the mean annual rainfall is expected to be less than the 1195 mm recorded during 1966–2015. The minimum annual rainfall for the next five decades is expected to be lower (697 mm for RCP 4.5 and 757 mm for RCP 8.5) than the minimum recorded during the past 50 years (854 mm). The high interannual variability observed graphically was confirmed by the Mann–Kendall test (Table 3.4). The results show no statistically significant trend (*p*-values > 0.05), whereas the Sens' slope estimator indicates an average increase (decrease) of 0.1 mm (2.94 mm) per year with the scenario RCP 4.5 (RCP 8.5) during the period 2021–2070.

Table 3.4. Results of Mann–Kendall and Sens's slope tests on annual rainfall

Scenario	Z Statistics	*p*-Value	Sens' Slope
RCP 4.5	0.03	0.97	0.1
RCP 8.5	−1.54	0.12	−2.94

Such high variability and insignificant trend in annual precipitation have been reported in previous studies (Djan'na Koubodana et al., 2020; Lawin, Hounguè, Biaou, et al., 2019) in the Mono catchment. Moreover, the mean annual cycle indicates changes in seasons and in monthly precipitations (Figure 3.8).

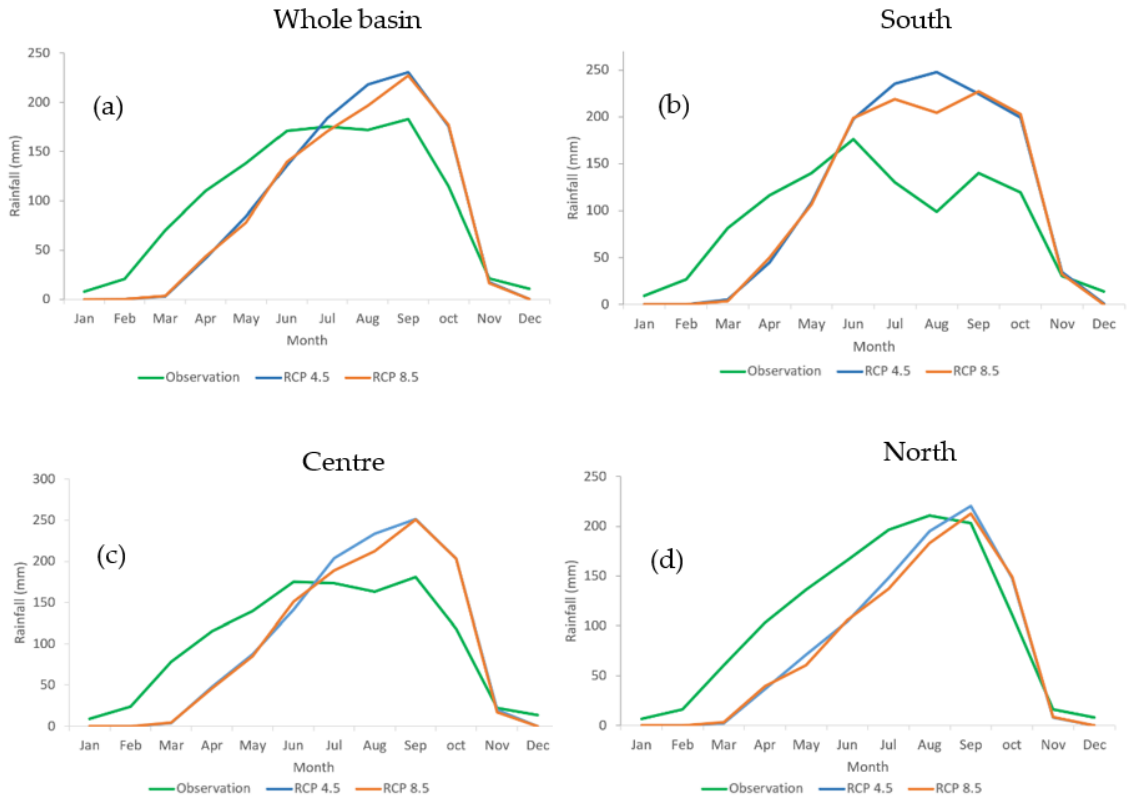

Figure 3.8. Rainfall annual cycles over the catchment

Overall, the start of the rainy seasons is likely to be delayed all over the catchment. For instance, the first rainfall events that usually occur in March in the south, are likely to shift in April based on the projections by RCP 4.5 and RCP 8.5. Moreover, the amounts of rainfall recorded in April and May in the past are expected to decrease in the future, according to the climate change scenarios. The bimodal rainfall cycle in the south will become "transitional" under the scenario RCP 4.5 and unimodal under RCP 8.5, whereas the central part will shift to a unimodal regime in the future. Such changes would lead to modifications in the agricultural calendar of the concerned agro-ecological zones and can be detrimental for crop production and for food security.

There is an increase of peaks during rainy seasons and a decrease of precipitation during the dry season. Therefore, rainy seasons may become wetter and dry seasons dryer compared to the past. Receiving higher amounts of precipitation during a shorter period of time will translate into rainfall intensification which may increase flood risk and the probability of extreme events in the area (Soriano et al., 2019). The percentage of future changes in the annual cycle with respect to the past is presented in Figure 3.9.

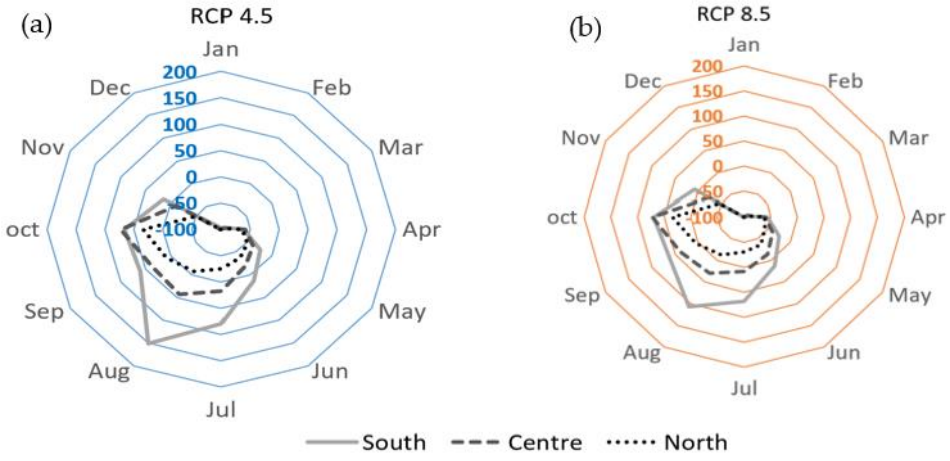

Figure 3.9. Relative change of monthly rainfall under climate scenarios

Figure 3.9 indicates that highest increases are expected in the south during July and August and more specifically in August where a greater than 100% increase was found. These projections need to be given attention because the period of July and August in the southern part is usually characterised by a rainfall cessation time during which farmers harvest and prepare the land for the second sowing season of the year (FAO, 2020). Furthermore, the highest decreases of precipitation, 93–100%, are expected to occur from December to March all over the catchment. In the north, almost all months, except September and October, showed a reduction of rainfall amounts.

Historically, the Mono catchment experiences recurrent flood events (Ntajal, Lamptey, Mianikpo, et al., 2016). Nonetheless, considering the potential decrease of rainfall (even statistically not significant), the increase of temperature discussed above, and the changes in future land use/cover mainly characterized by a "savannification" of forests and agricultural lands (Thiam et

al., 2022), drought-related studies should be undertaken alongside flood assessments in the Mono river catchment.

3.4. Conclusion

This study assessed future climate conditions in the Mono River Basin by using the TOPSIS multicriteria decision method to identify best-performing regional climate models. RCMs were ranked based on four statistical and categorical metrics (NSE, R^2, POD, FAR) applied at 38 measurement stations. Finally, six RCMs were selected out of the initial list of 15 to make an ensemble that is further used to evaluate potential changes in future climate by 2070 and under climate change scenarios RCP 4.5 and RCP 8.5. Both scenarios suggest a 1 to 1.5 °C increase of annual temperature in the catchment, especially in the northern and southern parts. On the other hand, a statistically insignificant decreasing trend was found in annual precipitation. The seasonal cycle of rainfall during the period 2021–2070 will be characterized by shorter rainy seasons and an increase of precipitation. This intensification of rainfall may exacerbate existing flood risks in the Mono River Basin. However, the compound effect of temperature rise, dry season prolongation and land use/cover changes may introduce drought as a major hazard in the study area in addition to floods. Moreover, the concordance between the results of the two climate change scenarios used indicates a relatively high possibility that the projections actually occur. Nevertheless, the possibilities of potential artefacts in models can be investigated and addressed by future studies in the Mono catchment. The findings of this study should be furthered by assessing the impact of the projected changes on flood, drought, agriculture, and health to support decision making and the identification of appropriate adaptation measures.

4. Climate and land use change impacts on flood hazards in the Mono River Catchment in Benin and Togo[3]

Abstract

Flooding is prominent in west Africa and are expected to exacerbate due to global changes. This study assessed the impact of future climate and land use changes on flood hazards in the Mono river catchment of Benin and Togo. Climate scenarios from the representative concentration pathways, RCP 4.5 and RCP 8.5, and land use projection at the horizon 2070 were used for runoff simulation at the Athiémé outlet, and flood mapping in the lower Mono river basin. The planned Adjarala dam was also simulated to evaluate its potential impact. The Soil and Water Assessment Tool (SWAT) was used to investigate the impact of the projected changes on runoff, while flood water extent was simulated using the two-dimensional TELEMAC-2D model. TELEMAC-2D was validated with satellite observation and in a participatory way with local stakeholders. SWAT showed good performance during the calibration (KGE=0.83) and validation (KGE=0.68) steps. Results show an increase of the magnitude of flood extremes under future climate and land use change scenarios. Events of 10-years return periods during 1987-2010 are expected to become 2-years return period events under the climate and land use change scenarios considered. The planned Adjarala dam showed potentials for extreme peaks and flood extent reduction. However, flow duration curves revealed that the discharge of the river during low flow periods may also be reduced if the Adjarala dam is built. Adaptation measures as well as sustainable land use and dam management options should be identified to alleviate the projected changes.

Keywords: Flood hazard, Mono river catchment, Climate change, Land use change, SWAT, TELEMAD-2D

[3] This chapter (4) was originally published as: Houngue, N. R., Almoradie, A. D. S., Thiam, S., Komi, K., Adounkpè, J.G., Begedou, K., & Evers, M. (2023). Climate and land use change impacts on flood hazards in the Mono River Catchment in Benin and Togo. *Sustainability*, 15. https://doi.org/10.3390/su15075862

4.1. Introduction

The compound effect of climate change and land use/land cover change jeopardizes human security around the world (Adger et al., 2014; Vivekananda, 2022). It has been established that the trends of precipitation and temperature observed since the 1950s are imputable to human-induced climate change (Trisos et al., 2022). With a 50% increase of built-up area, 11.5% increase of croplands, and 2.4% decrease of forest area from 2000 to 2020, the global state of land use and land cover has substantially changed over the past decades (Potapov et al., 2022). Acting in a feedback loop, changes in land use and climate conditions affect the water cycle, and exacerbates hydrological hazards including floods, landslides, and droughts (Collins et al., 2013; Piao et al., 2007). Furthermore, the magnitude and frequencies of those events are expected to increase in the coming decades.

However, there are uncertainties about the potential trends and patterns of these hazards in the future. According to the 6th assessment report of the Intergovernmental Panel on Climate Change (IPCC, 2021b), heavy precipitation and flooding are expected to intensify and be more frequent in most parts of Africa. In addition, the continent is expected, with medium confidence, to experience hydrological droughts. However, precipitation indices in west Africa show mixed patterns with few statistically significant trends (Barry et al., 2018). The projected changes in heavy precipitation over west Africa have low confidence due to data scarcity and limited evidence (Callaghan et al., 2021; IPCC, 2021b; Maidment et al., 2015). Moreover, the uncertainty array is further widened with potential uncertainties from climate and hydrological models (Moges et al., 2021; Pechlivanidis et al., 2017). Therefore, local and regional studies are needed to establish area-specific hazard profiles and to accordingly support decision making.

During the disastrous flood event of 2010 that caused about USD 300 million of loss and damages in Benin and Togo, intense precipitations and the overflow of the Mono river were pointed out among other causes (UNDP, 2010; WB & UNDP, 2011). Recent studies reported the increasing trend of temperature and above-normal precipitation over the past 50 years, in the Mono river catchment shared by Benin and Togo (Amoussou, 2010; Lawin, Lamboni, et al., 2019). In addition, the lower part of the catchment is prone to higher risks of flooding (Kissi et al., 2015; Ntajal, Lamptey, Sogbedji, et al., 2016). Wetzel et. al. (Wetzel et al., 2022) findings on flood vulnerability in the Lower Mono River Basin (LMRB) identified that poverty is a relevant driver of vulnerability that is strongly influenced by insufficient income generated through agriculture. Moreover, the study also identified that critical infrastructure that includes streets and buildings used as flood shelters as well as storage facilities (mainly for agricultural products) are relevant exposed elements. Extreme precipitation events in the Mono catchment are expected to become more frequent in the future (Amoussou et al., 2020; Houngue et al., 2022), despite the ambiguous projected trends (Batablinle et al., 2018; Batablinlè et al., 2019). To the horizon 2050, precipitations in the Mono catchment are expected to be characterised by high interannual variabilities, changes in seasons, and a mixture of above and below normal precipitations compared to the period 1981-2010 (Djan'na Koubodana et al., 2020; Lawin, Hounguè, Biaou, et al., 2019). Furthermore, the future land use and land cover (LULC) in the Mono catchment is

expected to be characterised by a decrease of forests, and an expansion of settlement and built-up areas (Koubodana et al., 2019; Thiam et al., 2022). Moreover, the two riparian countries intend to build a joint dam, the Adjarala dam, on the Mono river for hydropower energy production, flood protection and for agricultural purposes (CNEE, 2014).

Considering the past and projected changes in the Mono river catchment, this study aims to assess the impact of climate and LULC changes, as well as the influence of the forthcoming Adjarala dam on flood hazards in the lower part of the catchment. Climate change data from the representative concentration pathways RCP 4.5 and RCP 8.5, LULC maps and the Adjarala dam information were used for future runoff simulation and, ultimately, for flood mapping. Discharge simulations were performed with the Soil and Water Assessment Tool (SWAT), whereas flood modelling was carried out with the TELEMAC-2D model. The novelty of this study resides in the integrated runoff-flood modelling that was carried out, the assessment of climate and land use change impacts, and the simulation of the Adjarala dam.

4.2. Materials and Methods

4.2.1. The study area

Located between latitudes 6.28◦ N and 9.39◦ N and longitudes 0.62 ◦E and 1.99 ◦E, the Mono river catchment extends over the territories of Benin and Togo Republics (Figure 4.1). It has a surface area of 23,736.64 km2 and hosts the hydroelectric dam of Nangbéto.

The climate is sub-equatorial in the south and tropical in the northern part of the catchment. Main economic activities in the study area are small-scale farming, livestock breeding, fishing and trading. Average annual temperature recorded over the past 30 years ranges between 26°C and 28°C, with an average annual precipitation of 1200mm. Land use and land cover types in the catchment are predominantly savannah, forest, croplands, settlements and water bodies. In this study, the entire Mono river catchment was used for hydrological modelling whereas only the portion of the river located downstream of the Nangbéto dam, and designated as Lower Mono River (LMR), was considered for flood hazard mapping with a hydrodynamic model. The downstream of the catchment is characterized by low elevation and flat lands which favors the persistence of flood events in the area. The main economic activities in the Mono catchment are agriculture, fisheries, livestock breeding and trade.

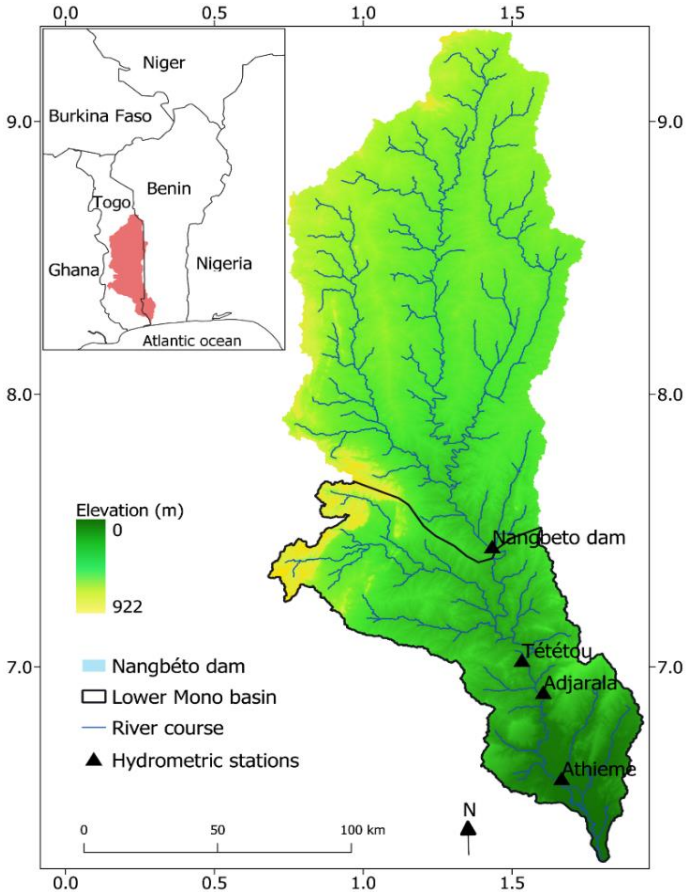

Figure 4.1. Map of study area

4.2.2. Data

4.2.2.1. Hydro-climatic data

Precipitation and minimum and maximum temperature were collected for the period 1967-2010. Precipitation data was taken at 38 gauging stations and temperature from 3 synoptic stations. These observation data were provided by met services of Benin and Togo (METEO-Benin, DGMN-Togo). In addition, future precipitation and temperature data excerpted from the Coordinated Regional Downscaling Experiment (CORDEX) database, https://esgf-data.dkrz.de/projects/esgf-dkrz/https://esgf-data.dkrz.de/projects/esgf-dkrz/, were used. The period 2021-2070 was considered and the Representative Concentration Pathways (RCP) scenarios RCP 4.5 and RCP 8.5 were used for future projections. Processed and ready-to-use climate model data for future projection were provided by Houngue et.al (Houngue et al., 2022) who systematically selected 6 Regional Climate Models (RCM) that were found to be the best performing in the Mono river basin. The 6 RCMs are presented in Table 4.1.

Table 4.1. List of regional climate models used

RCM	Institute	Driving model	Designation
CCLM4-8-17	Climate Limited-area Modelling Community (CLMcom)	MOHC-HadGEM2-ES	MOHC-CCLM4
CCLM4-8-17	Climate Limited-area Modelling Community (CLMcom)	MPI-M-MPI-ESM-LR	MPI-CCLM4
RACMO22T	Royal Netherlands Meteorological Institute (KNMI)	ICHEC-EC-EARTH	ICHEC-RACMO22T
RCA4	Swedish Meteorological and Hydrological Institute (SMHI)	MOHC-HadGEM2-ES	MOHC-RCA4
RCA4	Swedish Meteorological and Hydrological Institute (SMHI)	MPI-M-MPI-ESM-LR	MPI-RCA4
REMO2009	Helmholtz-Zentrum Geesthacht, Climate Service Center, Max Planck Institute for Meteorology (MPI-CSC)	MOHC-HadGEM2-ES	MPI-REMO

Potential evapotranspiration (PET) was computed using the Hargreaves method (Hargreaves & Samani, 1985). The Hargreaves method (Equation 4.1) is temperature-based and recommended when climate data are limited.

$$E_0 = 0.0023 \times H_0 \times (T_{max} - T_{min})^{0.5} \times (T_{mean} + 17.8) \quad (4.1)$$

where E_0 is PET (mm/day), H_0 is extra-terrestrial radiation (MJ/m2/day), T_{max} is the maximum air temperature for a given day (°C), T_{min} is the minimum air temperature of the day (°C), and T_{mean} is the mean air temperature of the day (°C).

Runoff data and rating curves were provided by water directorate of Benin, DGEau-Benin, and the management of the Nangbéto dam (Centrale Electrique du Bénin, CEB) at 3 stations: Athiémé (1964-2010), Nangbéto (1987-2019) and Tététou (1965-1991). Runoff data were used for model calibration and validation.

4.2.2.2. Land use and land cover (LULC) maps

LULC maps from the past, 1986, and the future 2030, 2050 and 2070 were used (Figure 4.2) as input for runoff simulation. The maps were taken from the study of Thiam et.al (Thiam et al., 2022). Thiam et.al, 2022 performed past land use classification and future land use modelling using machine learning, a participatory approach with stakeholders' perspective on land use scenarios, and the CA-Markov chain model embedded in the Land Change Modeler (LCM) of IDRISI

software. The LULC maps present 5 classes: savanna, forest, water bodies, settlement and cropland. The authors used the map of 2020 as reference to check the accuracy of the projections.

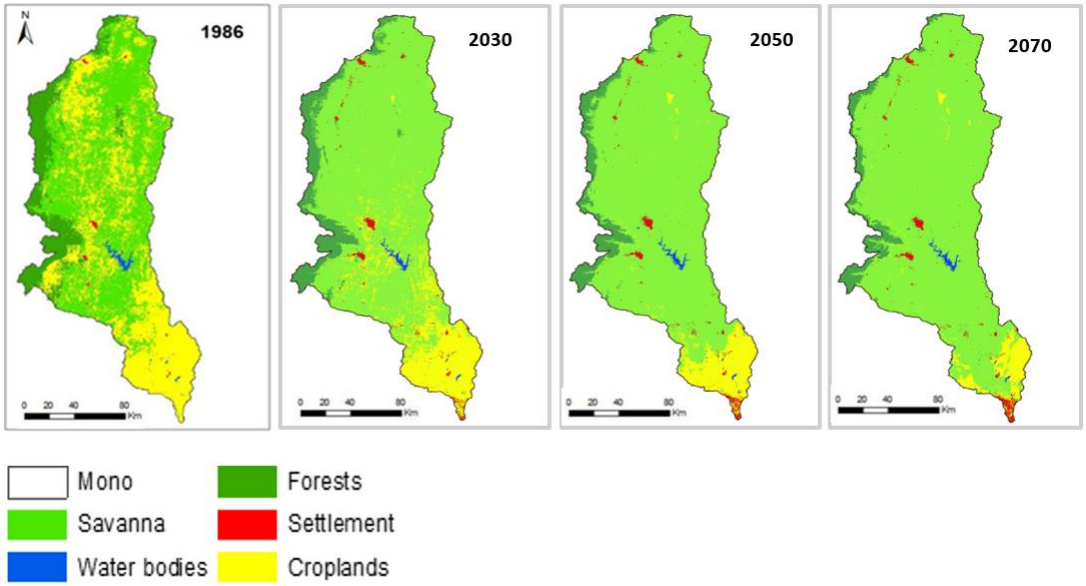

Figure 4.2. LULC maps by Thiam et al. 2022

An classified LULC map of 2020 was compared to the one generated by the Land Change Modeler (simulated LULC map 2020). Good results were observed: Kappa Index Agreement resulted in a Kappa for no information (Kno) of 0.91, a standard Kappa (Kstandard) of 0.89, and a Kappa for grid-cell level location of 0.95 (Klocation). The LULC maps from 1986-2070 indicate a reduction of croplands and forests while savanna and settlements are expected to keep increasing in the Mono river basin. Forest areas showed 58% decrease, while settlements and built-up areas are expected to undergo a 384.47% increase. Land use and land cover changes in the Mono catchment are mainly driven by rapid population growth, overexploitation of lands, cites' expansion and rainfall variability (Koubodana et al., 2019; Thiam et al., 2022).

4.2.2.3. Soil data

Soil map (Figure 4.3) was derived from the Harmonized World Soil Database (HWSD) v1.2 of the Food and Agriculture Organisation of the United Nations (FAO) https://www.fao.org/soils-portal/data-hub/soil-maps-and-databases/harmonized-world-soil-database-v12/en/ and provides, among others, information on soil textures. Soil textures in the catchment comprise clay, loam and sandy-clay-loam. The map has a 30 arc second resolution, about 1 km, and serves as the basis in the SWAT model for soil parameters (soil bulk density, water storage capacity, and hydraulic conductivity) computation using pedotransfer functions.

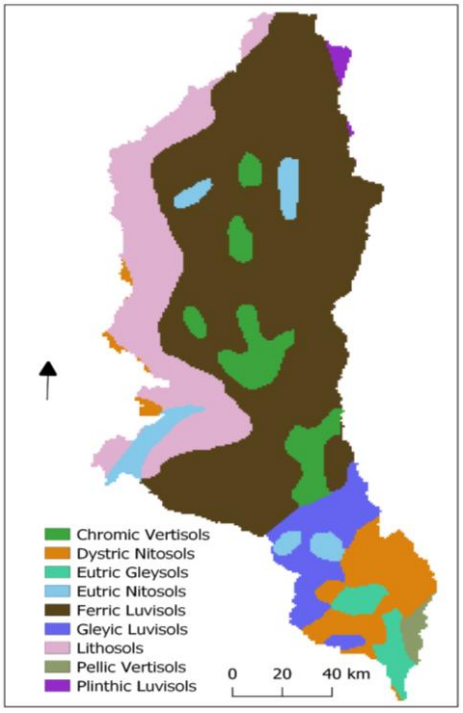

Figure 4.3. Soil map

The catchment is dominated by Luvisols, occupying 61.58% of the surface area. Luvisols are characterised by a higher proportion of clay in the subsoil than in the surface (IUSS Working Group WRB, 2006). They have a sandy clay loam texture. The western part of the catchment, hosting the high elevations areas, is made of Lithosols which cover 17.06% of the catchment area. Lithosols are usually found in mountainous regions and are characterised by rocky, gravelly or stony soils (IUSS Working Group WRB, 2006; Laplante, 1959). The rest of the catchment is made of Nitosols, Vertisols, and Eutric Gleysols, covering respectively 11.26%, 7.44% and 2.47% of the catchment area. The Vertisols have a clay texture, while Nitosols and the Eutric Gleysols are mainly made of loam.

4.2.2.4. Digital Elevation Model (DEM)

Digital surface model from the Advanced Land Observing Satellite (ALOS) provided by the Japan Aerospace Exploration Agency (JAXA) was used for elevation information. ALOS data has 1 x 1 arc second (about 30 m) resolution and displays height about sea level. As shown on Figure 4.1, elevation in the Mono catchment ranges from 0 to 922 m, with highest elevations located in the western and northern parts, while the downstream in the south hosts the lowest elevations (Figure 4.1).

4.2.2.5. Reservoirs data

Two reservoirs were taken into account in this study: the reservoir of the existing Nangbéto dam and that of the upcoming Adjarala dam. The Adjarala dam is located 100 km downstream of Nangbéto dam. The characteristics of these reservoirs are presented in Table 4.2.

Table 4.2. Reservoirs characteristics

Dam parameter	Description	Unit	Value at Nangbéto	Value at Adjarala
MORES	Month the reservoir became operational		September	January
IYRES	Year the reservoir became operational		1987	2022
RES_ESA	Reservoir surface area when the reservoir is filled to the emergency spillway	ha	18000	9500
RES_EVOL	Volume of the water needed to fill the reservoir to the emergency spillway	10^6 m^3	1715	630
RES_PSA	Reservoir surface area when the reservoir is filled to the principal spillway	ha	4200	8260
RES_PVOL	Volume of the water needed to fill the reservoir to the principal spillway	10^6 m^3	373.5	523
RES_VOL	Initial reservoir volume	10^6 m^3	373.5	523

Source: CNEE, 2014; HOUESSOU, 2016

The reservoir of the Nangbéto dam was represented as an existing reservoir while the reservoir of Adjarala was simulated as a “scenario”, since the dam is not yet operational.

4.2.2.6. Cross-sections

A good representation of river bathymetry is needed to adequately model the water flow in a river section. Cross-sections can be derived from field measurements and if field measurements are not available or possible due to resource constraints, cross-sections can be extracted from DEM. However, caution should be observed when using DEM for cross-section because of the resolution and errors on bed elevation due to uncorrected water surface elevation. Due to COVID-19 travel restrictions, the fieldwork cross-section measurement did not proceed according to what was initially planned. With this, cross-sections were derived by extracting the river bed elevation from the DEM and were corrected using the slope-area method supported by a 1D river model. ArcGIS with the HEC-GeoRAS and HEC-RAS 1D model was used as a tool to derive cross-sections since these data were not available. The method behind is elaborated on in section 4.2.6.1. Seventy-seven (77) cross-sections were derived having their locations identified following the criteria of changes in width and slope and areas with meanders or bends.

4.2.3. River runoff simulation

The Soil and Water Assessment Tool (SWAT) is a physically-based hydrological model for water quality and quantity simulation. The water balance in SWAT is based on equation 4.2 (Arnold et.al, 2012).

$$SW_t = SW_o + \sum_{i=1}^{t}\left(R_d - Q_{surf} - ET_a - W_{perc} - Q_{gw}\right) \quad (4.2)$$

where SW_t is the final soil water content; SW_o the initial soil water content; R_d the amount of precipitation, S_{surf} the surface runoff, ET_a the evapotranspiration, W_{perc} the percolation, and Q_{gw} the amount of return flow on day *i*.

SWAT has successfully been used with good results in various west African catchments (J Schuol & Abbaspour, 2006) such as the Niger basin (Badou et al., 2018; Begou et al., 2016), the Volta basin (AMPOFO et al., 2021; Awotwi et al., 2015) and the Ouémé basin in Benin (Bossa et al., 2014; Hounkpè et al., 2019). Koubodana et.al, (Koubodana et al., 2020) applied SWAT in the Mono River catchment and reported good results as well.

As a semi-distributed model, SWAT splits the catchment into sub-basins that are further divided into hydrological response units (HRU). An HRU is a unique combination of land use, soil type and slope. HRU are the computation units in SWAT (Adnan et al., 2019). For the Mono river catchment, 153 sub-basins and 552 HRUs were derived.

The impacts of climate and LULC changes on the runoff of the Mono river, was evaluated over the period 2022-2070. In order to account for the continuous LULC change in the catchment the LULC map of 2030 was used for the period 2022-2030, the map of 2050 for the period 2031-2050, and the map of 2070 for 2051-2070.

This study used the sequential uncertainty fitting, SUFI-2, embedded in the calibration and uncertainty programs, SWAT-CUP v5.1.6, for calibration, sensitivity analysis and uncertainty analysis. One specificity of SWAT-CUP is that its calibration parameters are not assigned single values, rather, intervals are defined. This approach accounts for the uncertainties in the definition of parameters value, because nothing like a unique perfect set of parameters exists (K. C. Abbaspour, 2015). For that purpose, a 95% prediction uncertainty (95PPU) is calculated at the 2.5% and 97.5% levels of the cumulative distribution of the output variable obtained through Latin Hypercube sampling.

The calibration and validation periods were identified based on the available data, the peak flow events and the construction of the Nangbéto dam. Discharge data in the Mono river catchment is characterised by a substantial level of missing, especially after the construction of the Nangbéto dam in 1987. From 1967-2010, 28% of discharge records are missing, out of which 72% are in 1988-2010 and occurred mainly during the high flow period April-October. Since the focus of this

study is on flood events, only years with no more than 30% missing between April-October were used. These are 1964-1986, 1988, 1989, 1990, 1991, 1992 and 2010. The first 3 years, 1964-1966 were used as warm-up period. As recommended, the different hydrological events in the study area should be accounted for during both calibration and validation phases, and the mean and standard deviation should be similar during the two periods (Abbaspour, 2020). In that regard, the calibration period was made of the years 1967-1977, 1990, 1991, 1992, and the model was validated on 1978-1986, 1988, 1989 and 2010. The two periods contain years before and after the construction of the dam as well as low and high peaks. The mean discharge values during calibration and validation are 106.40 m^3/s and 111.38 m^3/s respectively, while the standard variations are 177.15 m^3/s and 170.40 m^3/s.

Thirteen (13) calibration parameters were selected based on previous studies in Benin and Togo (Badou et al., 2018; Hounkpe, 2016; Djan'na Koubodana et al., 2021), and in the west African region (Poméon et al., 2018; Jürgen Schuol, Abbaspour, Srinivasan, et al., 2008; Jürgen Schuol, Abbaspour, Yang, et al., 2008). The Global Sensitivity program embedded in SWAT, was used to assess the sensitivity of the parameters after a 1000-runs simulation. Table 4.3 presents the list of parameters, their ranking based on the sensitivity analysis, and the ranges used. The goodness-of-fit between simulation and observation was based on the Kling-Gupta efficiency (KGE) (Gupta et al., 2009), the coefficient of determination (R^2) and the percentage of bias (PBIAS). In addition, the p-factor and r-factor provided by the SUFI-2 program, indicate respectively the percentage of measured data bracketed by the 95PPU, and the average thickness of the 95PPU band divided by the standard deviation of the measured data.

Table 4.3. SWAT calibration parameters

Rank	Parameter	Definition	Range
1	r_CN2	SCS runoff curve number	-0.5 - 0
2	r_ESCO	Soil evaporation compensation factor	-0.4 - (-0.1)
3	v_GW_REVAP	Groundwater "revap" coefficient	0.04 - 0.12
4	r_SOL_AWC	Available water capacity of the soil layer	0 - 0.5
5	r_SOL_BD	Moist bulk density	-0.1 - 0.5
6	v_RCHRG_DP	Deep aquifer percolation fraction	0 - 0.5
7	v_REVAPMN	Threshold depth of water in the shallow aquifer for "revap" to occur	70 - 120
8	r_SOL_K	Saturated hydraulic conductivity	-0.3 - 0.3
9	v_GWQMN	Threshold depth of water in the shallow aquifer required for return flow to occur	600 - 1200
10	v_GW_DELAY	Groundwater delay	5 - 15
11	v_ALPHA_BF	Baseflow alpha factor	0.1 - 0.3
12	v_SURLAG	Surface runoff lag time	5 - 15
13	r_EPCO	Plant uptake compensation factor	-0.3 - 0.3

With the assumption that everything remains equal, those parameter values were applied to simulate future climate and land use change impacts on the runoff of the Mono river.

4.2.4. Runoff and flood scenarios

Five scenarios organized in 3 groups are investigated in this study: a base-case scenario, scenarios without the Adjarala dam, and scenarios with the Adjarala dam. The base-case (BC) scenario is the reference situation since the construction of the Nangbéto dam. It serves as a basis for comparison and represents the past-to-present conditions in the catchment. The year of construction of the Nangbéto dam is taken as the starting point of the BC in order to assure similar hydrological conditions when comparing past-to-present runoff with projected ones.

The scenarios without Adjarala dam are scenarios that account simultaneously for climate and land use change projections. Climate and land use change scenarios were not simulated separately, but concomitantly and in subsets in the SWAT model. Climate data from 2022-2030 are used together with the LULC map of 2030 to simulate runoff from 2022 to 2030; likewise, for the period 2031-2050 (and 2051-2070), climate data from 2031-2050 (2051-2070) is used in combination with LULC map of 2050 (2070) to obtain runoff projections for the period under consideration. Therefore, the scenarios referred to as RCP 4.5 and RCP 8.5 in this study, already embed LULC scenarios and stand for “RCP 4.5 + LULC scenario” and “RCP 8.5 + LULC scenarios” respectively.

Scenarios with Adjarala consist of climate scenarios and LULC scenarios simulated all together with Adjarala dam. They are referred to as “RCP 4.5 + Adjarala dam” and “RCP 8.5 + Adjarala dam”.

4.2.5. Flow trend and pattern analysis

The trend of discharge was assessed using the Mann-Kendall test (Mann, 1945) at 95% confidence level. The Z statistics from the Mann-Kendall test indicates trend (increasing or decreasing) and the significance of the test. A positive Z means an increasing trend while a negative value suggests a decrease in the time series. The result of the test is considered to be statistically significant (not significant) when $Z > 1.96$ ($Z < 1.96$). The Mann-Kendall test was applied to the time series of daily discharge under the scenario RCP 4.5 and RCP 8.5.

Mean hydrographs were derived to analyze the overall pattern of the flow in a year. The mean hydrographs were obtained by averaging daily discharge over all the years of the study period. The mean hydrographs were derived for the scenarios RCP 4.5 and RCP 8.5, before and after the construction of the Adjarala dam.

In addition to the mean hydrographs, flow duration curves (FDCs) were used to assess the effects of the yet-to-be-built Adjarala dam. FDCs are obtained with the following steps:

- discharge records are ordered from highest to lowest values and each discharge value is assigned a rank $r, r = 1, \dots, n$, where n is the total number of records and 1 is assigned to the largest value;
- probabilities of exceedance are calculated as:

$$p = \frac{r}{n} \times 100 \qquad (4.3)$$

- discharge values are represented on the y-axis with a logarithmic scale and the probabilities of exceedance on the x-axis with an arithmetic scale.

The probability of exceedance indicates the percentage of time that a given discharge is equalled or exceeded (Vogel & Fennessey, 1994), e.g. when a discharge value Q has a percentage of exceedance p, it does not mean that the discharge is Q for p% of the time, but that Q is equalled or exceeded p% of the time. The shape of the FDC informs on the hydrological characteristics of the stream under consideration. A very curved FDC shows the flashy or ephemeral state of the stream; a steep shape in the upper end indicates that high runoffs in the study area are rainfall-caused, unlike snowmelt floods which would depict a flatter shape in the upper end of the curve (Berhanu et al., 2015). A flat slope at the lower end of the FDC indicates a high storage or a regulation of the streamflow (either artificially or naturally), while a steep slope .indicates a lower storage (Searcy, 1959). In this study, discharges with 0-5% percentage of exceedance are characterized as extremely high, 5%-20% high, 20%-70% medium, 70%-95% low, and 95%-100 extremely low (Gordon et al., 2004).

4.2.6. Flood hazard simulation

Flood (hazard) or a hydrodynamic model can be a valuable tool to support flood emergency managers and planners in making decisions and as well to create community awareness to mitigate the impact of flooding. Flood models can be used for both event and long-term management of floods, this can be from near-real time flood forecasting to understanding the impact of future scenarios in the context of climate and land-use change and evaluating the adequacy of current and planned mitigation measures. Such examples are the work of Icyimpaye et. al. (Icyimpaye et al., 2022) in Nyabugogo River, Rwanda. The study coupled the hydrological and hydrodynamic model that aimed to forecast flooding and assessed the effectiveness of the proposed measures to mitigate the impact of floods.

Flood models can be classified into one dimensions (1D) or 2D or a coupled 1D-2D model. Due to the nature of the directional flow of water on rivers and floodplains, 1D models are generally used for simulating water flow in the channel and a 2D for the floodplain. However, for wide rivers, a 2D model can also be used to simulate water flow because water may also flow in 2 dimensions. 2D models often requires more computational time and resources compared to 1D, nevertheless, this type of model is really useful for spatio-temporal hazard impact assessment because it provides a better understanding and information about the affected area. The article of Mitsopoulos et al. (Mitsopoulos et al., 2022) presented an interesting study on the coupling and optimizing of a 1D and 2D hydrodynamic model using HEC-RAS for early warning of flash floods.

Compared to just a 1D or 2D hydrodynamic mode, the coupling of 1D and 2D yielded a faster simulation with spatial information on flooding in the floodplain.

In the current study, the TELEMAC-2D developed by Laboratoire National d'Hydraulique et Environnement (LNHE), part of the R&D group of Électricité de France was used. It simulates free-surface flows in two dimensions of horizontal space solving the Saint-Venant equations using the finite-element or finite-volume method in a computational mesh of triangular elements. For pre- and post-processing of the TELEMAC-2D model, the Kalypso 1D/2D software from Björnsen Consulting Engineers (BCE) GmbH Germany was used. It presents a structured user-oriented graphical unit interface to visually set up the model (https://kalypso.bjoernsen.de). ArcGIS with the HEC-GeoRAS and HEC-RAS 1D model was used as a tool to derive cross-sections since these data were not available.

4.2.6.1. Data input pre-processing

The slope-area method (Equation 4.4) was used to correct the DEM derived 77 cross-sections. The cross-section DEM was extracted using the HEC-GeoRAS tool and adjustments were supported and verified by the HEC-RAS 1D modelling tool. The following are examples of adjusted and unadjusted cross-sections (Figure 4.4 and Figure 4.5).

$$Q = \frac{1}{n} A R^{\frac{2}{3}} S^{\frac{1}{2}} \rightarrow \frac{Q \times n}{S^{1/2}} = \frac{\left(x/4\right)^{5/3} \times (y)^{5/3}}{\left((x^2 + 4y^2)^{1/2}\right)^{2/3}} \tag{4.4}$$

where,

$Q =$ discharge (m^3/s)
$n =$ Manning's roughness coefficient (range between 0.01 and 0.75)
$A =$ cross-section area (m^2)
$R =$ the hydraulic radius, equal to the area divided by the wetted perimeter (m)
$S =$ the head loss per unit length of the channel, approximated by the channel slope

Different land uses can affect water flow where the greater the roughness coefficient the lesser the flow velocities. To represent these in the equations, an empirically derived roughness coefficient is introduced using the table of Chow (1959) approximating it to Ks values. Landsat satellite imagery (present time) was used for the identification of land use types using the works of Thiam et. al. (Thiam et al., 2022).

As a requirement for the model, using ArcGIS, the river and its banks and DEM spatial model boundary and distinct features (e.g., roads) were delineated and exported to shape and ascii files respectively.

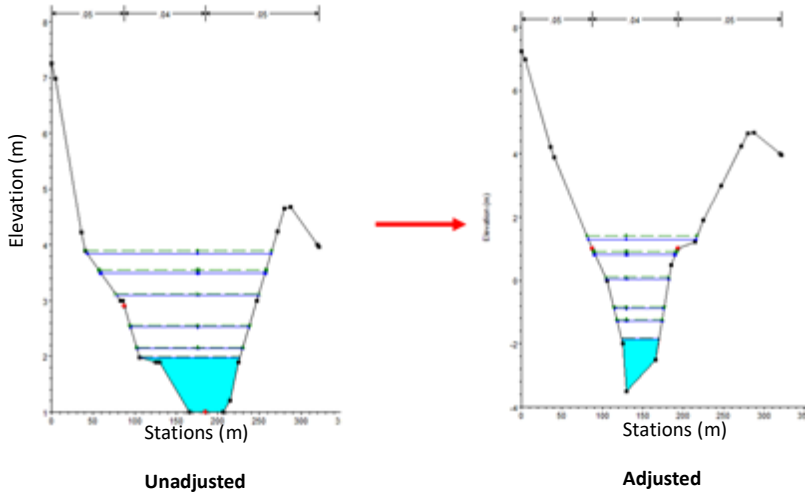

Figure 4.4. Example section of unadjusted and adjusted cross-section

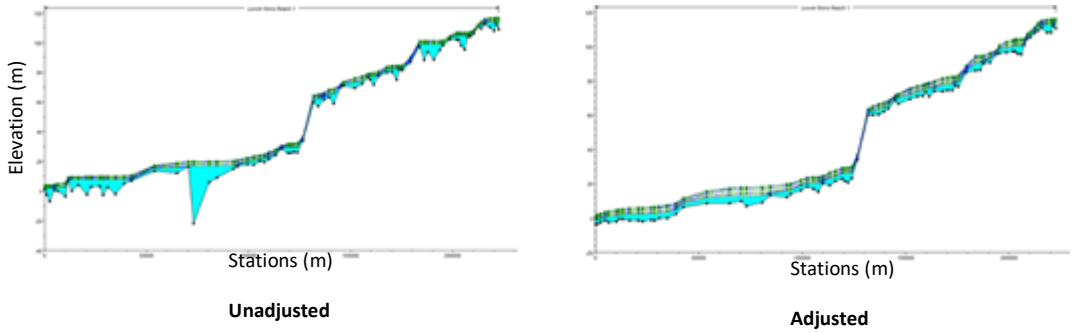

Figure 4.5. Upstream to outflow longitudinal profile of the unadjusted and adjusted cross-section

4.2.6.2. Model-setup

The LMR was initially divided into four sections (S1-S4) (Figure 4.6) for the reasons of model run time efficiency, availability of historical discharge and flexibility in the integration of scenarios and measures. However, during the first investigation and run analysis, it was decided to combine both S1 and S2 sections because of the rather flat terrain in these sections. Coupling these two sections allowed us to have a better representation of the flow and interaction of floodwater in the terrain. Furthermore, knowing that computational parallelization is possible, a multi-core CPU were used when running the model.

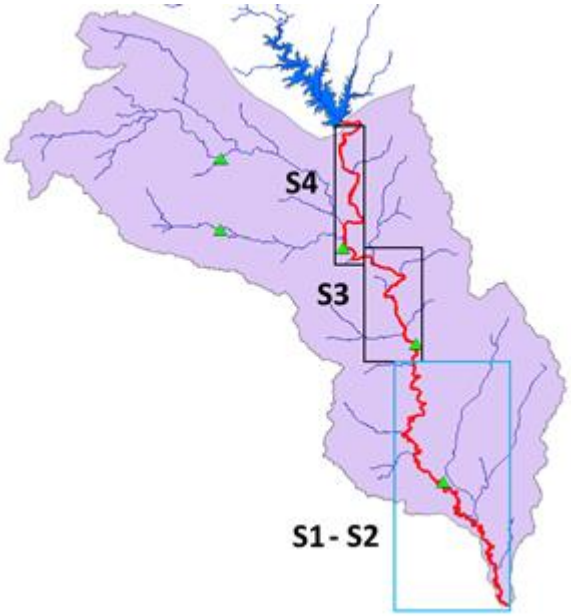

Figure 4.6. Lower Mono River (LMR) basin study area showing the divided sections for flood modelling

In setting-up the model in Kalypso, the discharge data was imported, location of model boundary was defined, computational mesh to represent river and floodplain were created, mesh elevation and roughness coefficient were assigned, upstream and downstream boundary conditions were defined, and calculation units and simulation settings were set. At the end, the model set-up was exported to a file format for Telemac2D and the model was run using the command line terminal script for Telemac2D. Table 4.4 is the summary of the set-up of the sections.

Table 4.4. Model set-up of the three sections

Input data	Section		
	S1-S2	S3	S4
DEM	30 meters	30 meters	30 meters
River bathymetry	30 m DEM – Corrected theoretically Length – 139.5 km	30 m DEM – Corrected theoretically Length – 52.83 km	30 m DEM – Corrected theoretically Length – 53.11 km
Land use for flow resistance	Farmland, water, settlement and savanna	Farmland, water, settlement and savanna	Farmland, water, settlement and savanna
Mesh 2D elements	Number of elements – 477,889 Area – 2,064 km^2	Number of elements – 174,876 Area – 182.7 km^2	Number of elements – 183,325 Area – 237 km^2
Upstream boundary	Athiémé/Adjarala discharge	Tététou discharge	Nangbéto discharge
Downstream boundary	Sea water level (constant)	Athiémé/Adjarala rating curve	Tététou rating curve
Discharge time series	August 2010-April 2011	August 2010-April 2011	August 2010-April 2011
Rating curve	Not available	Yes	Yes

4.2.6.3. Calibration and validation

Calibration of a hydrodynamic model generally makes use of observed water level data to compare with the model output. However, due to the unavailability of observed water level data, the model results were calibrated and validated by comparing it with a satellite image of a flooding event with a similar discharge. Moreover, stakeholders were also engaged in a workshop on identifying the most flood-prone areas based on their field and expert knowledge.

In this context, first, the low and medium flow discharge was used to simulate a riverbank full. Then the 1963 and 2010 extreme events were used as a reference case to compare with satellite imagery of a similar flood discharge in the year 2019. The 1963 and 2010 extreme events had a maximum peak discharge in Athiémé of about 900m^3/s. Flooding in the Mono river as shown in Figure 4.7 can last up to several months. Thus, the model has to run a 70 to 90-day event to capture the rise and fall of water level in the Mono river.

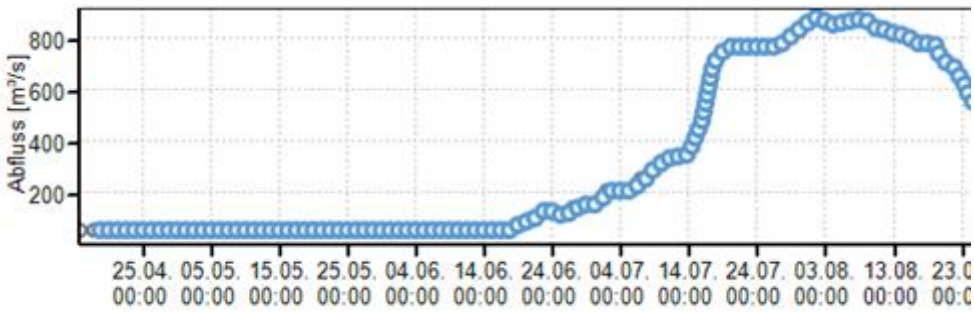

Figure 4.7. Hydrograph Athiémé station- 2010 event

The extreme event was spatially validated with the processed satellite imagery from MODIS by UNOSAT for the flood event 2019 (https://unosat.org/products/2763) and inputs from the stakeholder workshop (Figure 4.8). Unfortunately, UNOSAT published a flood map that only shows the side of Togo. Hence the southeast coastal part is not presented. The flood event of 2010 was more or less comparable to that of 2019 in terms of peak discharge. The results show an almost similar flood extent. However, remotely sensed information cannot capture shallow water depths which is why some parts look like there is no flooding.

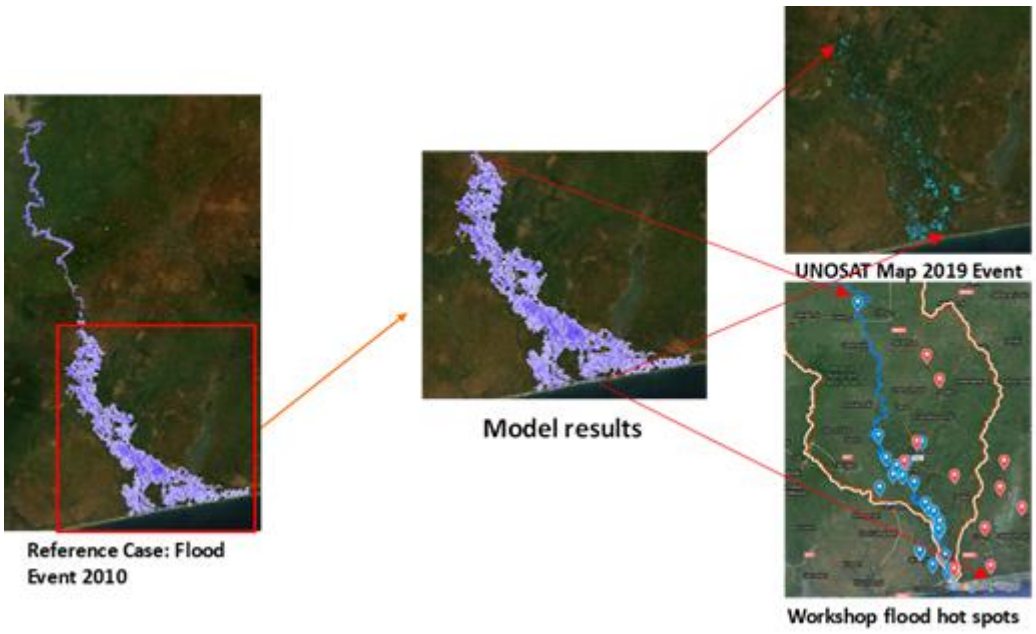

Figure 4.8. Model results verification

4.2.7. Analysis of extremes and flood hazard scenarios

For the analysis of extremes, max discharge return periods (HQ) of 2, 5, 10, 50 and 100 years were statistically derived for the historical (base case) and future scenarios. The Extreme Valued Distribution (EVD) statistical analysis Gumbel (GEV) and Pearson III were used to derive HQ for

stations Nangbéto, Tététou and Athiémé. The work of Millington et.al. (2011) (Millington et al., 2011) presented an interesting study on the comparison of GEV and Pearson III in the upstream of the Thames river basin under different global climate models.

For the base case, discharge data of 33 years (1987-2019) were used for Nangbéto station, 27 years (1965-1991) for Tététou and 24 years (1987-2010) for Athiémé. Future scenarios on climate (RCP 4.5 and 8.5) and land-use change, with and without Adjarala dam from the years 2022 to 2070 were used to derive future return periods (HQs) of discharge. Estimates of discharge with future scenarios were modelled by the hydrological model at the station Athiémé. Figure 4.9 presents the plot of the Base Case HQ.

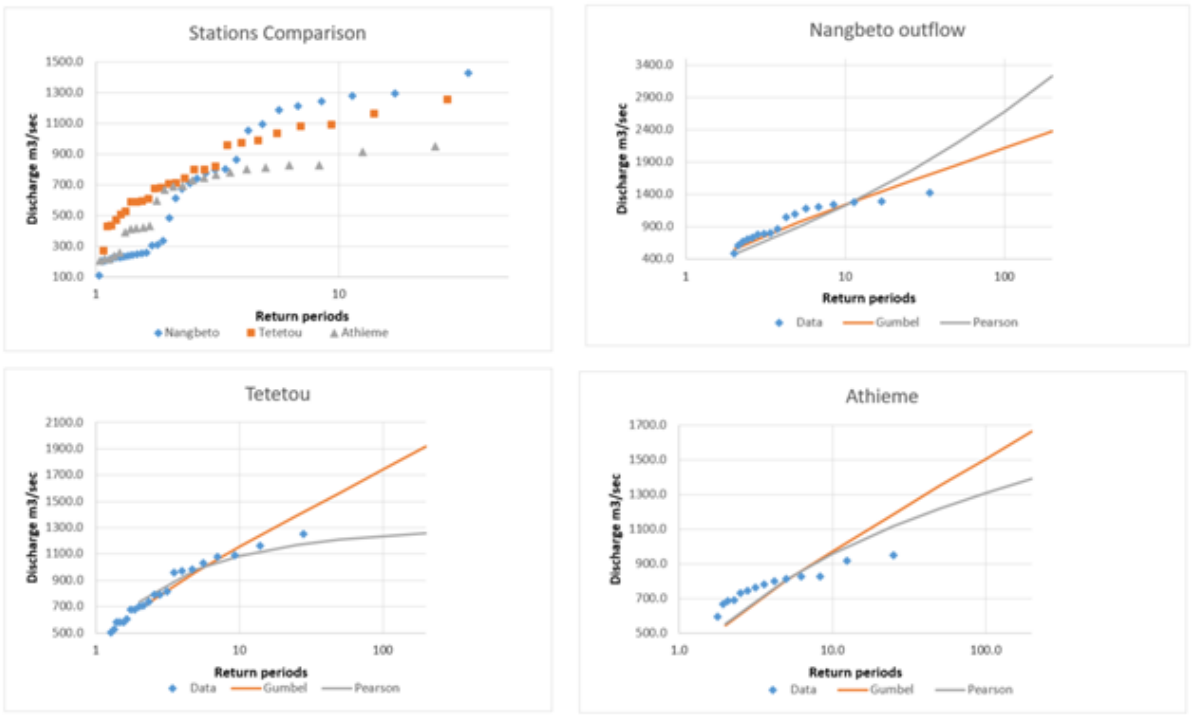

Figure 4.9. Base Case (HQ) for different stations

After the analysis of extremes, these HQs were transformed into a hydrograph (Figure 4.10) having the shape derived from several high-flow event hydrographs. This was then used as an input to the hydrodynamic model to have an idea of the severity of these flooding scenarios.

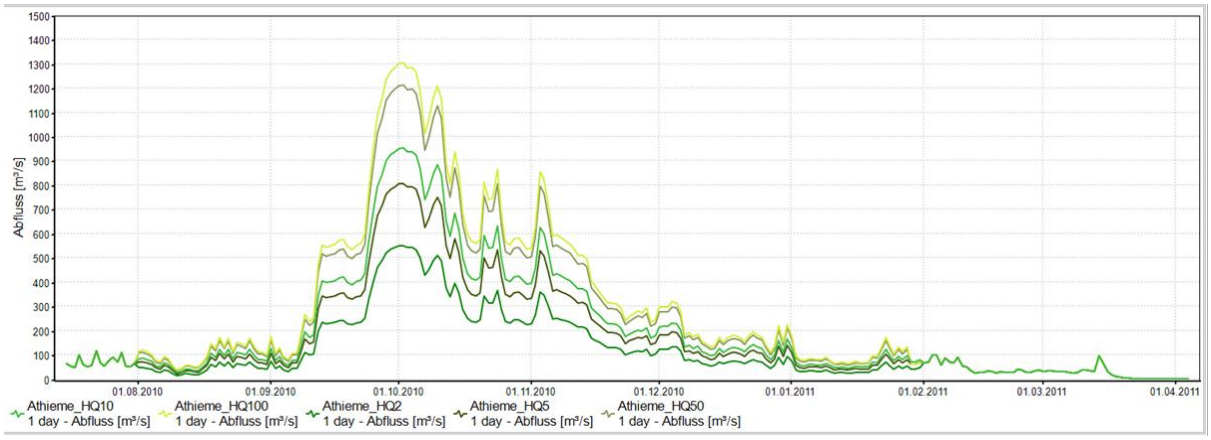

Figure 4.10. Base Case HQ derived hydrograph for Athiémé station

4.3. Results and discussion

4.3.1. Runoff simulation

4.3.1.1. Model calibration and validation

Figure 4.11. shows the simulation results during calibration and validation phases. A visual inspection indicates that the pattern of observed discharge at the Athiémé station is well represented. That is supported by the statistics presented in Table 4.5.

Overall, the values of p-factor and r-factor show that the parameter ranges that were used, well represent the observation and with relatively low uncertainty. As reported by Schuol et.al. 2008 (Jürgen Schuol, Abbaspour, Srinivasan, et al., 2008), a p-factor and a r-factor near 1, indicate quite good results. The p-factor of 0.91 during calibration (0.85 during validation), means that 91% (85%) of observation was bracketed within the 95% certainty range defined by the 95PPU band. Moreover, the ability of the model to capture the flow during the period 1970-1985, which is known as a drought-dominated period over west Africa (Sharon E Nicholson, 2013), and the capacity of the model to represent the peaks, confirms the good performance of the SWAT model in both drought and flood periods in the Mono basin. The lower R^2 and KGE statistics noticed during validation are imputable to the abnormally high values simulated at the beginning of 2010. This overestimation may be due to outliers in rainfall records. Despite this lower R^2 value, the model showed good results during validation, compared to calibration statistics that were very good. In addition, the bias level declined during the validation period.

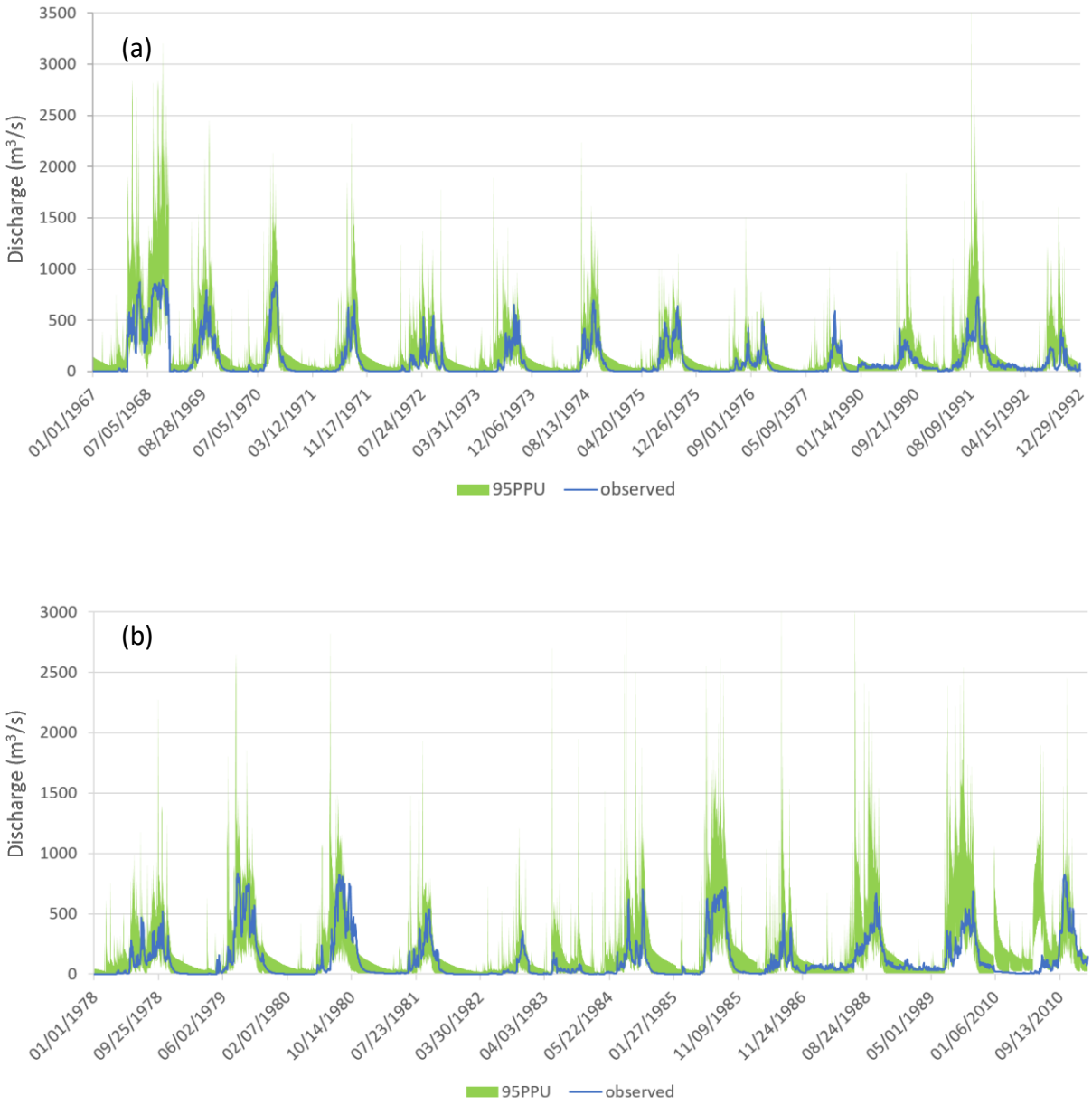

Figure 4.11. Observation and 95PPU of the simulation during (a) calibration and (b) validation

Table 4.5. Goodness of fit during SWAT calibration and validation

Goodness-of-fit	KGE	R^2	PBIAS	p-factor	r-factor
Calibration	0.83	0.80	-13	0.91	1.31
Validation	0.68	0.57	2.3	0.85	1.46

The fact that calibration and validation periods were not selected as continuous periods (e.g. 1967-1976 and 1977-1986), but rather based on a balanced combination of hydrologic conditions (dam and no-dam years, high and low peak years), has led to better results, compared to a previous studies conducted with SWAT in the Mono catchment (Djan'na Koubodana et al., 2021). In the study by Koubodana et.al (Djan'na Koubodana et al., 2021), known to date as the only published work with SWAT in the Mono catchment, the authors created two distinct models: one for the period before Nangbéto dam's construction (1964-1986) and another one for the period after the dam (1988-2011). The model calibration with that approach, yielded very good results for the period before the construction of the dam (KGE=0.82, R2=0.68), but a lower performance during the period post-dam (KGE=0.54, R2=0.2). The decline of the statistics may be attributed to the high level of missing discharge data during the post-dam period, 39% (the majority occurring in high flow season), which substantially reduced the actual exploitable data.

4.3.1.2. Future runoff under climate and land use scenarios

Figure 4.12 presents the pattern of the discharge under climate and land use change scenarios.

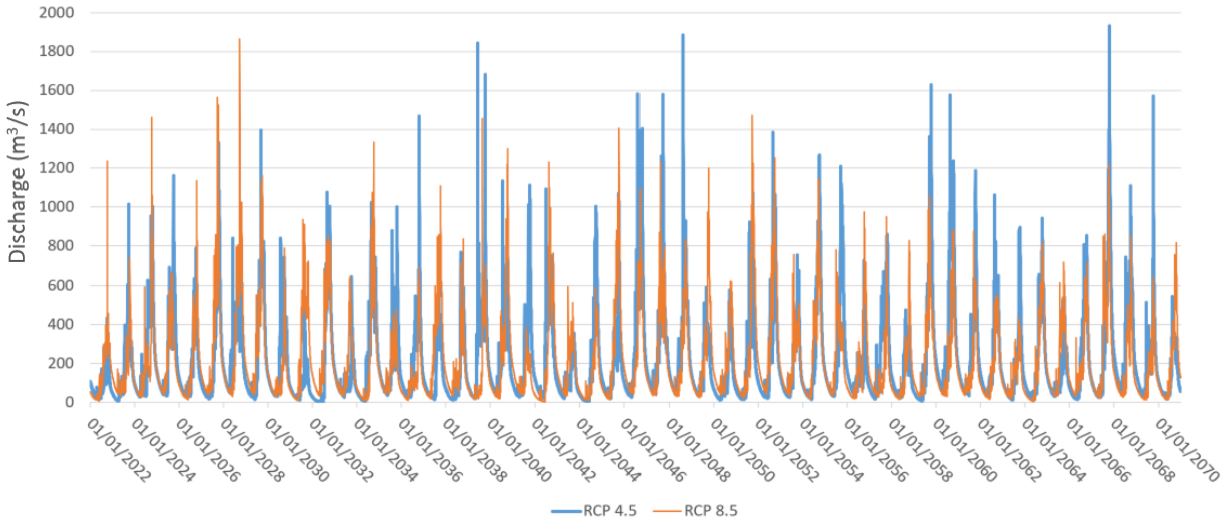

Figure 4.12. Daily runoff under climate and land use change scenarios.

During the period 2022-2070, the runoff is expected to be characterized by a mixture of high and low peaks. The scenario RCP 4.5 projects higher peak values than the scenario RCP 8.5. This is attributable to rainfall and temperature projections in the Mono basin. As reported by Houngue et.al. (Houngue et al., 2022), RCP 4.5 projects wetter conditions (higher precipitations peaks and lower temperatures) than the high pathway scenario, RCP 8.5, in the Mono basin. With reference to 1966-2015, the average annual temperature in 2021-2070 presented a 1.5°C increase under RCP 8.5, while the intermediate pathway scenario, RCP 4.5, showed a 1°C increase.

The Mann-Kendall test performed on annual peaks of runoff from 2022-2070, revealed a statistically-insignificant increase with the scenario RCP 4.5 and a significant decrease under RCP

8.5. That is in line with rainfall and temperature scenarios mentioned above. However, regardless of the projected trend, a succession of low and high annual peaks is expected in some years; for instance, 2058 (464.5 m^3/s) and 2059 (1629 m^3/s) under RCP 4.5 and the years 2045 (592.1 m^3/s) and 2046 (1407 m^3/s) under RCP 4.5.

The highest discharge recorded in the Mono catchment, from 1960-2010, is about 900 m^3/s, and was observed in 1963 and in 2010. That discharge magnitude triggered one of the most disastrous flood events in the catchment (UNDP, 2010; WB & UNDP, 2011). Taking 900m^3/s as reference during the period 2022-2070, it was noticed that discharge under RCP 8.5 has more years (24 years) above 900 m^3/s than the scenario RCP 4.5 (19 years). This means that despite the lower peak values projected by the scenario RCP 8.5, potentially high flood events are likely to occur often under that scenario. That assumption is corroborated by the discharge values at return periods 2, 5, 10, 50, and 100. Table 4.6 presents the return period and associated discharge values for scenario RCP 4.5, RCP 8.5, and the base case scenario.

Table 4.6. Return periods of runoff with climate and land use scenarios

	Runoff (m^3/s)		
Return period	Base case	RCP 4.5	RCP 8.5
2	554.80	1014.32	927.28
5	810.30	1373.82	1228.53
10	956.2	1584.36	1408.91
50	1218.00	1981.44	1758.66
100	1308.50	2125.34	1889.02

Comparing the base case (BC) with the future scenarios shows, that the peak runoff becomes more frequent in the future. For example, the base case HQ10 will become HQ2.

Figure 4.13 presents the mean hydrograph for the period 1988-2010 (after the construction of the Nangbéto dam) and the hydrographs under future climate (2022-2070) and land use change scenarios.

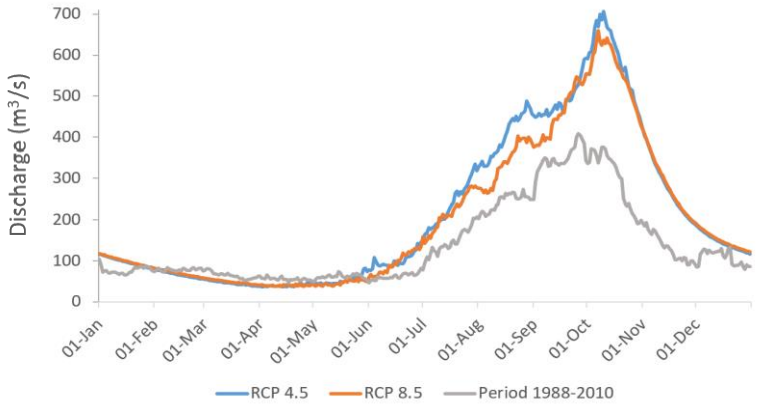

Figure 4.13. Past and future mean hydrographs

Overall, the peaks are expected to increase during 2022-2070 with a longer overland flow. That is attributable to rainfall projections in the Mono catchment which are expected to be more intense due to climate and land use changes. As reported by Amoussou et.al (Amoussou et al., 2020), the annual maximums of daily precipitation are expected to increase between 2028-2050. The authors assessed extreme rainfall patterns in the Mono catchment and concluded that a significant increase in the intensity of extreme rainfall events is expected. The analysis of the precipitation data used in this study revealed an increase of peaks, a delay in the start of the rainy season and a shorter season (Houngue et al., 2022). Moreover, the findings of the study of Wetzel et. al. (Wetzel et al., 2022) on assessing flood risk dynamics in the LMR shows that there is a strong causality between economic dependence on agriculture and the destruction of ecosystems and soil degradation that are driven by the type of agriculture and the agricultural techniques. These soil degradation and destruction of ecosystems will also have an impact on the extremity of flooding. This will produce more run-off and sedimentation in the river channels. Those factors compounded with the decrease of forest areas and the extension of settlements in the catchment (Koubodana et al., 2019; Thiam et al., 2022) may trigger low infiltration rates and a higher runoff. The works of Thiam et. al. (Thiam et al., 2022) shows a 58% decrease of forest in the year 2070 that would have an effect on the ecosystems and soil degradation.

The boxplots in Figure 4.14 illustrate the interannual variability of discharge under the scenarios RCP 4.5 and RCP 8.5.

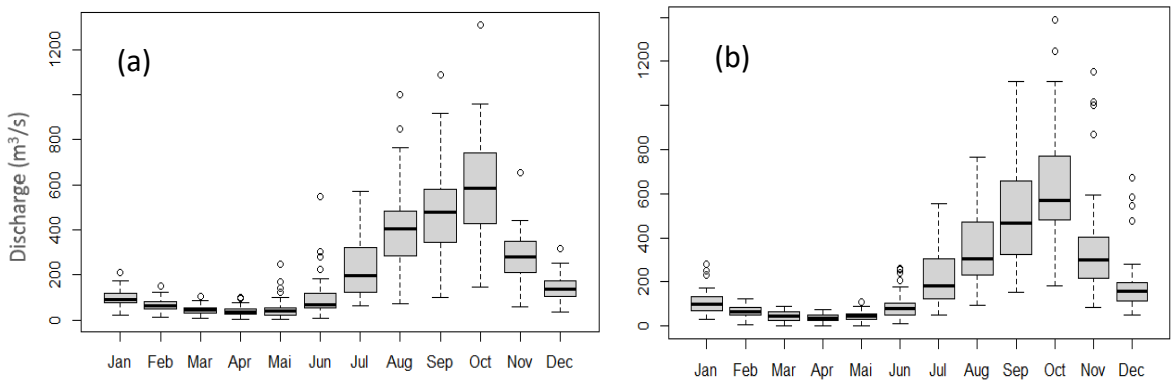

Figure 4.14. Boxplots of discharge with scenarios (a) RCP 4.5 and (b) RCP 8.5

Despite the projected overall increase of discharge, high interannual variabilities are expected at monthly scale, especially during the high peak season. The highest variations are noticed from July to November.

4.3.1.3. Effect of the Adjarala dam

After adding the second, yet to be built, Adjarala dam in the model, the annual maxima have globally reduced (Figure 4.15). The average annual maximum dropped from 1050.63 m^3/s to 814.42 m^3/s under RCP 4.5, and from 995.29 m^3/s to 816.72 m^3/s under RCP 8.5.

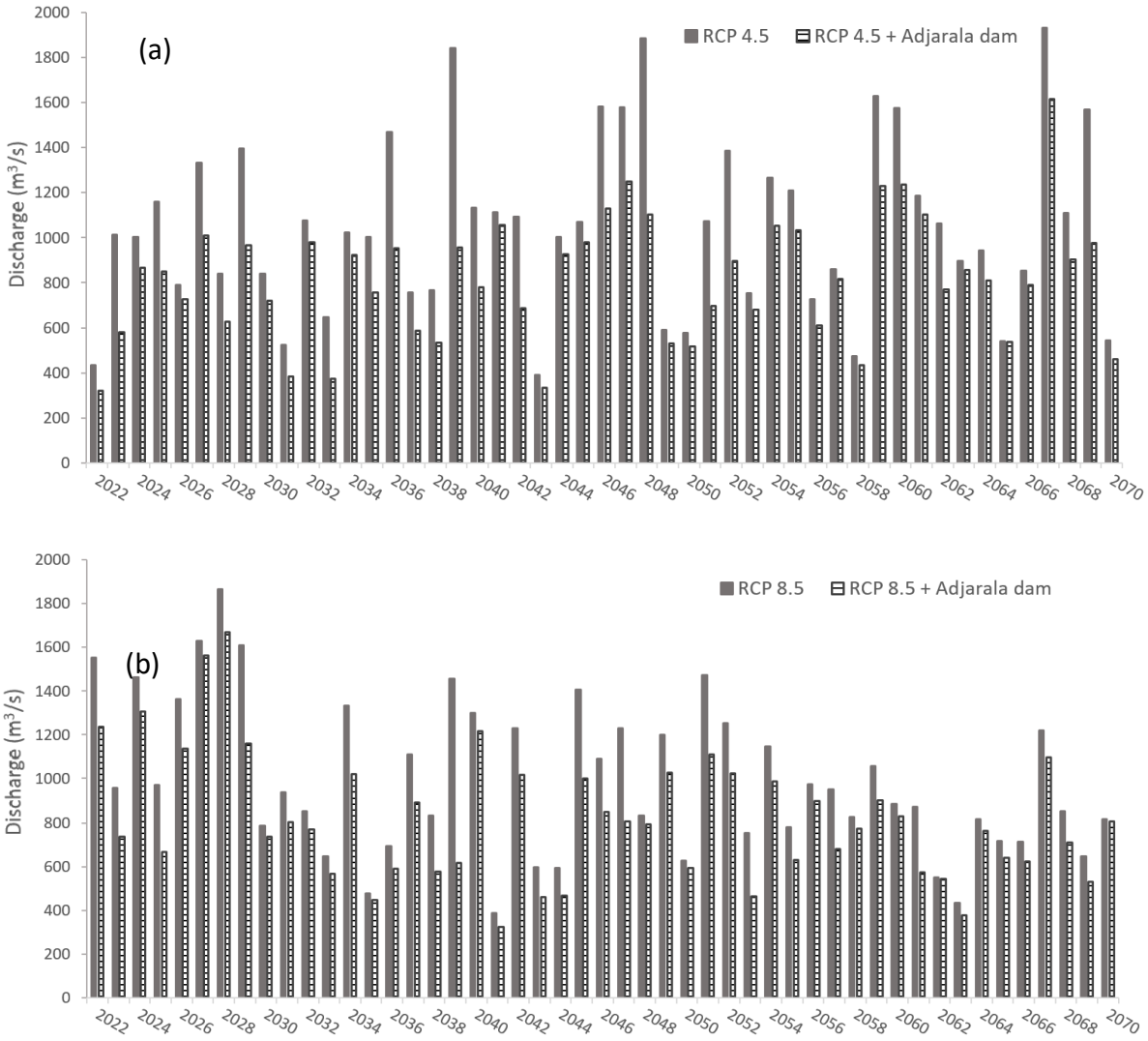

Figure 4.15. Annual maximum discharge from 2022-2070 under (a) RCP 4.5 and (b) RCP 8.5

Table 4.7 presents a comparison of return periods of annual maximum discharge, with and without the Adjarala dam.

Table 4.7. Return periods of runoff with climate, land use and Adjarala dam scenarios

Return period	Runoff (m^3/s)				
	Base case	LU + RCP		LU + RCP + Adjarala dam	
		RCP 4.5	RCP 8.5	RCP 4.5	RCP 8.5
2	554.80	1014.32	927.28	810.85	772.01
5	810.30	1373.82	1228.53	1050.35	1127.80
10	956.2	1584.36	1408.91	1173.24	1420.99
50	1218.00	1981.44	1758.66	1370.50	2279.85
100	1308.50	2125.34	1889.02	1430.94	2755.42

The results show that constructing the Adjarala dam may reduce the recurrence of extreme discharges. Nonetheless, the peaks are expected to remain above the levels experienced till date (the base case). Under the scenario RCP 8.5, HQ50 and HQ100 are expected to rather increase if the Adjarala dam is constructed. Those obviously off-track values may be due to the limited length of the time series used (49 years) and to outliers.

Figure 4.16 presents the mean hydrographs over 2022-2070, with and without the Adjarala dam. The mean hydrographs indicate that from a long-term perspective, building the Adjarala dam may reduce the discharge at Athiémé, but only slightly.

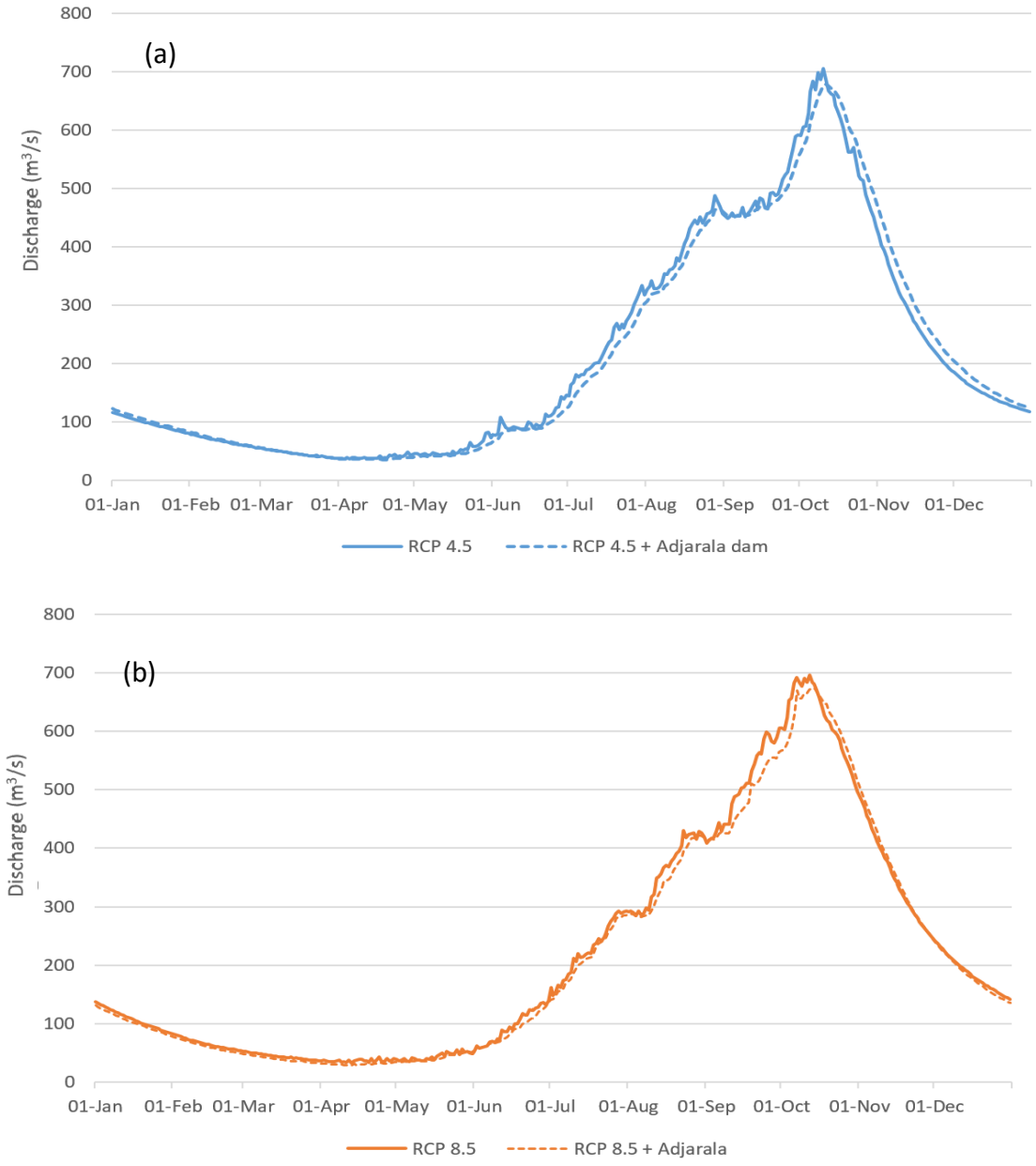

Figure 4.16. Mean hydrograph 2022-2070 under scenarios (a) RCP 4.5 and (b) RCP 8.5, with and without the Adjarala dam

This is probably attributable to the characteristics of the reservoir which might be relatively small for a substantial and long-term flood reduction under future climate and land use change scenarios in the Mono catchment. In that regard, the Netherlands Commission for Environmental Assessment (CNEE, 2014), has reported that the intended volume and surface area of the reservoir of the Adjarala dam, as announced in the dam project, might be underestimated due to potential improper elevation considerations.

The flow duration curves (FDC) presented in Figure 4.17 illustrate the percentage of time that a certain amount of discharge is reached or exceeded during the period 2022-2070.

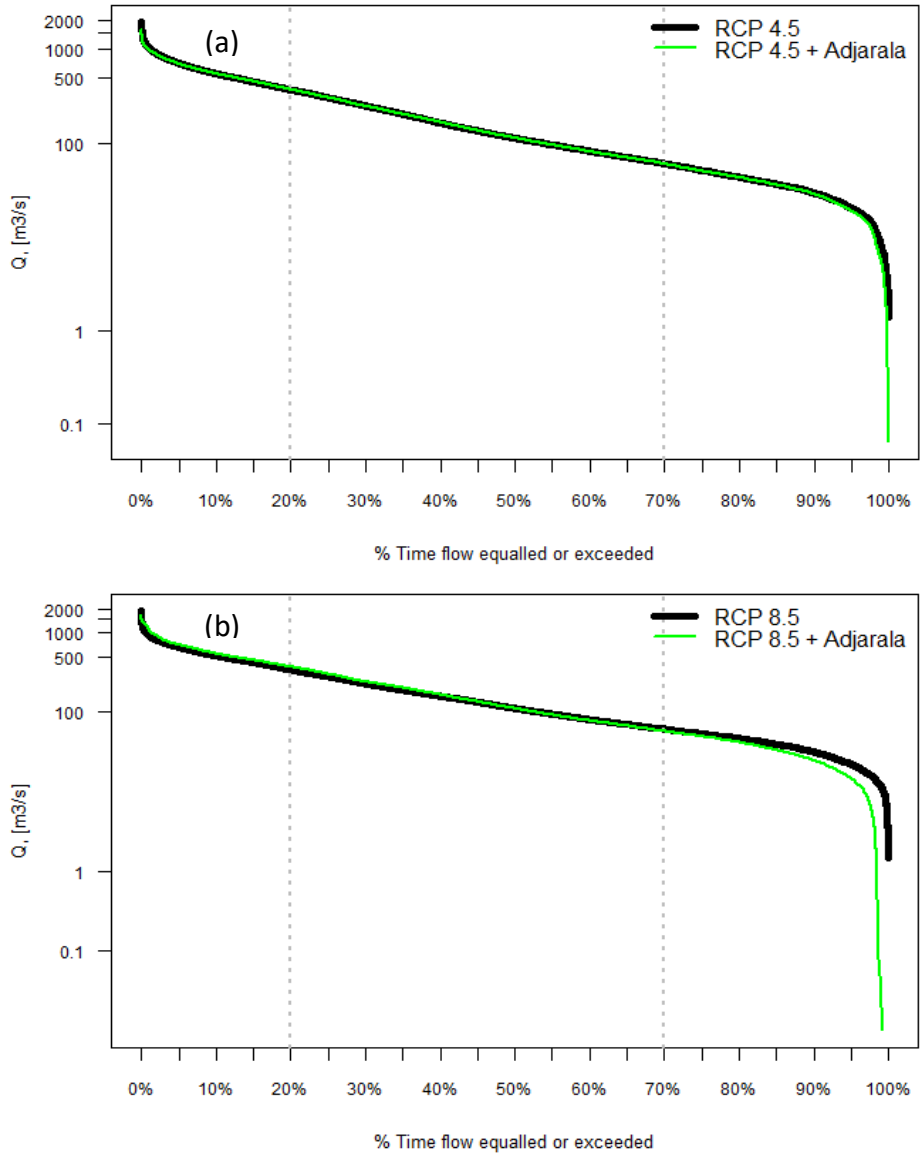

Figure 4.17. Flow duration curves (FDCs) with and without the Adjarala dam under scenarios (a) RCP 4.5 and (b) RCP 8.5

The shapes of FDCs from scenarios 'with' and 'without' the Adjarala dam are similar, indicating that the overall hydrology of the flow is not expected to change. The FDCs show that peaks of 0-1% exceedance percentage are reduced with the Adjarala dam. That supports the assumption that the dam can reduce the peak of extremely high discharges. However, a lower effect is observed for medium (20-70%) and low (70%-95%) flows.

Furthermore, the very low flows (95%-100% exceedance probability) depict a remarkable decrease with the Adjarala dam, especially under the scenario RCP 8.5. It indicates that the construction of the Adjarala dam may cause the river to dry-out downstream sometimes in the future. It is worth recalling that the current simulation is basically based on the storage information for the reservoir of the Adjarala dam. The reservoir simulation did not account for other water uses such as irrigation and aquaculture, as announced by the two countries (CNEE, 2014). The peaks might therefore become lower and the dam more effective for flood protection if those components were integrated. However, beyond the flood reduction aspect tackled in this study, it is recommended to ensure a minimum environmental flow to sustain water availability for local communities and for ecosystem services (IUCN, 2003; WMO, 2019). As reported by King and Brown 2018 (King & Brown, 2018), the expansion of hydropower infrastructures in developing countries may jeopardise river systems and induce environmental and social impacts. Considering the potential reduction of discharge detected during very low flow periods, further studies on the management of the Adjarala dam, and on possible options for the regulation of the river flow are recommended.

4.3.2. Flood hazard

The flood modelling produced 25 hazard maps, modelling the return periods (HQ) 2,5,10,50 and 100 of the Base Case, RCP4.5 and RCP8.5, and with Adjarala dam. In this section, we present selected flood hazard maps that are representative of our findings and analysis. Moreover, RCP 4.5 return periods were selected for comparison because it shows that this climate scenario produces higher discharge compared to RCP 8.5.

4.3.2.1. Base Case and RCP 4.5 (H2 and HQ10)

The findings show that flooding considerably affects and is more dynamic from mid to downstream sections. Even with low return periods (i.e., HQ2- the probability of occurrence of 50% every year) many townships/communities are still affected. Figure 4.18 shows a comparison of Base Case and RCP 4.5 HQ2 and HQ10. Looking at HQ10 RCP4.5 (Figure 4.18.d) which has a peak of ~600 m^3/s more compared to the HQ10 base case (Figure 4.18.c), large areas which have not experienced flooding in the Athiémé township and the floodplains in the south to the east of Grand Popo may be inundated. HQ10 base case is an event comparable to the year 2010, one of the most devastating flood events recorded in the study area.

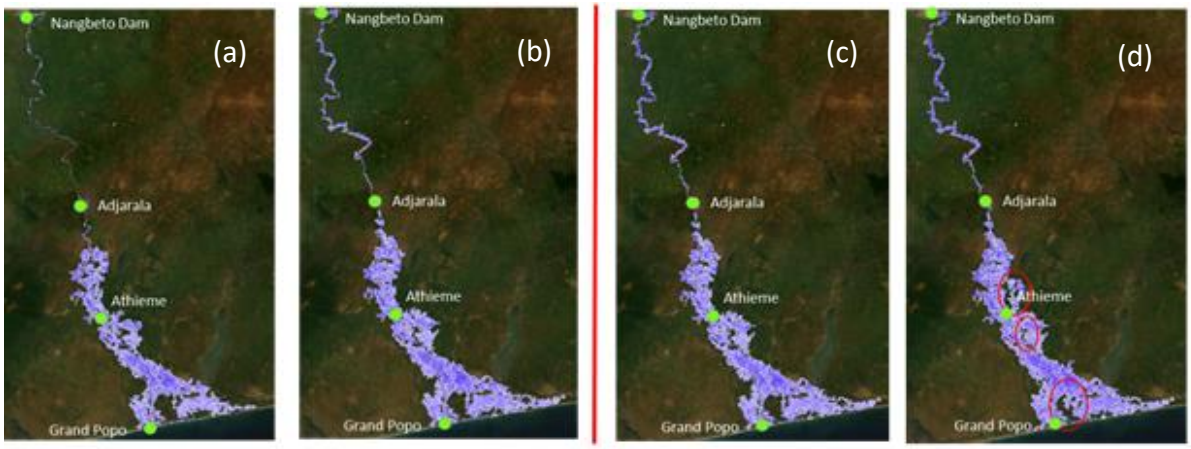

Figure 4.18. Flood hazard maps- Base case vs RCP 4.5 (HQ2 and HQ10)

4.3.2.2. RCP 4.5 and RCP 8.5 (HQ10 and HQ 100)

The following figures present the scenario RCP 4.5 and RCP 8.5 HQ10 and HQ100 with the base case. As shown again in these figures, even with an increase of >47% (HQ10 RCP 8.5) in the discharge peak of the HQ10 base case, the areas that did not experience flooding in the township of Athiémé and the southern flood plains may also be inundated (Figure 4.19-b and c). Furthermore, an increase of >98% (Figure 4.19-e) in the discharge peak of the HQ10 base case will also further exacerbate the flooding near the area of Lac Ahémé, in the southwest and also the areas in the Upper midsection.

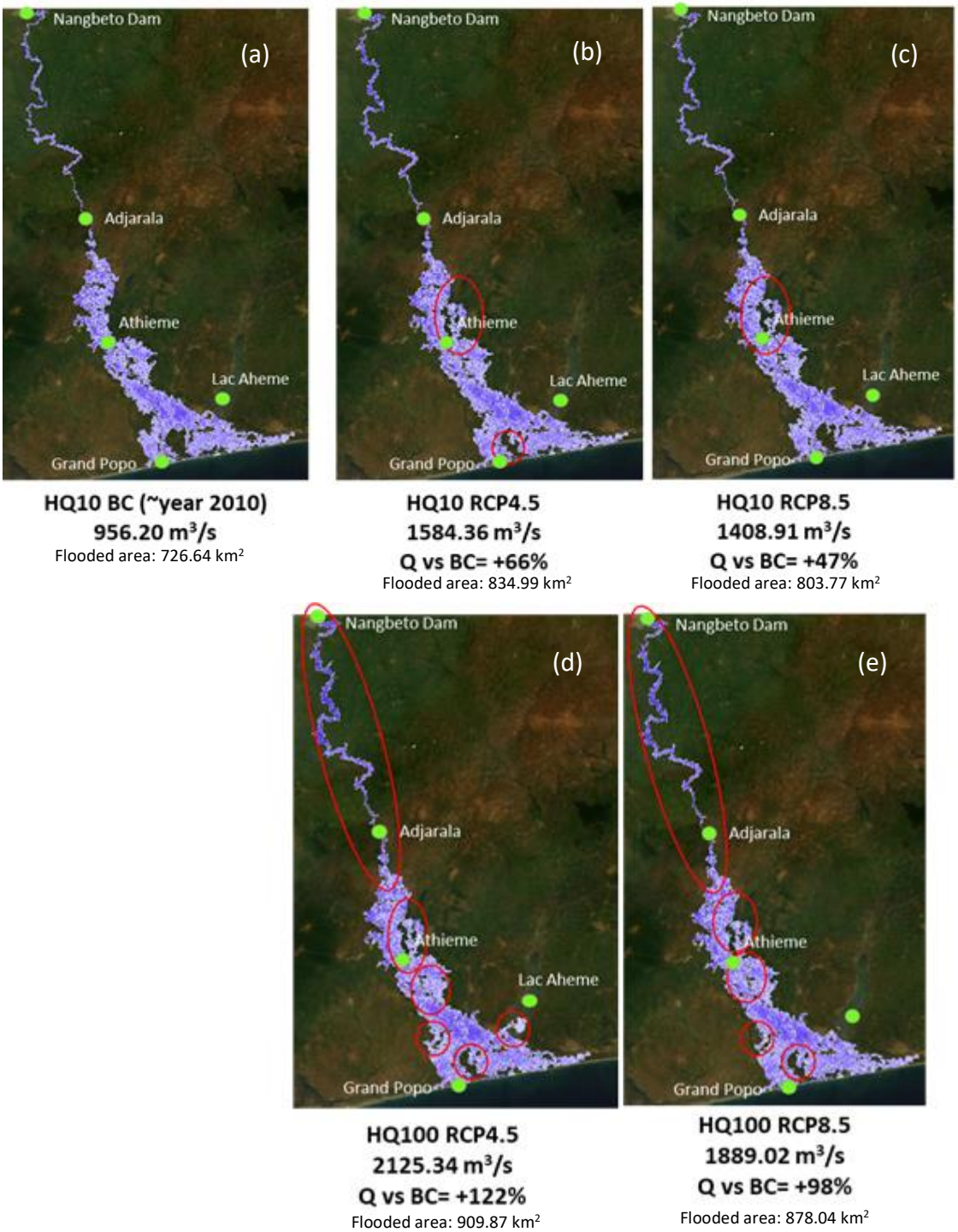

Figure 4.19. Flood hazard maps- HQ10 and HQ100.

4.3.2.3. Effect of the Adjarala dam on flood extent

Presenting the results of the Adjarala dam scenario, Figure 4.20 shows that for HQ10 RCP4.5 the Adjarala dam can potentially reduce the impact of flooding. This is clearly shown in the townships of Athiémé and the southern coastal areas. The assumptions for Adjarala dam were based on the parameters and projected operational management information provided by Communauté Electrique du Bénin (CEB), the institution in charge of electric infrastructures detained by Benin and Togo (CNEE, 2014). This however can be improved if new data and information are acquired.

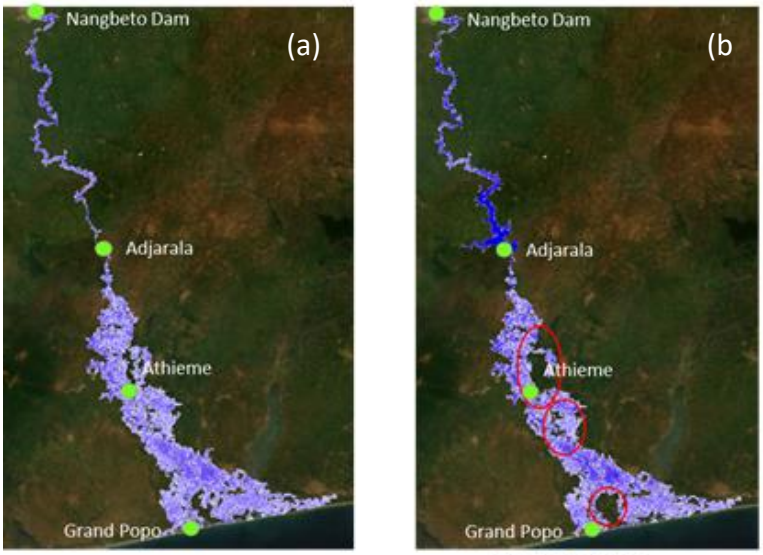

HQ10 RCP4.5
1584.36 m³/s
Flooded area: 834.99 km²

HQ10 RCP4.5
Adjarala Dam
1173.24 m³/s
Q w/dam= -26%
Flooded area: 825.41 km²

Figure 4.20. Flood hazard map- RCP 4.5- (b) with and (a) without Adjarala Dam

In addition to the findings, in Figure 4.21, the simulation shows that certain sections on the western coast drain the water coming from the flood plains. These existing flood plains and drains play a vital role in storage and drainage thus it needs to be preserved to not exacerbate flooding.

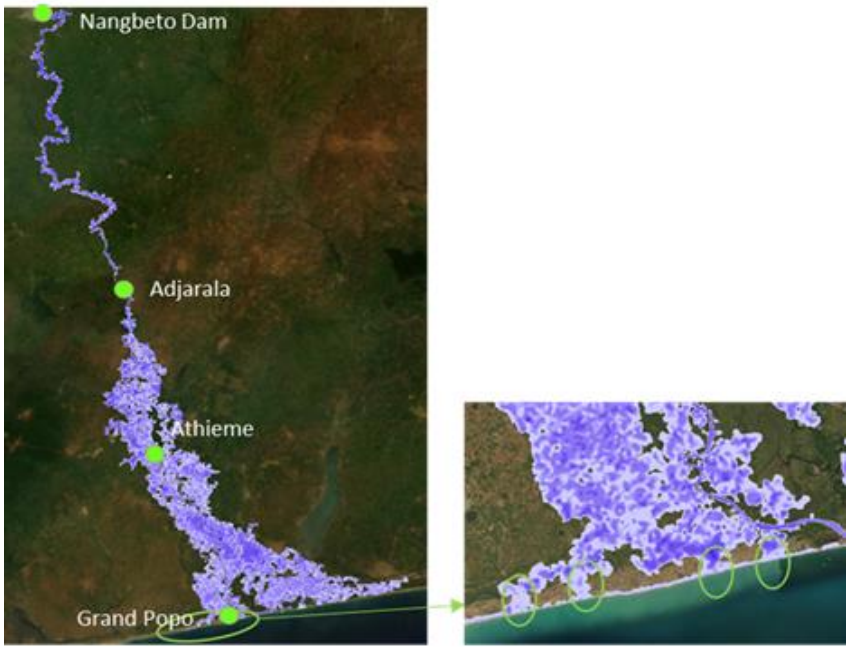

Figure 4.21. Flood hazard maps- Western coast drainage

4.3.2.4. Limitations

The model has been set up with the limited data we have collected and to compensate for this, scientifically derived inputs such as the cross-section were also used as input. If additional information and data are made available in the future, this will significantly improve the model results, especially in the southern section.

The east and west coastal area and the south-eastern floodplain are beyond the scope of the basin boundary defined in this study. We tried to integrate these into the model but in our investigation, the interaction here is more complex, thus current results in the coastal area must be dealt with caution because of uncertainty. This requires an in-depth investigation integrating the other system and as well (new) data regarding discharge, storm surge/tides and bathymetry. See the Figure 4.22 below for the areas (in red) that need caution for further use.

Figure 4.22. Modelled area for further investigation

4.4. Conclusion

This study assessed the combined impact of climate and land use change on floods in the Lower Mono River catchment, and the potential effect of the forthcoming Adjarala dam. Results show that flood extreme events will persist in the future based on the climate and LULC change scenarios investigated. A high interannual variability of runoff is expected from 2022 to 2070, with possibilities of drought and flood occurring in consecutive years. During the wet season, more intense precipitation is expected that translates to more extreme flood events. This is clearly seen on the mean hydrographs from 2022-2070 that depict higher runoff during the peak season August-November. In addition, HQ10 events of the base case become HQ2 under the climate and land use change scenarios. Although the sole investigation of land-use change impact on flooding was not explicitly investigated here, it is already clear that urban growth will also exacerbate flooding producing higher runoffs. This will have an increased impact on communities and the agricultural economy which is the main economic activity in the study area. The Adjarala dam may reduce the magnitude of extreme flood events in the future. However, it may also affect water availability during low flow periods, and thus, jeopardize environmental flow and related benefits in the LMR basin. Based on the observed variability of spatio-temporal impacts on flood hazard in the LMR basin, both local and basin scales need to be taken into account by decision makers. Expansion of settlements in flooded areas that are currently not settled should be avoided. The integrated and participatory approach used in this study with the engagement of stakeholders for flood maps validation, should be maintained and furthered for the identification of sustainable adaptation measures. Further studies could investigate the capabilities of other models for flood hazards mapping in the LMR basin. In addition, improved model performances may be achieved with more in situ data, e.g., longer discharge time series, measured cross-sections of the river, and tide data. Furthermore, a system analysis of floods, involving water intrusion from the sea, and the influence of the nearby Ahémé lake, are recommended in order to have a holistic perspective of floods hazards in the LMR basin. Finally, vulnerability and risk assessments are recommended for effective preparedness, response and adaptation to floods in the LMR basin.

5. Water cooperation in face of climate and land use changes in the transboundary Mono river basin[4]

Abstract

Effective cooperation between riparians is essential for sustainable development in transboundary river catchments. It is relevant in the current context of global changes. This study focuses on the Mono river catchment shared by Benin and Togo in west Africa. The study aims at assessing the present state of water cooperation in the Mono river catchment, and the readiness of the two countries to manage and respond to potential climate and land changes in a transboundary way. The water cooperation quotient (WCQ) was used to perform a participative assessment of the level of cooperation in the basin. Stakeholders and experts from NGOs, academia and technical sector, as well as decision making and policy implementation institutions, were involved in the assessment. Results indicate existing grounds for transboundary water cooperation (WCQ = 72/100). That finding updates the results published in 2017 by the Strategic Foresight Group (SFG). Mechanisms of data exchange, alternative dispute resolution, and frameworks for joint and sustainable coordination of flood, drought and ecosystems management are still lacking.

Keywords: Water cooperation, Transboundary basin, WCQ, Mono river catchment, Climate change, Land use change.

[4] This chapter (5) is submitted for publication and is under review as: Houngue, N. R., Evers, M., & Almoradie, A. D. S. (2023). Water cooperation in face of climate and land use changes in the transboundary Mono river basin. *Environment, development and sustainability.*

5.1. Introduction

Water is abundant on earth and represents an important resource for living beings. However, less than 3% of water stock on earth is freshwater, out of which, only 0.26% is stored in lakes and rivers which supply most human water consumption needs (Shiklomanov, 1993). Freshwater, from both surface and underground, is essential for socio-economic development.

Climate change is likely to affect freshwater availability, quality and demand. Changes in air and water temperature, and the modification of precipitation pattern (intensity, magnitude and distribution) are expected to increase water related risks (Bayramoglu et al., 2020). Sectors like agriculture, food security, health and sanitation, transport and industries are the most vulnerable and at risk (UNFCC, 2011). Moreover, inadequate land use is expected to aggravate climate change effects.

Climate and land cover changes have accelerated over the past five decades in West Africa (Abdulraheem et al., 2022; Herrmann et al., 2020; Ofori et al., 2021). The impacts of those changes have been extensively analysed in various catchments of the region (Coulibaly et al., 2018; Dembélé et al., 2022; Idrissou et al., 2022; Stanzel et al., 2018; Yéo et al., 2016). Transboundary catchments involving many countries, require attention in the current global change conditions. In fact, the compound effect of climate and land use change, and the difference of socio-politico-economic development strategies in riparian nations, emphasize the need to establish cooperation channels among the countries. Due to the borderless nature of water, riparian countries are bounded, and the actions from upstream countries may affect downstream residents (Benzie & Persson, 2019).

Climate change impact studies in the Mono river catchment, revealed an increase of mean temperature since the 1960s, and that is expected to continue until the end of the century (Amoussou, 2010a; Koubodana et al., 2020; E. Lawin, Lamboni, et al., 2019). Precipitation from the 2020s until 2100 are expected to be characterised by high variabilities, extreme rainfall, and delays and shift of seasons (Houngue et al., 2022; Lawin, Hounguè, et al., 2019). These changes will translate into modifications in the runoff of the Mono River, and potential flood and drought events (Batablinlè et al., 2021; Houngue, 2018). Moreover, changes in land use and land cover (LULC), including decline of forests and expansion of built-up areas, have been reported over the period 1980-2010, and are expected to keep on until 2070 (Koubodana et al., 2019; Thiam et al., 2022). Population growth, urbanization, climate change, soil degradation, and the lack of environmental and political commitment, among others, were reported as the drivers of land use and land cover change (LULCC) in the Mono catchment (Thiam et al., 2022). Moreover, the development plans being set up by the Governments of Benin and Togo in the Mono region may increase water demand and competition in the catchment. There are plans to build dams for agriculture and fish farming purposes, to extend fluvial transportation and tourism, and to develop water supply infrastructure (Benin Government, 2021; Togo Government, 2018). In addition to the existing Nangbéto dam, the two countries are planning to build a second hydropower dam on the Mono river, at Adjarala. Obahoundje et al., (Obahoundje et al., 2021)

reported that water demands for irrigation, consumption, livestock, industries and dams operation, will not be met under the future climate and land use change conditions projected for the Mono catchment, and if the Adjarala dam was built. A strong cooperation is therefore needed to effectively and sustainably adapt to existing flood risks (Kissi et al., 2015; Ntajal et al., 2017; Wetzel et al., 2022), and to prepare for the projected impacts of future climate, land use and socio-economic development actions.

Water cooperation plays a key role for water security. In that regard, transboundary water cooperation over rivers, lakes and aquifers is set as an indicator (indicator 6.5.2) of the Sustainable Development Goal 6 (SDG 6). The indicator 6.5.2, defined as "the proportion of transboundary basin area with an operational arrangement for water cooperation", focuses on the importance of transboundary cooperation. A first round of reports on the indicator were produced in 2017/2018 by countries around the world, while the second and latest reports were published in 2020/2021 (UN-Water, 2018, 2021). The Water Cooperation Quotient (WCQ) developed by the Strategic Foresight Group (SFG) in 2013 and updated in 2015 and 2017, serve as a metric for transboundary water cooperation assessment (SFG, 2013, 2015, 2017).

Considering the projected changes in the Mono river catchment, this study aims at assessing the current state of water cooperation in the catchment, as an indicator of the readiness of the two countries to jointly respond to potential climate and land use change impacts. The WCQ of the Mono River catchment was computed in a participatory way with national and local stakeholders. The results were compared with scores published by the SFG and official information communicated by Benin and Togo in their report on the SDG6 indicator 6.5.2. The WCQ is a dynamic metric, and this study attempts to provide an updated quotient for the Mono catchment since the last computation carried out in 2017 by the SFG.

5.2. Materials and Methods

5.2.1. The study area

The Mono River catchment located in west Africa is shared by the Republics of Benin and Togo, and covers an area of 23,736.64 Km^2. 89% of the catchment area is in Togo, while 11% is on Benin territory. The Mono River serves as natural border between both countries in the downstream. The two countries dispose of two joint bodies: the Mono Basin Authority (MBA), and a company (named Communauté Electrique du Bénin - CEB) that manages the common Nangbéto hydropower dam. It was reported that the effect of the Nangbéto dam constructed in 1987 is twofold: a positive impact characterised by the reduction of high flow peaks and the increase of baseflow; and undesirable consequences related to water releases from the dam, that create flooding in the downstream (MBA, 2022). Flood events are recurrent in the Mono catchment and communities living in the downstream are at higher risk (Kissi et al., 2015; Ntajal et al., 2017; Ntajal, Lamptey, & Sogbedji, 2016). Thus, 12,839 people lost their houses and 3,337 hectares of crops were inundated in 2007 in the commune of Grand-Popo at the downstream. Yet, a second and common hydropower dam is planned by the two countries over the Mono river, at the

downstream of the existing Nangbéto dam. The number of inhabitants living in the catchment is estimated to 5,266,832 in 2022, and is expected to reach 13,354,360 in 2050 (MBA, 2022). The main economic activities of the population are agriculture, fishing, livestock breeding (by transhumant breeders and small-scale farmers), and trade.

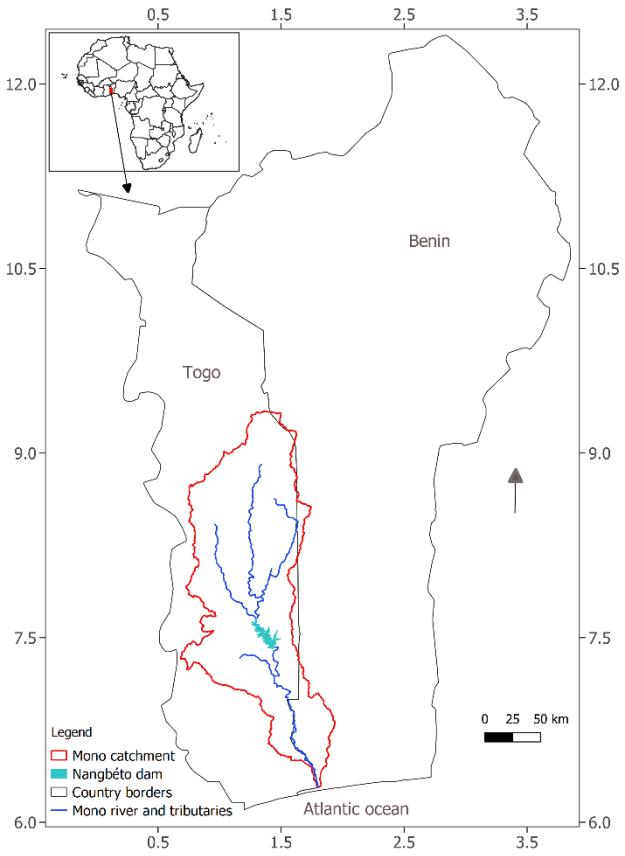

Figure 5.1. Location of the transboundary Mono river catchment

5.2.2. The water cooperation quotient

The water cooperation quotient (WCQ) is a metric developed by the Strategic Foresight Group (FSG) and meant to assess water cooperation and risk of conflicts in transboundary river basins. The first attempt to quantify transboundary water cooperation with the WCQ was done in 2013 (SFG, 2013). The computation was updated in 2015 and the last version was published in 2017 (SFG, 2015, 2017). The motto emphasized in each of those reports is that “any two countries engaged in active water cooperation do not go to war for any reason”. The Quotient is presented as an assessment and decision-making tool that Governments of riparian countries can build on to establish strong and basin-specific cooperation. The WCQ is linked to SDG 6, but also SDG 16 on peace, justice and strong institutions. In the 2017 report, the WCQ was computed for 231

watercourses in 146 countries all over the world, including the Mono river basin. The report was based on publically available information like the Global Environmental Facility (GEF) database, and the transboundary water treaties database of the Oregon State University. Information were also elicited from various experts. The Quotient computation method was developed by the SFG with experts from around the world.

The computation of the Quotient is based on 10 parameters organised into 3 groups: technical parameters, political parameters and, parameters for alternative conflict resolution and environmental protection. These are:

Technical parameters

1. Agreement
2. communication mechanism
3. technical projects
4. exchange of data

Alternative conflict resolution and environmental protection parameters

5. alternate dispute resolution
6. Flood, drought and infrastructure protection

Political parameters

7. Water infrastructure
8. Inclusion
9. Political commitment
10. institutional functioning

Climate and land use changes are accounted for in the quotient through parameter 6 on flood, drought and ecosystem. To compute the WCQ according to the FSG method, each parameter is assigned a weight of 1, 5 or 3 when it belongs to technical, political or to conflict resolution and environmental protection group respectively. Each parameter is assessed based on criteria presented in Table 5.1.

Table 5.1. WCQ parameters description

Parameter group	Parameter	Criteria	Weight
Technical cooperation	Agreement	The riparian countries have a legally binding agreement acknowledging the water relationship between them. The agreement may provide for allocation of water resources or for cooperation with or without any reference to allocation	1
	Communication mechanism	There is a mechanism for regular and formal communication between riparian countries in various forms, including meetings of officials of water ministries. The mechanism may include meetings of Water Ministers, but not other ministers such as Foreign Ministers and Finance Ministers and certainly not Heads of Government. The mechanism may be in the form of committees within respective water ministries. Regional economic cooperation organisations with water charters are not taken into consideration under the parameter of Communication Mechanism unless they are the only cooperative body on water and they are specifically dealing with shared watercourses.	1
	Technical Projects	The riparian countries engage in collaborative scientific and technical projects in relation to their shared watercourse such as small demonstration projects relating to navigation, irrigation, electricity or livelihood creating activities. It is to be noted that these projects are not those that are carried out by individual countries domestically but are those that are either basin wide or international in nature and are often implemented by or through River Basin Organisation or River Basin Commission (RBO/RBCs) or jointly by the riparian countries. It is to be further noted that these projects are different from large infrastructure projects	1
	Exchange of data	The riparian countries agree to exchange data on quantity and quality of shared water resources where the data is collected nationally, but exchanged on a regular basis through an agreed channel or it is collected and shared through a basin organisation.	1
alternative conflict resolution methods and/or	Alternative Dispute Resolution	The riparian countries have a well-defined mechanism for resolving disputes, which could be either through a River Basin Organisation, to which they belong, or through reference to a specific third party. If the countries approach the International Court of Justice (ICJ) to complain against other riparian countries, it is not to be taken into account in this context.	3

environmental, drought or flood control measures	Floods, Droughts and Ecosystem Protection	The riparian countries agree on long term coordination and cooperation mechanisms to manage floods, drought and ecosystem in a collaborative way, including early warning, rapid response, pollution control, coordination on deforestation, coordination on farming patterns and agricultural trade, and explicit long term coordination mechanism for emergency response.	3
Political cooperation	Water Infrastructure	Riparian countries agree that all infrastructure related to transboundary water resources such as dams, reservoirs, irrigation networks, navigation are built with active collaboration and transparency in a way that takes into account the interest of all relevant riparian countries and not merely the host country of the concerned project. They could have any one of the following: a. Infrastructure in any country built only with prior approval and consent of other riparian countries. b. Infrastructure built through joint or coordinated planning; joint investment. c. Infrastructure that has joint ownership. It is essential however, that the countries have no other projects that do not have prior approval and have been built over the objections of any of the other riparians.	5
	Inclusion	All countries in the basin, without exception, are members of the regional or basin wide arrangement.	5
	Political Commitment	The riparian countries commit to cooperate at the highest political level with either one or both of the following components: 1. Regular engagement at a level higher than Water Ministers, such as: a) Foreign Ministers b) Heads of Governments And/Or 2. Co-ordination and harmonization of national laws/policies to satisfy common standards.	5
	Institutional Functioning	The riparian countries have (a) A permanent, independent and joint organisation for transboundary water cooperation such as a River Basin Organisation with an independent secretariat or (b) Permanent, though separate entities located in the respective riparian countries, acting as a joint mechanism for water governance, and having regular formal communication in the form of meetings and approval authority for projects in any of the countries In addition and essentially, The riparian countries make joint strategic plans and implement them ensuring that the projects are executed within an agreed time frame and are not reduced to mere statements of intention.	5

Thus, the maximum score that a basin can reach is 30. The score is afterward translated into percentage to get the WCQ. Therefore, a score of 30/30 would be equivalent to a WCQ of 100, and a score of 10/30 corresponds to WCQ 33.33. However, when a watercourse is shared by only two countries, parameter 8 on inclusion turns out to be irrelevant and should not be evaluated. Thus, the maximum score corresponding to WCQ 100 in that case would be 25. The WCQ of the Mono river, shared only between Benin and Togo, will therefore be computed on that basis and it is given by:

$$WCQ = S/25 \times 100 \quad (5.1)$$

where S is the score obtained after assigning weights to parameters.

The parameters are assigned the full weight only when the associated criteria are fully met. A weight of 0 is applied when the criteria are not fulfilled, including partially.

5.2.3. Stakeholders engagement

Experts from 26 institutions were involved in the participatory computation of the WCQ of the Mono catchment. 13 institutions from Benin, 11 from Togo, and 2 common institutions jointly managed by the two countries (CEB and the Mono Basin Authority), were consulted during a 3-day workshop. The experts are the stakeholders of the transboundary CLIMAFRI project (Implementation of Climate-sensitive Adaptation strategies to Reduce Flood Risk in the transboundary Lower Mono River catchment in Benin and Togo). They were identified through a purposive sampling carried out at the beginning of the project, based on their local knowledge and their key role in flood and water management in the Mono River basin. The stakeholders come from different sectors and their diversity enriched the assessment process with mixed perspectives. The list of stakeholders is presented in details in the following section (*2.4. Computation of the water cooperation quotient*). During day 1, stakeholders were introduced to the concept and context of transboundary water cooperation as well as the WCQ. The aim was to assure a common understanding of parameters definition, criteria and weighting, and to pave the way for the actual computation process. Day 2 was dedicated to computation in small groups. Finally, all stakeholders came together on day 3 to discuss and consensually compute the WCQ of the Mono catchment.

5.2.4. Computation of the water cooperation quotient

The calculation of the WCQ was done in two steps: first, at sub-group level and after, with all stakeholders together. The stakeholders were organised into three main groups: non-governmental organisations (NGOs), research/academia/technical, and policy implementation/public administration. Table 5.2 presents the repartition in each group.

Table 5.2. Stakeholder groups for WCQ computation

NGOs	Research/Academia/Technical	Policy implementation/Public admin
JVE Benin	INRAB (Benin)	ANPC Benin
JVE-Togo	ITRA (Togo)	ANPC Togo
Red-Cross Benin	DG-Eau Benin	MCVDD (Benin)
Red-Cross Togo	DRE Togo	Ministry of Environment (Togo)
Caritas Benin	WASCAL Benin experts	Ministry of Agriculture (Benin)
Caritas Togo	WASCAL Togo experts	Ministry of Agriculture (Togo)
PNE-Benin	Directorate of Vegetal	FNEC Benin
GIZ Benin	Production (Togo)	Mono Basin Authority - MBA
Eau-Vive Togo		Commune of Athiémé
		CEB - Management of Nangbéto dam

JVE : Jeunes volontaires pour l'environnement (*Young Volunteers for the Environment*)
PNE : Programme national de l'eau (*National Water Partnership*)
GIZ : Deutsche Gesellschaft für Internationale Zusammenarbeit (*German Agency for International Cooperation*)
INRAB : Institut National des Recherches Agricoles du Bénin (*National Agricultural Research Institute of Benin*)
ITRA: Institut Togolais de Recherche Agronomique (*Agronomic Research Institute of Togo*)
DG-Eau Benin : Direction Générale de l'Eau (*General Directorate of Water of Benin*)
DRE Togo: Direction des Ressources en Eau du Togo (*Directorate of Water Resources of Togo*)
WASCAL: West African Climate Service Centre on Climate Change and Adapted Land Use
ANPC : Agence Nationale de la Protection Civile (*National Civil Protection Agency*)
MCVDD : Ministre du Cadre de Vie et du Développement Durable (*Ministry of Living Environment and Sustainable Development*)
FNEC : Fond National pour l'Environnement et le Climat (*National Fund for Environment and Climate*)

Most of the institutions involved exist or have their counterpart in both countries (e.g. Red-Cross, JVE, ANPC, water directorates, agricultural research institutes, ministries of environment and agriculture). Although the NGOs act at country level, they are national representations of big international organisations. They work on the ground and deal with environmental, water-related and disaster management topics in the two countries. Red-Cross and Caritas usually intervene for flood risk preparation, response and resilience in the Mono catchment. NGOs like JVE (Benin and Togo), PNE and Eau-Vive Togo are part of the Platform of Civil Society Organisations of the Mono basin (GWP, 2017). The 2nd group of researchers and technical stakeholders comprises experts of water, climate, and land use topics. The members of the 3rd group are from policy, decision making and implementation side.

The WCQ was computed in each group based on discussions, and the expert knowledge and judgment of the stakeholders. Finally, a plenary discussion was engaged in order to carry out a consensual computation by all stakeholders together.

5.3. Results and discussion

5.3.1. Group assessment

The results from groups computation are summarized in Table 5.3.
NGOs group, group 1, has a score of 25/25. Group 2 (research/academia/technical experts) got a score of 24/25, while group 3 (policy implementation and public administration experts) came up with a score of 18/25. Thus, the WCQ values as computed by group 1, group 2 and group 3 are respectively 100, 96 and 72. The value obtained by group 1 suggests a perfect and active water cooperation in the Mono basin. Members of group 2 found flaws only in the data exchange parameters. These are researchers and technical experts who generate and regularly used data, and are therefore in good position to report on actual data exchange between the two countries. Data exchange was also weighted 0 by group 3.

Table 5.3. Results of WCQ group computation

Parameter	Weight allocated		
	NGOs	Research/ Academia/ Technical	Policy implementation/ Public administration
1. Agreement	1	1	1
2. Communication mechanism	1	1	1
3. Technical projects	1	1	1
4. Data exchange	1	0	0
5. Alternative dispute resolution	3	3	0
6. Flood, drought and ecosystem protection	3	3	0
7. Water infrastructure	5	5	5
9. Political commitment	5	5	5
10. Institutional functioning	5	5	5
Score (S)	**25**	**24**	**18**

In addition, group 3 allocated 0 to parameter 5 (alternative dispute resolution) and parameter 6 (flood, drought and ecosystem). The members of the group indicated that an agreement was hard to reach for parameters that were given 0. The reasons given by stakeholders who initially did not agree with the weight 0 are:

- ***Data exchange***: data exchange occurs in the framework of projects and publications led together by institutions and researchers from the two countries;
- ***Alternative dispute resolution***: the existence of the Mono Basin Authority sets the ground for conflict resolution in the catchment;
- ***Flood, drought and ecosystem protection***: institutions from the Benin and Togo work sometimes together for flood and ecosystem protection: e.g. managers of the Nangbéto dam inform authorities of the two countries before opening water gates; the creation of

the transboundary biosphere reserve of the Mono delta (GIZ, 2013) is an example of joint ecosystem protection.

Table 5.4 presents an overview of the reasons why all the three groups assigned full weight to parameter 1, 2, 3, 7, 9 and 10.

Table 5.4. Parameters that were equally weighted during group computation

Parameter	Reason
1. Agreement	Existence of the Convention on the Statute of the Mono River and Creation of the Mono Basin Authority
2.Communication mechanism	The Council of Ministries in charge of water resources meets once a year in ordinary session or in extraordinary session if needed.
3.Technical projects	The Nangbéto dam that was jointly built in 1987 and is commonly managed by Benin and Togo through CEB; upcoming Adjarala dam project led by both countries
4. Data exchange	*not equally weighted by all groups. Reasons explained above*
5.Alternative dispute resolution	*not equally weighted by all groups. Reasons explained above*
6.Flood, drought and ecosystem protection	*not equally weighted by all groups. Reasons explained above*
7.Water infrastructure	The Nangbéto dam that was jointly built in 1987 and is commonly managed by Benin and Togo through CEB; upcoming Adjarala dam project led by both countries
9.Political commitment	Commitment of both Governments to cooperate
10.Institutional functioning	Existence and functioning of the MBA and CEB

5.3.2. All-together assessment of the WCQ

This step built on the results and discussion from group assessments. Here, the discussion and search of consensus were focused on parameters that were not equally weighted in the first step.

Data exchange

Stakeholders agree that there is currently no agreement between the riparians to share data collected at national level on water quality and quantity, on a regular basis and through a predefined channel. Therefore, the parameter was assigned 0.

Alternative dispute resolution

Despite the existence of the MBA, the Mono basin does not dispose of a well-defined mechanism for dispute resolution at the moment. Stakeholders highlighted however, the intervention of NGOs and national institutions towards communities affected by the Adjarala dam project in order to calm tensions and mediate. Nonetheless, a formal dispute and conflict management mechanism agreed upon by the two countries is lacking. Thus, this parameter is given 0.

Flood, drought and ecosystem protection

Benin and Togo respond separately to flood events in the Mono basin, even in the valley where communities from both countries equally endure flood impact, and even when alerts are simultaneously given to the two countries by Nangbéto managers. Drought has not been a critical concern in Togo and Benin since the 1970s-1980s (Nicholson et al., 2000). However, future climate projections in the Mono catchment indicate potential dry years in the next five decades. So far, the two countries are lacking official and well-defined early warning systems for those hazards, emergency response mechanisms, and a common and long-term coordination of environmental issues including pollution, deforestation and farming patterns. Such a framework is even more necessary considering the changes projected for in the catchment. Finally, stakeholders agree to allocated 0 to this parameter.

Stakeholders emphasized however, the fact that assigning 0 to those three parameters does not mean a nonfulfillment of all the criteria. Rather, some things are being done and there a need to improve and to establish appropriate cooperation frameworks.

Ultimately, the score as computed by all the stakeholders is 18/25. Therefore, water cooperation in the Mono catchment has a WCQ of 72

5.3.3. Discussion

The results obtained in this study, either at group level or consensually by all stakeholders, differ from the score published by the SFG report in 2017. The report indicates a score of 1/25, and thus WCQ = 4. That WCQ value was attributed to the fact that the MBA was created only in 2014, shortly before the preparation of the report in 2017. Only parameter 1 on agreement was taken as fulfilled. All other parameters were considered as unfulfilled, although the criteria e.g., for water infrastructure and political commitment are actually met on the ground. This raises questions on how detailed are the information used by the SFG on the one hand, and on the other, whether authorities from Benin and Togo, regularly communicate and make necessary information on the Mono basin publicly available. Furthermore, in spite of the detailed criteria description provided in the methodology of the SFG to quantify transboundary water cooperation, subjective analyses based on stakeholders' experience on the ground played a role in their perception. However, the involvement of stakeholders and their diversity has proven to be important for water cooperation assessment in the Mono catchment. Overall, the current state of water cooperation in the Mono catchment does not fulfil necessary criteria for an effective transboundary management of projected climate and land use change impacts. In that regard, Benin and Togo in their country report on SDG indicator 6.5.2, point out that no mutual assistance or mitigation measure with respect to transboundary water pollution and extreme

meteorological events resulting from climate change is in place (Benin, 2020; Togo, 2020). Data exchange, establishment of long-term coordination and cooperation agreements for flood, drought and ecosystems, political commitment, and institutional functioning will be essential to achieve that goal. Stakeholders pointed out the lack of socio-cultural dimensions in the parameters. For example, as in other west African countries, it is common in Benin and Togo to have disputes settled by traditional Chiefs without recourse to legal or judicial proceedings (Bagayoko & Koné, 2017; Fauvelle-Aymar, 2001). Likewise, gods' belief and fear of their chastisement prevent some communities from overexploiting forest and fish resources which therefore, contribute to the protection of the resources (DJOSSOU, 2014; Juhé-Beaulaton, 2007, 2008; Nobimè, 2020). These socio-cultural realities are specific to Benin and Togo, and they are important leverages for the protection of natural resources in both countries.

5.4. Conclusion

This study assessed the current state of water cooperation in the Mono catchment and its capacity to stand future climate and land use changes in a transboundary way. It was found that grounds for transboundary cooperation and joint coordination exist in the catchment, namely through the creation of the MBA and the existing actions at national level. However, the riparians of the Mono catchment, considering their current level of cooperation, do not dispose of all the mechanisms and frameworks to jointly coordinate their response and to sustainably manage the adverse impacts of future climate and land use changes. The riparian countries mainly respond separately at national scale. Therefore, emphasis should be put on data sharing, dispute resolution alternatives, and the harmonization of laws and policies to foster political commitment and institutional functioning.

6. Conclusion and recommendations

This thesis aimed at assessing climate and land use change impacts on floods in the Mono river catchment, while evaluating the capacity the riparian to respond to the impacts in a transboundary manner. Floods were analysed based on scenarios: RCP climate change scenarios, land use change scenarios and the scenarios of the construction of the Adjarala dam. The quantitative and model-based approaches used in this study were complemented with stakeholders' engagement. The key findings as well as limitations and outlook are presented below.

6.1. Key highlights

6.1.1. Alternatives to deal with gaps in precipitation data

The performance of three satellite-based precipitation product (CHIRPS, PERSIANN, TAMSAT), and one gauge-based product (GPCC) were evaluated as an alternative to station data that contain substantial gaps. Based on a grid-to-point analysis, all four products performed poorly at daily scale, but captures very well the seasonal cycles. GPCC exhibited the best results with respect to extreme precipitation representation. Further insight was explored using the products as input to the HBV hydrological model. CHIRPS depicted poor results when used for runoff simulation, and is therefore not recommended for flood modelling in the Mono river catchment. PERSIANN, GPCC and TAMSAT are rather recommended for such purposes. The study revealed that regardless of the product used to fill-in gaps in observation datasets, the resulting runoff remains almost identical to when observation datasets are used without being filled. The findings point out that using a strong interpolation method like Kriging in the Mono catchment could be enough to compute realistic areal precipitation, without any need to fill-in the missing values. That is specifically convenient when using lumped hydrologic models or when the focus is to display catchment averages for trend and pattern analyses.

6.1.2. RCM selection and future climate trend assessment

The CORDEX database provide a wide range of RCMs for climate change scenarios assessments. However, RCMs perform differently from one location to the other. This study proposed a systematic approach to select RCMs that best represent the temperature and precipitation patterns in the Mono river catchment. The TOPSIS MCDA method applied, led to the selection of 6 RCMs that were used to explore future climate in the catchment. This systematic ranking and selection of RCMs is a novelty in the Mono catchment and represent a major contribution for impact studies. Temperature depicts an increasing trend during the period 2022-2070, and for both scenarios RCP 4.5 and RCP 8.5. The concordance of the two scenarios on the trend, suggest a high likelihood of the projected changes. From an average annual temperature of 26.9°C during the period 1966–2015, it is expected to reach 27.8°C under RCP 4.5 and 28.4°C for RCP 8.5. As for

rainfall, it is expected to be characterized by variabilities, longer dry seasons and rainfall intensification during the period 2022-2070. Flood risks in the Mono catchment are expected to persist in the future due to rainfall intensification. However, the shrinkage of rainy seasons noticed on rainfall seasonal cycles, together with the increase of temperature, and changes in land use, may lead to drought episodes. Unlike flood, drought in the Mono catchment is so far not recurrent. Nonetheless, it may become a major hazard in the catchment based on the projected changes. Therefore, it is recommended to account for drought as a potential hazard in the next 50 years, and to identify appropriate adaptation measures.

6.1.3. Impact of climate change, land use change and Adjarala dam on floods

Extreme flood events will continue in the future, based on the climate change and land use change scenarios investigated in this study. A high interannual variability of runoff is expected from 2022 to 2070, with possibilities of drought and flood occurring in consecutive years. Floods that were known as 10-year return period events, HQ10, since the construction of the Nangbéto dam, are expected to become HQ2 events under climate and land use change effect. Therefore, it is recommended to strengthen flood protection measures and to avoid the expansion of settlements in flood prone areas that not yet settled. The Adjarala dam may reduce the magnitude and extent of extreme floods. For example, the Adjarala dam in combination with scenario RCP 4.5 reduces the magnitude of HQ10 by 26%. However, the new dam may reduce as well water availability during low flow period. This may affect ecosystems and the socio-economic activities of local communities. The projected impacts of climate and land use changes, call for both local and basin-scale measures to sustainably adapt.

6.1.4. Transboundary water cooperation

The investigation of transboundary water cooperation between riparians of the Mono river revealed that some cooperation elements are in place. These include the creation of the MBA, the existence of the Council of water Ministers from both countries, the common management of the Nangbéto dam, and the joint planning of the Adjarala dam. However, there is a lack of essential mechanisms like regular data sharing, early warning system for hazards, and an absence of long-term agreements for the management of environmental issues, including pollution and deforestation. This raises concerns on the coordinated response capacity of the two countries, in view of the cross-border projections of climate and land use in the catchment. This study provided an updated value of the WCQ. The participatory assessment of water cooperation with stakeholders and experts resulted in a WCQ of 72/100, which is different for the 4/100 score published in 2017 by the SFG. This is due to the dynamic aspect of the Quotient, and the added value of involving a diversity of stakeholders for both countries. An active and strong cooperation in the Mono catchment will require well-defined frameworks for data sharing, dispute resolution, and formal mechanisms for the management of ecosystems, flood, drought and other hazards. Joint actions will complement existing strategies at national scale.

6.2. Limitations and recommendations for future research

This thesis provides valuable findings towards a better understanding of climate and land use change impacts in the transboundary Mono river catchment. However, there is room to improve on some of the methods used, and to explore additional research elements.

The attempt of using remotely-sensed datasets to deal with gaps in precipitation records was based on four products, despite the enormous number of satellite-based and reanalysis datasets that exist. The selection of those four products was basically guided by how well they performed in other west African catchments. However, more products, including reanalysis datasets can be explored. In addition, the fours datasets were used in their raw state without correction. Undertaking a correction may improve their performance and provide an opportunity of using them for flood studies.

This study made use of the TOPSIS MCDA method to rank RCMs based on four statistical metrics used as criteria. For a stronger analysis, more criteria may be introduced to fine-tune the ranking and selection process. Moreover, using the ensemble (average) derived from the selected RCMs may be limiting, because some RCMs can outperform ensembles. Therefore, it is recommended to first compare the ensemble with individual RCMs. Furthermore, the assessment of future climate was based only on temperature and rainfall. This is due to the limited observation data available for other variables. However, the pattern of evapotranspiration, computed with a temperature-based method, can also be explored for a broader understanding of future climate impacts.

Climate and land use change impacts were not evaluated separately. This would have provided an in-depth view on the contribution of each of them to the projected changes in runoff, extremes, and flood hazard. Moreover, the effect of the Adjarala dam as analysed in this study did not account for other purposes of the dam like agriculture. Although SWAT was successfully calibrated and validated with good results, exploring other physically-based hydrological models could the subject of further studies. The same applies for new flood models that can be tested in the Mono basin. In addition to the SUFI-2 calibration programme used in this study, other programmes such as GLUE and Parasol, embedded in the SWAT model can also be examined. One limitation of this study was the restriction of flood modelling only along the main course of the Mono river. This was mainly due to the lack of data from major tributaries. The availability of long and good quality discharge data would improve the calibration of models and their subsequent output. Another limitation that can be addressed in further studies is the absence of measured cross-section information from the field. This was alternatively compensated with sections correction, however, field measurements could improve the results. It is also recommended to analyse the effect of tides and the Ahémé lake on floods in the lower Mono river basin.

Transboundary water cooperation, including transboundary hazards management in this study were addressed mainly from a general and quantitative perspective. Thus, the participatory approach involving stakeholders remained in the scope of quantifying the cooperation, and lacks an in-depth investigation of the management strategies in each country. Therefore, further

studies can focus on extensive examination of processes and practical operation: e.g., legislations and policies in place, the actors involved and their interconnection, the flood preparation, response and resilience chain, identification of country-specific socio-cultural realities in play, and how cooperation operates at local level among communities that cohabitate on both sides of frontiers. Understanding the mechanisms in each country will help to analyse commonalities and differences in order to establish an active and mutually benefiting cooperation.

7. References

Abbaspour, K. (2020). *SWATCUP "How to do": Validation.* Youtube. https://www.youtube.com/watch?v=7E9qxRzwmV4

Abbaspour, K. C. (2015). *SWAT-CUP SWAT Calibration and Uncertainty Programs. A User Manual*. https://swat.tamu.edu/media/114860/usermanual_swatcup.pdf

Abdulraheem, K. A., Adeniran, J. A., & Aremu, A. S. (2022). Carbon and precursor gases emission from forest and non-forest land sources in West Africa. *International Journal of Environmental Science and Technology*, *19*, 12003–12018. https://doi.org/10.1007/s13762-022-04304-7

Adeyewa, D. Z., & Nakamura, K. (2003). Validation of TRMM Radar Rainfall Data over Major Climatic Regions in Africa. *Journal of Applied Meteorology and Climatology*, *42*(2), 331–347. http://journals.ametsoc.org/jamc/article-pdf/42/2/331/3916451/1520-0450

Adger, W. N., Pulhin, J. M., Barnett, J., Dabelko, G. D., Hovelsrud, G. K., Levy, M., Spring, Ú. O., & Vogel, C. H. (2014). Human security. In C. B. Field, V. R. Barros, D. J. Dokken, K. J. Mach, M. D. Mastrandrea, T. E. Bilir, M. Chatterjee, K. L. Ebi, Y. O. Estrada, R. C. Genova, B. Girma, E. S. Kissel, A. N. Levy, S. MacCracken, P. R. Mastrandrea, & L. L. White (Eds.), *Climate Change 2014: Impacts, Adaptation, and Vulnerability. Part A: Global and Sectoral Aspects. Contribution of Working Group II to the Fifth Assessment Report of the Intergovernmental Panel on Climate Change* (pp. 755–791). Cambridge University Press, Cambridge. https://www.ipcc.ch/site/assets/uploads/2018/02/WGIIAR5-Chap12_FINAL.pdf

Adnan, M., Kang, S., Zhang, G., Saifullah, M., Anjum, M. N., & Ali, A. F. (2019). Simulation and Analysis of the Water Balance of the Nam Co Lake Using SWAT Model. *Water*, *11*. https://doi.org/https://doi.org/10.3390/w11071383

Akinsanola, A. A., & Ogunjobi, K. O. (2017). Evaluation of present-day rainfall simulations over West Africa in CORDEX regional climate models. *Environmental Earth Sciences*, *76*(10), 1–20. https://doi.org/10.1007/s12665-017-6691-9

Akinsanola, A. A., Ogunjobi, K. O., Gbode, I. E., & Ajayi, V. O. (2015). Assessing the Capabilities of Three Regional Climate Models over CORDEX Africa in Simulating West African Summer Monsoon Precipitation. *Advances in Meteorology*, *2015*. https://doi.org/10.1155/2015/935431

Alifu, H., Hirabayashi, Y., Imada, Y., & Shiogama, H. (2022). Enhancement of river flooding due to global warming. *Scientific Reports*, *12*. https://doi.org/10.1038/s41598-022-25182-6

Almoradie, A., Cortes, V. J., & Jonoski, A. (2015). Web-based stakeholder collaboration in flood risk management. *Journal of Flood Risk Management*, *8*(1), 19–38. https://doi.org/10.1111/jfr3.12076

Amoussou, E. (2010). *Variabilité pluviométrique et dynamique hydro-sédimentaire du bassin versant du complexe lagunaire Mono-Ahémé-Couffo (Afrique de l'Ouest)* [Université de Bourgogne]. https://www.theses.fr/2010DIJOL001.pdf

Amoussou, E., Awoye, H., Vodounon, H. S. T., Obahoundje, S., Camberlin, P., Diedhiou, A., Kouadio, K., Mahé, G., Houndénou, C., & Boko, M. (2020). Climate and extreme rainfall events in the mono river basin (West Africa): Investigating future changes with regional climate models. *Water (Switzerland)*, *12*(3). https://doi.org/10.3390/w12030833

Amoussou, E., Tramblay, Y., Totin, H. S. V., Mahé, G., & Camberlin, P. (2014). Dynamique et modélisation des crues dans le bassin du Mono à Nangbéto (Togo/BEN). *Hydrological Sciences Journal*, *59*(11), 2060–2071. https://doi.org/10.1080/02626667.2013.871015

AMPOFO, S., GYEKYE, E., AMPADU, B., & SACKEY, I. (2021). Modelling Soil and Water Dynamics in the Black Volta Basin Using the Soil and Water Assessment Tool (SWAT) Model. *Ghana Journal of Science, Technology and Development*, *7*(2. February 2021). https://doi.org/10.47881/259.967x

Arnell, N. W., & Gosling, S. N. (2016). The impacts of climate change on river flood risk at the global scale. *Climatic Change*, *134*, 387–401. https://doi.org/10.1007/s10584-014-1084-5

Asadullah, A., McIntyre, N., & Kigobe, M. (2008). Evaluation of five satellite products for estimation of rainfall over Uganda. *Hydrological Sciences Journal*, *53*(6), 1137–1150. https://doi.org/10.1623/hysj.53.6.1137

Ashouri, H., Hsu, K.-L., Sorooshian, S., Braithwaite, D. K., Knapp, K. R., Cecil, L. D., Nelson, B. R., & Prat, O. P. (2015). PERSIANN-CDR Daily precipitation climate data record from multisatellite observations for hydrological and climate studies. *American Meteorologial Society*, *January*, 69–84. https://doi.org/10.1175/BAMS-D-13-00068.1

Atiah, W. A., Amekudzi, L. K., Aryee, J. N. A., Preko, K., & Danuor, S. K. (2020). Validation of satellite and merged rainfall data over Ghana, West Africa. *Atmosphere*, *11*. https://doi.org/10.3390/ATMOS11080859

Awotwi, A., Kumi, M., Pe, J., Yeboah, F., & Ik, N. (2015). Earth Science & Climatic Change Predicting Hydrological Response to Climate Change in the White Volta. *Journal of Earth Science & Climatic Change*, *6*(1), 1–7. https://doi.org/10.4172/2157-7617.1000249

Badou, D. F., Diekkrüger, B., Kapangaziwiri, E., Mbaye, M. L., Yira, Y., Lawin, E. A., Oyerinde, G. T., & Afouda, A. (2018). Modelling blue and green water availability under climate change in the Beninese Basin of the Niger River Basin, West Africa. *Hydrological Processes*, *32*(16), 2526–2542. https://doi.org/10.1002/hyp.13153

Bagayoko, N., & Koné, F. R. (2017). *Les Mécanismes traditionnels de gestion des conflits en afrique subsaharienne*.

Barry, A. A., Caesar, J., Tank, A. M. G. K., Aguilar, E., Mcsweeney, C., Ahmed, M., Nikiema, M. P., Narcisse, K. B., Sima, F., Stafford, G., Touray, L. M., Ayilari-naa, J. A., Mendes, C. L., Tounkara, M., Gar-glahn, E. V. S., Coulibaly, M. S., Dieh, M. F., Oyegade, J. A., Sambou, E., & Laogbessi, E. T. (2018). West Africa climate extremes and climate change indices. *International Journal of Climatology*, *38*(February), 921–938. https://doi.org/10.1002/joc.5420

Batablinlè, L., Agnidé, L. E., Japhet, K. D., Ernest, A., & Expédit, V. (2021). Future changes in

precipitation, evapotranspiration and streamflows in the Mono Basin of West Africa. *Proceedings of the International Association of Hydrological Sciences*, *384*, 283–288. https://doi.org/10.5194/piahs-384-283-2021

Batablinlè, L., Lawin Agnidé, E., Celestin, M., & Zakari, M. D. (2019). Variability of Future Rainfall over the Mono River Basin of West-Africa. *American Journal of Climate Change*, *08*(01), 137–155. https://doi.org/10.4236/ajcc.2019.81008

Batablinle, L., Lawin, E., Agnide, S., & Celestin, M. (2018). Africa-Cordex simulations projection of future temperature, precipitation, frequency and intensity indices over Mono Basin in West Africa. *Journal of Earth Science & Climatic Change*, *09*(09), 1–12. https://doi.org/10.4172/2157-7617.1000490

Bates, B. C., Kundzewicz, Z. W., Wu, S., & Palutikof, J. P. (2008). Climate Change and Water. In *Climate change nd water. Technical Paper of the Intergovernmental Panel on Climate Change*. IPCC Secretariat. https://doi.org/10.1016/j.jmb.2010.08.039

Bayramoglu, B., Chakir, R., & Lungarska, A. (2020). Impacts of Land Use and Climate Change on Freshwater Ecosystems in France. *Environmental Modelling & Assessment*, *25*, 147–172. https://doi.org/10.1007/s10666-019-09673-x

Begou, J. C., Jomaa, S., Benabdallah, S., Bazie, P., Afouda, A., & Rode, M. (2016). Multi-Site Validation of the SWAT Model on the Bani Catchment : Model Performance and Predictive Uncertainty. *Water*, *8*. https://doi.org/10.3390/w8050178

Benin. (2020). *Établissement de rapports sur l'indicateur mondial 6.5.2 des ODD*. https://unece.org/sites/default/files/2021-11/Benin_2ndReporting_SDG652_2020_web_small.pdf

Benin Government. (2021). *Programme d'Action du Gouvernement: Synthèse et principaux projets*. https://beninrevele.bj/doc/197/download

Benzie, M., & Persson, Å. (2019). Governing borderless climate risks: moving beyond the territorial framing of adaptation. *International Environmental Agreements: Politics, Law and Economics*, *19*, 369–393. https://doi.org/10.1007/s10784-019-09441-y

Bergström, S. (1992). *THE HBVMODEL-its structure and applications*.

Berhanu, B., Seleshi, Y., Demisse, S. S., & Melesse, A. M. (2015). Flow Regime Classification and Hydrological Characterization: A Case Study of Ethiopian Rivers. *Water*, *7*, 3149–3165. https://doi.org/10.3390/w7063149

Beyer, R., Krapp, M., & Manica, A. (2020). An empirical evaluation of bias correction methods for palaeoclimate simulations. *Climate of the Past*, *16*(4), 1493–1508. https://doi.org/10.5194/cp-16-1493-2020

Boé, J., Terray, L., Habets, F., & Martin, E. (2007). Statistical and dynamical downscaling of the Seine basin climate for hydro-meteorological studies. *International Journal of Climatology*, *27*, 1643–1655. https://doi.org/10.1002/joc.1602

Bokhari, S. A. A., Ahmad, B., Ali, J., Ahmad, S., Mushtaq, H., & Rasul, G. (2018). Future Climate

Change Projections of the Kabul River Basin Using a Multi-model Ensemble of High-Resolution Statistically Downscaled Data. *Earth Systems and Environment*, *2*(3), 477–497. https://doi.org/10.1007/s41748-018-0061-y

Bormann, H., & Diekkrüger, B. (2003). Possibilities and limitations of regional hydrological models applied within an environmental change study in Benin (West Africa). *Physics and Chemistry of the Earth*, *28*(33–36), 1323–1332. https://doi.org/10.1016/j.pce.2003.09.008

Bossa, A. Y., Diekkrüger, B., & Agbossou, E. K. (2014). *Scenario-Based Impacts of Land Use and Climate Change on Land and Water Degradation from the Meso to Regional Scale*. 3152–3181. https://doi.org/10.3390/w6103152

Brunet-Moret, Y. (1971). Etude de l'homogénéité de séries chronologiques de précipitations annuelles par la méthode des doubles masses. *Cahiers de l'ORSTOM. Série Hydrologie*, *8*(4), 3–31.

Brunetti, M. T., Melillo, M., Gariano, S. L., Ciabatta, L., Brocca, L., Amarnath, G., & Peruccacci, S. (2021). Satellite rainfall products outperform ground observations for landslide prediction in India. *Hydrology and Earth System Sciences*, *25*, 3267–3279. https://doi.org/10.5194/hess-25-3267-2021

Callaghan, M., Schleussner, C., Nath, S., Lejeune, Q., Knutson, T. R., Reichstein, M., Hansen, G., Theokritoff, E., Andrijevic, M., Brecha, R. J., Hegarty, M., Jones, C., Lee, K., Lucas, A., Maanen, N. Van, Menke, I., Pfleiderer, P., Yesil, B., & Minx, J. C. (2021). Machine-learning-based evidence and attribution mapping of 100,000 climate impact studies. *Nature Climate Change*, *11*(November 2021), 966–972. https://doi.org/10.1038/s41558-021-01168-6

CCAFS. (2014). *GCM downscaled data portal*. Statistical Downscaling (Delta Method) CMIP3 Data. http://www.ccafs-climate.org/statistical_downscaling_delta/

Chen, J., Arsenault, R., Brissette, F. P., & Zhang, S. (2021). Climate Change Impact Studies: Should We Bias Correct Climate Model Outputs or Post-Process Impact Model Outputs? *Water Resources Research*, *57*(5), 1–22. https://doi.org/10.1029/2020WR028638

Cloke, H. L., Wetterhall, F., He, Y., Freer, J. E., & Pappenberger, F. (2012). Modelling climate impact on floods with ensemble climate projections. *Quarterly Journal of the Royal Meteorological Society Q. J. R. Meteorol. Soc*. https://doi.org/10.1002/qj.1998

CNEE. (2014). *Barrage hydroélectrique d'Adjarala. Avis sur l'examen de qualité de l'EIES*. https://www.eia.nl/docs/mer/diversen/pos099_cnee_adjarala.pdf

Collins, M., Knutti, R., Arblaster, J., Dufresne, J.-L., Fichefet, T., Friedlingstein, P., Gao, X., Gutowski, W. J., Johns, T., Krinne, G., Shongwe, M., Tebaldi, C., Weaver, A. J., & Wehner, M. (2013). Long-term Climate Change: Projections, Commitments and Irreversibility. In T. F. Stocker, D. Qin, G.-K. Plattner, M. Tignor, S. K. Allen, J. Boschung, A. Nauels, Y. Xia, V. Bex, & P. M. Midgley (Eds.), *Climate Change 2013: The Physical Science Basis. Contribution of Working Group I to the Fifth Assessment Report of the Intergovernmental Panel on Climate Change* (pp. 1029–1136). Cambridge University Press.

Coulibaly, N., Coulibaly, T. J. H., Mpakama, Z., & Savané, I. (2018). The impact of climate change

on water resource availability in a trans-boundary Basin in West Africa: The case of Sassandra. *Hydrology*, *5*. https://doi.org/10.3390/hydrology5010012

Crochemore, L., Ramos, M. H., & Pappenberger, F. (2016). Bias correcting precipitation forecasts to improve the skill of seasonal streamflow forecasts. *Hydrology and Earth System Sciences*, *20*(9), 3601–3618. https://doi.org/10.5194/hess-20-3601-2016

Das, P., Zhang, Z., & Ren, H. (2022). Evaluation of four bias correction methods and random forest model for climate change projection in the Mara River Basin, East Africa. *Journal of Water and Climate Change*, *13*(4), 1900–1919. https://doi.org/10.2166/wcc.2022.299

Deblauwe, V., Droissart, V., Bose, R., Sonké, B., Blach-Overgaard, A., Svenning, J. C., Wieringa, J. J., Ramesh, B. R., Stévart, T., & Couvreur, T. L. P. (2016). Remotely sensed temperature and precipitation data improve species distribution modelling in the tropics. *Global Ecology and Biogeography*, *25*(4), 443–454. https://doi.org/10.1111/geb.12426

Deepthi, B., Sunil, A., Nair, S. C., Mirajkar, A. B., & Adarsh, S. (2020). Ranking of Cmip5-Based General Circulation Models Using Compromise Programming and Topsis for Precipitation: a Case Study of Upper Godavari Basin, India. *International Journal of Big Data Mining for Global Warming*, *02*(02), 2050007. https://doi.org/10.1142/s2630534820500072

Dembélé, M., Vrac, M., Ceperley, N., Zwart, S. J., Larsen, J., Dadson, S. J., Mariéthoz, G., & Schaefli, B. (2022). Contrasting changes in hydrological processes of the Volta River basin under global warming. *Hydrology and Earth System Sciences*, *26*, 1481–1506. https://doi.org/10.5194/hess-26-1481-2022

Dembélé, M., & Zwart, S. J. (2016). Evaluation and comparison of satellite-based rainfall products in Burkina Faso , West Africa. *International Journal of Remote Sensing*, *37*(17), 3995–4014. https://doi.org/10.1080/01431161.2016.1207258

Dinku, T. (2019). Challenges with availability and quality of climate data in Africa. In A. M. Melesse, W. Abtew, & S. Gabriel (Eds.), *Extreme Hydrology and Climate Variability: Monitoring, Modelling, Adaptation and Mitigation* (Issue January, pp. 71–80). https://doi.org/10.1016/B978-0-12-815998-9.00007-5

Dinku, T., Funk, C., Peterson, P., Maidment, R., Tadesse, T., Gadain, H., & Ceccato, P. (2018). Validation of the CHIRPS satellite rainfall estimates over eastern Africa. *Quarterly Journal of the Royal Meteorological Society*, *144*(January), 292–312. https://doi.org/10.1002/qj.3244

Djan'na Koubodana, H., Adounkpe, J., Tall, M., Amoussou, E., Atchonouglo, K., & Mumtaz, M. (2020). Trend Analysis of Hydro-climatic Historical Data and Future Scenarios of Climate Extreme Indices over Mono River Basin in West Africa. *American Journal of Rural Development*, *8*(1), 37–52. https://doi.org/10.12691/ajrd-8-1-5

DJOSSOU, B. O. (2014). *Le vodun et la gestion durable des ressources naturelles*. Villakaro. https://villakaro.org/blog/2014/12/30/le-vodun-et-la-gestion-durable-des-ressources-naturelles/

DREF. (2011). *DREF final report Czech Republic : Floods Red Cross and Red Crescent action* (Issue DREF operation n° MDRTG003). https://reliefweb.int/report/togo/togo-floods-dref-

operation-n°-mdrtg003-final-report

Earle, A., Cascão, A. E., Hansson, S., Jägerskog, A., Swain, A., & Öjendal, J. (2015). Transboundary water management and the climate change debate. In *Earthscan Studies in Water Resource Management*. Routledge. https://doi.org/10.4324/9780203098929

Edwards, D. C., & Mckee, T. B. (1997). Characteristics of 20th century drought in the United States at multiple timescales. *Climatology Report*, *97–2*. http://weather.uwyo.edu/upperair/sounding.html

Evers, M., Almoradie, A. D. S., & de Brito, M. M. (2018). Enhancing flood resilience through collaborative modelling and multi-criteria decision analysis (MCDA). In A. Fekete & F. Fiedrich (Eds.), *Urban Disaster Resilience and Security* (pp. 221–236). Springer International Publishing AG. https://doi.org/10.1007/978-3-319-68606-6_14

Fallah, A., Rakhshandehroo, G. R., Berg, P., Sungmin, O., & Orth, R. (2020). Evaluation of precipitation datasets against local observations in southwestern Iran. *International Journal of Climatology*, *40*, 4102–4116. https://doi.org/10.1002/joc.6445

FAO. (2020). *global information and early warning system on food and agriculture (GIEWS): Country brief Togo*. https://www.fao.org/giews/countrybrief/country/TGO/pdf_archive/TGO_Archive.pdf

Fauvelle-Aymar, F.-X. (2001). Rois et Chefs en Afrique subsaharienne. In *Vingtième Siècle. Revue d'histoire* (pp. 176–178). Les Sciences Po. https://doi.org/10.3917/ving.069.0176

Funk, C. C., Peterson, P. J., Landsfeld, M. F., Diego, H. P., Verdin, J. P., Rowland, J. D., Romero, B. E., Husak, G. J., Michaelson, J. C., & Verdin, A. P. (2014). *A quasi-global precipitation time series for drought monitoring: U.S. Geological Survey Data Series 832*. https://doi.org/http://dx.doi.org/10.3133/ds832.

Gado, A. A. O. R. (2019). *Hydrological Modeling for Water Balance Components and Flood Hazard Assessment under Climate Change in Mono, Lower Basin, Benin and Togo* [Pan-African University]. http://repository.pauwes-cop.net/bitstream/handle/1/343/ABDEL AZIZ GADO MASTER THESIS_ FINAL VERSION_.pdf?sequence=1&isAllowed=y

Gbobaniyi, E., Sarr, A., Sylla, M. B., Diallo, I., Lennard, C., Dosio, A., Dhiédiou, A., Kamga, A., Klutse, N. A. B., Hewitson, B., Nikulin, G., & Lamptey, B. (2014). Climatology, annual cycle and interannual variability of precipitation and temperature in CORDEX simulations over West Africa. *International Journal of Climatology*, *34*(7), 2241–2257. https://doi.org/10.1002/joc.3834

Gbode, I. E., Ogunjobi, K. O., Dudhia, J., Ajayi, V. O., & Liu, C. (2021). Impacts of global warming on West African monsoon rainfall. In N. Oguge, D. Ayal, L. Adeleke, & I. da Silva (Eds.), *African Handbook ofClimate Change Adaptation* (pp. 2469–2483). Springer. https://doi.org/10.1016/j.atmosres.2020.105334

Gehne, M., Kiladis, G. N., Hamill, T. M., & Trenberth, K. E. (2016). Comparison of Global Precipitation Estimates across a Range of Temporal and Spatial Scales. *Journal of Climate*, *29*, 7773–7795. https://doi.org/10.1175/JCLI-D-15-0618.1

Githungo, W., Otengi, S., Wakhungu, J., & Masibayi, E. (2016). Infilling monthly rain gauge data gaps with satellite estimates for ASAL of Kenya. *Hydrology*, *3*(4). https://doi.org/10.3390/hydrology3040040

GIZ. (2013). *Deutsche Gesellschaft für Internationale Zusammenarbeit*. Transboundary Biosphere Reserve in the Mono Delta. https://www.giz.de/en/worldwide/27427.html

Gordon, N. D., Mcmahon, T. A., Finlayson, B. L., Gippel, C. J., & Nathan, R. J. (2004). *Stream Hydrology: An Introduction for Ecologists Second Edition*. John Wiley. https://www.researchgate.net/profile/Brian-Finlayson-2/publication/240311031_Stream_hydrology_an_introduction_for_ecologists/links/00b7d52e75ff67894d000000/Stream-hydrology-an-introduction-for-ecologists.pdf?origin=publicationDetail&_sg%5B0%5D=b3K62xUc7o3

Grillakis, M. G., Tsanis, I. K., & Koutroulis, A. G. (2010). Application of the HBV hydrological model in a flash flood case in Slovenia. *Natural Hazards and Earth System Science*, *10*(12), 2713–2725. https://doi.org/10.5194/nhess-10-2713-2010

Gründemann, G. J., van de Giesen, N., Brunner, L., & van der Ent, R. (2022). increase in magnitude under future climate change. *Communications Earth and Environment*, *3*, 1–9. https://doi.org/10.1038/s43247-022-00558-8

Gunavathi, S., & Selvasidhu, R. (2021). *Assessment of Various Bias Correction Methods on Precipitation of Regional Climate Model and Future Projection*. https://doi.org/10.21203/rs.3.rs-339080/v1

Gupta, H. V, Kling, H., Yilmaz, K. K., & Martinez, G. F. (2009). Decomposition of the mean squared error and NSE performance criteria : Implications for improving hydrological modelling. *Journal of Hydrology*, *377*(1–2), 80–91. https://doi.org/10.1016/j.jhydrol.2009.08.003

GWP. (2017). *Global Water Paternership*. LA PLATEFORME DES OSC DU BASSIN DU MONO (POSC MONO) Mise Sur Les Fonds Baptismaux. http://gwppnebenin.org/la-plateforme-des-osc-du-bassin-du-mono-posc-mono,1121.html

Hargreaves, G. H., & Samani, Z. (1985). Reference crop evapotranspiration from ambient air temperature. *Winter Meeting American Society of Agricultural Engineers*, 1–13. https://doi.org/10.13031/2013.26773

Hattermann, F. F., Vetter, T., Breuer, L., Su, B., Daggupati, P., Donnelly, C., Fekete, B., Florke, F., Gosling, S. N., Hoffmann, P., Liersch, S., Masaki, Y., Motovilov, Y., Muller, C., Samaniego, L., Stacke, T., Wada, Y., Yang, T., & Krysnaova, V. (2018). Sources of uncertainty in hydrological climate impact assessment: A cross-scale study. *Environmental Research Letters*, *13*(1). https://doi.org/10.1088/1748-9326/aa9938

Her, Y., Yoo, S., Cho, J., Hwang, S., Jeong, J., & Seong, C. (2019). Uncertainty in hydrological analysis of climate change : multi- parameter vs . multi-GCM ensemble predictions. *Scientific Reports*, 1–22. https://doi.org/10.1038/s41598-019-41334-7

Herrmann, S. M., Brandt, M., Rasmussen, K., & Fensholt, R. (2020). Accelerating land cover

change in West Africa over four decades as population pressure increased. *Communications Earth and Environment*, *1*(53), 1–10. https://doi.org/10.1038/s43247-020-00053-y

Hirsch, A. L., Guillod, B. P., Seneviratne, S. I., Beyerle, U., Boysen, L. R., Brovkin, V., Davin, E. L., Doelman, J. C., Kim, H., Mitchell, D. M., Nitta, T., Shiogama, H., Sparrow, S., Stehfest, E., van Vuuren, D. P., & Wilson, S. (2018). Biogeophysical Impacts of Land-Use Change on Climate Extremes in Low-Emission Scenarios: Results From HAPPI-Land. *Earth's Future*, *6*, 396–409. https://doi.org/10.1002/2017EF000744

Hirsch, A. L., Wilhelm, M., Davin, E. L., Thiery, W., & Seneviratne, S. I. (2017). Can climate-effective land management reduce regional warming? *Journal of Geophysical Research*, *122*(4), 2269–2288. https://doi.org/10.1002/2016JD026125

Homsi, R., Shiru, M. S., Shahid, S., Ismail, T., Harun, S. Bin, Al-Ansari, N., Chau, K. W., & Yaseen, Z. M. (2020). Precipitation projection using a CMIP5 GCM ensemble model: a regional investigation of Syria. *Engineering Applications of Computational Fluid Mechanics*, *14*(1), 90–106. https://doi.org/10.1080/19942060.2019.1683076

Hong, Y., Tang, G., Ma, Y., Huang, Q., Han, Z., Zeng, Z., Yang, Y., Wang, C., & Guo, X. (2018). Remote Sensing Precipitation: Sensors, Retrievals, Validations, and Applications. In X. Li & H. Vereecken (Eds.), *Observation and measurement. Ecohydrology* (Issue January, pp. 107–128). Springer, Berlin, Heidelberg. https://doi.org/10.1007/978-3-662-48297-1_4

HOUESSOU, S. (2016). *Les inondations et les risques previsionnels liés aux barrages hydroelectriques*. Université d'Abomey-Calavi.

Houngue, N. R. (2018). *Assessment of mid-century climate change impacts on Mono river's downstream inflows*. Université de Lomé.

Houngue, N. R., Almoradie, A. D. S., & Evers, M. (2022). A Multi Criteria Decision Analysis Approach for Regional Climate Model Selection and Future Climate Assessment in the Mono River Basin , Benin and Togo. *Atmosphere*, *13*, 1–19. https://doi.org/10.3390/ atmos13091471 Academic

Hounguè, N. R., Ogbu, K. N., Almoradie, A. D. S., & Evers, M. (2021). Evaluation of the performance of remotely sensed rainfall datasets for flood simulation in the transboundary Mono River catchment, Togo and Benin. *Journal of Hydrology: Regional Studies*, *36*. https://doi.org/10.1016/j.ejrh.2021.100875

Hounkpè, B. Y. J., Diekkrüger, B., Badou, D. F., Bossa, A. Y., Lawin, E. A., Adounkpè, J., & Afouda, A. A. (2019). How Does Climate and Land Use Change Influence Flood Hazard in Benin ? In *Regional Climate Change Series : Floods* (pp. 44–49). WASCAL Publishing. https://doi.org/10.33183/rccs.2019.p44

Hounkpe, J. (2016). *ASSESSING THE CLIMATE AND LAND USE CHANGES IMPACT ON FLOOD HAZARD IN OUÉMÉ RIVER BASIN, BENIN (WEST AFRICA)* [University of Abomey-Calavi]. http://wascal-uac.org/thesis/JeanHOUNKPE.pdf

Icyimpaye, G., Abdelbaki, C., & Mourad, K. A. (2022). Hydrological and hydraulic model for flood

forecasting in Rwanda. *Modeling Earth Systems and Environment*, *8*(1), 1179–1189. https://doi.org/10.1007/s40808-021-01146-z

Idrissou, M., Diekkrüger, B., Tischbein, B., de Hipt, F. O., Näschen, K., Poméon, T., Yira, Y., & Ibrahim, B. (2022). Modeling the Impact of Climate and Land Use/Land Cover Change on Water Availability in an Inland Valley Catchment in Burkina Faso. *Hydrology*, *9*. https://doi.org/10.3390/hydrology9010012

Ingram, W. (2016). Extreme precipitation: Increases all round. *Nature Climate Change*, *6*, 443–444. https://doi.org/10.1038/nclimate2966

IPCC. (2007). Climate Change 2007: The Physical Science Basis. Contribution of Working Group I to the Fourth Assessment Report of the Intergovernmental Panel on Climate Change. In S. Solomon, D. Qin, M. Manning, Z. Chen, M. Marquis, K. B. Averyt, M. Tignor, & H. L. Miller (Eds.), *Weather*. Cambridge University Press, Cambridge, United Kingdom and New York, NY, USA. https://doi.org/10.1256/wea.58.04

IPCC. (2014). Climate Change 2014: Impacts, Adaptation, and Vulnerability. Part A: Global and Sectoral Aspects. In B. C. Field, R. V. Barros, J. D. Dokken, J. K. Mach, M. D. Mastrandrea, B. T.E, M. Chatterjee, K. L. Ebi, Y. . Estrada, R. C. Genova, G. B., E. S. Kissel, A. N. Levy, S. MacCracken, M. P.R, & L. . White (Eds.), *Contribution of Working Group II to the Fifth Assessment Report of the Intergovernmental Panel on Climate Change*. Cambridge University Press, Cambridge, United Kingdom and New York, NY, USA.

IPCC. (2018). Summary for Policymakers. In V. Masson-Delmotte, P. Zhai, H.-O. Pörtner, D. Roberts, J. Skea, P. R. Shukla, A. Pirani, W. Moufouma-Okia, C. Péan, R. Pidcock, S. Connors, J. B. R. Matthews, Y. Chen, X. Zhou, M. I. Gomis, E. Lonnoy, T. Maycock, M. Tignor, & T. Waterfield (Eds.), *Global warming of 1.5°C. An IPCC Special Report on the impacts of global warming of 1.5°C above pre-industrial levels and related global greenhouse gas emission pathways, in the context of strengthening the global response to the threat of climate change,* (In Press). Cambridge University Press. www.environmentalgraphiti.org

IPCC. (2021a). Summary for Policymakers. In V. Masson-Delmotte, P. Zhai, A. Pirani, S. L. Connors, C. Péan, S. Berger, N. Caud, Y. Chen, L. Goldfarb, M. I. Gomis, M. Huang, K. Leitzell, E. Lonnoy, J. B. R. Matthews, T. K. Maycock, T. Waterfield, O. Yelekçi, R. Yu, & B. Zhou (Eds.), *Climate Change 2021: The Physical Science Basis. Contribution of Working Group I to the Sixth Assessment Report of the Intergovernmental Panel on Climate Change* (p. 42). Cambridge University Press. https://www.ipcc.ch/report/ar6/wg1/

IPCC. (2021b). Summary for Policymakers. In V. Masson-Delmotte, P. Zhai, A. Pirani, S. L. Connors, C. Péan, S. Berger, N. Caud, Y. Chen, L. Goldfarb, M. I. Gomis, M. Huang, K. Leitzell, E. Lonnoy, J. B. R. Matthews, T. K. Maycock, T. Waterfield, O. Yelekçi, R. Yu, & B. Zhou (Eds.), *Climate Change 2021: The Physical Science Basis. Contribution of Working Group I to the Sixth Assessment Report of the Intergovernmental Panel on Climate Change* (pp. 3–32). Cambridge University Press. https://doi.org/10.1017/9781009157896.001

IUCN. (2003). *The Essentials of Environmental Flows* (M. Dyson, G. Bergkamp, & J. Scanlon (eds.)). IUCN Publications Services Unit. https://portals.iucn.org/library/sites/library/files/documents/2008-096.pdf

IUSS Working Group WRB. (2006). *World reference base for soil resources 2006* (2nd editio). FAO.

Jenkinson, A. F. (1955). the Frequency distribution of the annual maximum (or minimum) values of meteorological elements. *Quaterly Journal of the Royal Meteorological Society*, *81*(348), 158–171.

Jones, R., & Boer, R. (2004). Assessing Current Climate Risks. In B. Lim, E. Spanger-Siegfried, I. Burton, E. L. Malone, & S. Huq (Eds.), *Adaptation Policy Frameworks for Climate Change: Developing Strategies, Policies and Measures* (pp. 91–117). Cambridge University Press.

Juhé-Beaulaton, D. (2007). Bois sacrés et conservation de la biodiversité dans l ' aire culturelle aja-fon (sud Bénin et Togo). In C. Deslaurier & D. J. Beaulaton (Eds.), *Afrique, terre d'histoire : au coeur de la recherche avec Jean Pierre Chrétien* (pp. 115–127). Karthala.

Juhé-Beaulaton, D. (2008). Sacred Forests and the Global Challenge of Biodiversity Conservation: The Case of Benin and Togo. *Journal for the Study of Religion, Nature and Culture*, *2*(3), 351–372. https://doi.org/10.1558/jsrnc.v2i3.351

Kebede, A., Diekkrüger, B., & Moges, S. A. (2014). Comparative study of a physically based distributed hydrological model versus a conceptual hydrological model for assessment of climate change response in the Upper Nile, Baro-Akobo basin: a case study of the Sore watershed, Ethiopia. *International Journal of River Basin Management*, *12*(4), 299–318. https://doi.org/10.1080/15715124.2014.917315

Khan, N., Shahid, S., Ahmed, K., Ismail, T., Nawaz, N., & Son, M. (2018). Performance assessment of general circulation model in simulating daily precipitation and temperature using multiple gridded datasets. *Water (Switzerland)*, *10*(12). https://doi.org/10.3390/w10121793

King, J. M., & Brown, C. (2018). Environmental Flow Assessments Are Not Realizing Their Potential as an Aid to Basin Planning. *Frontiers in Environmental Science Received:*, *6*(October). https://doi.org/10.3389/fenvs.2018.00113

Kissi, A. E., Abbey, G. A., Agboka, K., & Egbendewe, A. (2015). Quantitative Assessment of Vulnerability to Flood Hazards in Downstream Area of Mono Basin , South-Eastern Togo : Yoto District. *Journal of Geographic Information System*, *7*(December), 607–619. https://doi.org/10.4236/jgis.2015.76049

Koubodana, D. H., Diekkrüger, B., Näschen, K., Adounkpè, J., & Atchonouglo, K. (2019). Impact of the accuracy of land cover data sets on the accuracy of land cover change scenarios in the Mono River Basin , Togo , West Africa. *International Journal of Advanced Remote Sensing and GIS*, *8*(1), 3073–3095. https://doi.org/10.23953/cloud.ijarsg.422

Koubodana, H. Djan'na, Adounkpe, J. G., Atchonouglo, K., Djaman, K., Larbi, I., Lombo, Y., & Kpemoua, K. E. (2021). Modelling of streamflow before and after dam construction in the Mono River Basin in Togo- Benin, West Africa. *Intl. J. River Basin Management*, *1*, 1–17. https://doi.org/10.1080/15715124.2021.1969943

Koubodana, H.D, Adounkpe, J., Tall, M., Amoussou, E., Atchonouglo, K., & Mumtaz, M. (2020).

Trend Analysis of Hydroclimatic Historical Data and Future Scenarios of Climate Extreme Indices over Mono River Basin in West Africa. *American Journal of Rural Development*, *8*(1), 37–52. https://doi.org/10.12691/ajrd-8-1-5

Koutsouris, A. J., Seibert, J., & Lyon, S. W. (2017). Utilization of global precipitation datasets in data limited regions: A case study of Kilombero Valley, Tanzania. *Atmosphere*, *8*(12). https://doi.org/10.3390/atmos8120246

Krysanova, V., Vetter, T., Eisner, S., Huang, S., Pechlivanidis, I., Strauch, M., Gelfan, A., Kumar, R., Aich, V., Arheimer, B., Chamorro, A., Van Griensven, A., Kundu, D., Lobanova, A., Mishra, V., Plötner, S., Reinhardt, J., Seidou, O., Wang, X., … Hattermann, F. F. (2017). Intercomparison of regional-scale hydrological models and climate change impacts projected for 12 large river basins worldwide - A synthesis. *Environmental Research Letters*, *12*(10). https://doi.org/10.1088/1748-9326/aa8359

Kwawuvi, D., Mama, D., Agodzo, S. K., Hartmann, A., Larbi, I., Bessah, E., Limantol, A. M., Dotse, S.-Q., & Yangouliba, G. I. (2022). Spatiotemporal variability and change in rainfall in the Oti River Basin, West Africa. *Journal of Water and Climate Change*, *13*(3), 1151–1169. https://doi.org/10.2166/wcc.2022.368

Laplante, L. (1959). *Etude pédologique du comté de Bagot*. https://sis.agr.gc.ca/siscan/publications/surveys/pq/pq5/pq5_report.pdf

Larbi, I., Hountondji, F. C. C., Annor, T., Agyare, W. A., Gathenya, J. M., & Amuzu, J. (2018). Spatio-temporal trend analysis of rainfall and temperature extremes in the Vea catchment, Ghana. *Climate*, *6*(4). https://doi.org/10.3390/cli6040087

Lawin, A. E. (2007). *Analyse climatologique et statistique du regime pluviométrique de la haute vallee de l'Ouémé à partir des données pluviographiques AMMA-CATCH Bénin. PhD dissertation*. Institut National Polytechnique de Grenoble, Université d'Abomey-Calavi.

Lawin, A. E., Hounguè, N. R., Biaou, C. A., & Badou, D. F. (2019). Statistical Analysis of Recent and Future Rainfall and Temperature Variability in the Mono River Watershed. *Climate*, *7*(8). https://doi.org/10.3390/cli7010008

Lawin, E., Hounguè, N. R., Biaou, C. A., & Badou, D. F. (2019). Statistical analysis of recent and future rainfall and temperature variability in the Mono River watershed (Benin, Togo). *Climate*, *7*(8). https://doi.org/10.3390/cli7010008

Lawin, E., Hounguè, R., M'Po, Y. N. T., Hounguè, N. R., Attogouinon, A., & Afouda, A. A. (2019). Mid-century climate change impacts on Ouémé River discharge at Bonou Outlet (Benin). *Hydrology*, *6*(72). https://doi.org/10.3390/hydrology6030072

Lawin, E., Lamboni, B., Manirakiza, C., & Kamou, H. (2019). Future Extremes Temperature: Trends and Changes Assessment over the Mono River Basin, Togo (West Africa). *Journal of Water Resource and Protection*, *11*, 82–98. https://doi.org/10.4236/jwarp.2019.111006

Le Coz, C., & Van De Giesen, N. (2020). Comparison of rainfall products over sub-saharan africa. *Journal of Hydrometeorology*, *21*(4), 553–596. https://doi.org/10.1175/JHM-D-18-0256.1

Lee, S., Kim, S. W., Hwang, S. O., Choi, J. N., Ahn, K. B., & Kim, J. (2020). Comparative analysis of the cloud behavior over inland and coastal regions within single climate characteristics. *Atmosphere*, *11*(12), 1–16. https://doi.org/10.3390/atmos11121316

Lischeid, G., Dannowski, R., Kaiser, K., Nützmann, G., Steidl, J., & Stüve, P. (2021). Inconsistent hydrological trends do not necessarily imply spatially heterogeneous drivers. *Journal of Hydrology*, *596*(March), 126096. https://doi.org/10.1016/j.jhydrol.2021.126096

Luo, M., Liu, T., Meng, F., Duan, Y., Frankl, A., Bao, A., & De Maeyer, P. (2018). Comparing bias correction methods used in downscaling precipitation and temperature from regional climate models: A case study from the Kaidu River Basin in Western China. *Water (Switzerland)*, *10*(8). https://doi.org/10.3390/w10081046

Lutz, A. F., ter Maat, H. W., Biemans, H., Shrestha, A. B., Wester, P., & Immerzeel, W. W. (2016). Selecting representative climate models for climate change impact studies: an advanced envelope-based selection approach. *International Journal of Climatology*, *36*(12), 3988–4005. https://doi.org/10.1002/joc.4608

Macadam, I., Rowell, D. P., & Steptoe, H. (2020). Refining projections of future temperature change in West Africa. *Climate Research*, *82*, 1–14. https://doi.org/10.3354/CR01618

Maidment, R. I., Allan, R. P., & Black, E. (2015). Recent observed and simulated changes in precipitation over Africa. *Geophysical Research Letters*, *42*(19), 8155–8164. https://doi.org/10.1002/2015GL065765.Received

Maidment, R. I., Grimes, D., Allan, R. P., Tarnavsky, E., Stringer, M., Hewison, T., Roebeling, R., & Black, E. (2014). The 30 year TAMSAT african rainfall climatology and time series (TARCAT) data set. *Journal of Geophysical Research: Atmospheres*, *119*, 10619–10644. https://doi.org/10.1002/2014JD021927.Received

Mann, H. B. (1945). Non-parametric test against trend. *Econometrica*, *13*(3), 245–259. https://doi.org/10.2307/1907187

Maraun, D., Wetterhall, F., Ireson, A. M., Chandler, R. E., Kendon, E. J., Widmann, M., Brienen, S., Rust, H. W., Sauter, T., Themeßl, M., Venema, V. K. C., Chun, K. P., Goodess, C. M., Jones, R. G., Onof, C., Vrac, M., & Thiele-Eich, I. (2010). Precipitation downscaling under climate change: Recent developments to bridge the gap between dynamical models and the end user. *Reviews of Geophysics*, *48*(3), 2–34. https://doi.org/10.1029/2009RG000314

Matheron, G. (1963). Principles of geostatistics. *Economic Geology*, *58*, 1246–1266.

Mazzoleni, M., Dottori, F., Cloke, H. L., & Baldassarre, G. Di. (2022). fl ood extent at the global level. *Communications Earth and Environment*, *3*, 1–10. https://doi.org/10.1038/s43247-022-00598-0

MBA. (2022). *BOUCLIER-CLIMAT / Mono Project Towards a climate risks shield in the Mono River Basin Strengthening adaptation and resilience to climate change through integrated water resources and flood management*. https://www.adaptation-fund.org/projects-document-view?URL=https://spxdocs/en/081250007292242895/14670_OSS_Regional_ConceptNote-BOUCLIER-MONO_Project_May22_Reviewed_Clean_LOE_PFG.pdf

Mckee, T. B., Doesken, N. J., & Kleist, J. (1993). The relationship of drought frequency and duration to time scales. *Eighth Conference on Applied Climatology*, *January*, 179–184.

Mendez, M., Maathuis, B., Hein-Griggs, D., & Alvarado-Gamboa, L. F. (2020). Performance evaluation of bias correction methods for climate change monthly precipitation projections over Costa Rica. *Water (Switzerland)*, *12*(2). https://doi.org/10.3390/w12020482

Millington, N., Das, S., & Simonovic, S. P. (2011). *The Comparison of GEV, Log-Pearson Type 3 and Gumbel Distributions in the Upper Thames River Watershed under Global Climate Models* (Issue September). https://ir.lib.uwo.ca/cgi/viewcontent.cgi?article=1039&context=wrrr

Mishra, V., Kumar, D., Ganguly, A. R., Sanjay, J., Mujumdar, M., Krishnan, R., & Shah, R. D. (2014). Journal of Geophysical Research : Atmospheres. *Journal of Geophysical Research: Atmospheres*, *119*, 2966–2989. https://doi.org/10.1002/2014JD021636

Mitsopoulos, G., Panagiotatou, E., Sant, V., Baltas, E., Diakakis, M., Lekkas, E., & Stamou, A. (2022). Optimizing the Performance of Coupled 1D/2D Hydrodynamic Models for Early Warning of Flash Floods. *Water (Switzerland)*, *14*. https://doi.org/10.3390/w14152356

Moges, E., Demissie, Y., Larsen, L., & Yassin, F. (2021). Review : Sources of hydrological model uncertainties and advances in their analysis. *Water*, *18*, 1–23. https://doi.org/10.3390/w13010028

Moriasi, D. N., Arnold, J. G., Van Liew, M. W., Bingner, R. L., Harmel, R. D., & Veith, T. L. (2007). Model Evaluation Guidelines for Systematic Quantification of Accuracy in Watershed Simulations. *Transactions of the ASABE*, *50*(3), 885–900. https://doi.org/10.13031/2013.23153

N'Tcha M'Po, Y., Lawin, A. E., Oyerinde, G. T., Yao, B. K., & Afouda, A. A. (2016). Comparison of Daily Precipitation Bias Correction Methods Based on Four Regional Climate Model Outputs in Ouémé Basin, Benin. *Hydrology*, *4*(6), 58–71. https://doi.org/10.11648/j.hyd.20160406.11

Nash, E., & Sutcliffe, V. (1970). River flow forecasting through conceptual models Part I - A discussion of principles. *Journal of Hydrology*, *10*, 282–290.

Niang, I., Ruppel, O. C., Abdrabo, M. A., Essel, A., Lennard, C., Padgham, J., & Urquhart, P. (2014). Africa. In V. R. Barros, C. B. Field, D. J. Dokken, M. D. Mastrandrea, K. J. Mach, T. E. Bilir, M. Chatterjee, K. L. Ebi, Y. O. Estrada, R. C. Genova, B. Girma, E. S. Kissel, A. N. Levy, S. MacCracken, P. R. Mastrandrea, & L. L. White (Eds.), *Climate Change 2014: Impacts, Adaptation and Vulnerability: Part B: Regional Aspects: Working Group II Contribution to the Fifth Assessment Report of the Intergovernmental Panel on Climate Change* (pp. 1199–1266). Cambridge University Press. https://doi.org/10.1017/CBO9781107415386.002

Nicholson, S. E., Some, B., & Kone, B. (2000). An Analysis of Recent Rainfall Conditions in West Africa, Including the Rainy Seasons of the 1997 El Nin˜o and the 1998 La Nin˜a Years. *Journal of Climate*, *13*, 2628–2640. https://doi.org/10.1007/s10803-018-3505-1

Nicholson, Sharon E. (2013). The West African Sahel : A Review of Recent Studies on the Rainfall

Regime and Its Interannual Variability. *ISRN Meteorology*, *2013*, 1–32. https://doi.org/10.1155/2013/453521

Nobimè, F. (2020). *Gestion endogène des ressources naturelles : un atout pour la préservation de la biodiversité*. Miodjou. https://miodjou.com/2020/07/07/gestion-endogene-des-ressources-naturelles-un-atout-pour-la-preservation-de-la-biodiversite/

Ntajal, J., Lamptey, B. L., Mahamadou, I. B., & Nyarko, B. K. (2017). Flood disaster risk mapping in the Lower Mono River Basin in Togo, West Africa. *International Journal of Disaster Risk Reduction*, *23*, 93–103. https://doi.org/10.1016/j.ijdrr.2017.03.015

Ntajal, J., Lamptey, B. L., Mianikpo, J., & Kpotivi, W. K. (2016). Rainfall trends and flood frequency analyses in the lower Mono River basin in Togo, West Africa. *International Journal of Advance Research*, *4*(10), 1–11.

Ntajal, J., Lamptey, B. L., & Sogbedji, J. M. (2016). Flood Vulnerability Mapping in the Lower Mono River Basin in Togo, West Africa. *International Journal of Scientific & Engineering Research*, *7*(10), 1553–1562. https://www.ijser.org/research-paper-publishing-october-2016_page6.aspx

Ntajal, J., Lamptey, B. L., Sogbedji, M. J., & Wilson-bahun, K. K. (2016). Rainfall trends and flood frequency analyses in the lower Mono River basin in Togo, West Africa. *International Journal of Advance Research*, *4*(10). https://www.researchgate.net/profile/Joshua-Ntajal/publication/322604015_Rainfall_Trends_and_Flood_Frequency_Analysis_in_the_Lower_Mono_River_Basin_Togo_West_Africa/links/5a6278974585158bca4c567d/Rainfall-Trends-and-Flood-Frequency-Analysis-in-the-Lower-M

Obahoundje, S., Youan Ta, M., Diedhiou, A., Amoussou, E., & Kouadio, K. (2021). Sensitivity of Hydropower Generation to Changes in Climate and Land Use in the Mono Basin (West Africa) using CORDEX Dataset and WEAP Model. *Environmental Processes*, *8*(3), 1073–1097. https://doi.org/10.1007/s40710-021-00516-0

OCHA. (2010). *Benin inondations: Rapport de situation numero 9*. https://reliefweb.int/report/benin/bénin-inondations-2010-rapport-de-situation-09-12-november-2010

Ofori, S. A., Cobbina, S. J., & Obiri, S. (2021). Climate Change, Land, Water, and Food Security: Perspectives From Sub-Saharan Africa. *Frontiers in Sustainable Food Systems*, *5*, 1–9. https://doi.org/10.3389/fsufs.2021.680924

Ogbu, K. N., Hounguè, N. R., Gbode, I. E., & Tischbein, B. (2020). Performance Evaluation of Satellite-Based Rainfall Products over Nigeria. *Climate*, *8*(10), 103. https://doi.org/10.3390/cli8100103

Pastén-Zapata, E., Eberhart, T., Jensen, K. H., Refsgaard, J. C., & Sonnenborg, T. O. (2022). Towards a More Robust Evaluation of Climate Model and Hydrological Impact Uncertainties. *Water Resources Management*, *36*, 3545–3560. https://doi.org/10.1007/s11269-022-03212-2

Pechlivanidis, I. G., Arheimer, B., Donnelly, C., Hundecha, Y., Huang, S., Aich, V., Samaniego, L.,

Eisner, S., & Shi, P. (2017). Analysis of hydrological extremes at different hydro-climatic regimes under present and future conditions. *Climatic Change*, *141*, 467–481. https://doi.org/10.1007/s10584-016-1723-0

Pfahl, S., O'Gorman, P. ., & Fischer, E. . (2017). Understanding the regional pattern of projected future changes in extreme precipitation. *Nature Climate Change*, *7*, 423–428. https://doi.org/10.1038/nclimate3287

Piao, S., Friedlingstein, P., Ciais, P., de Noblet-ducoudre, N., Labat, D., & Zaehle, S. (2007). Changes in climate and land use have a larger direct impact than rising CO2 on global river runoff trends. *The Proceedings of the National Academy of Sciences (PNAS)*, *104*(39), 15242–15247. https://doi.org/10.1073/pnas.0707213104

Pierce, D. W., Cayan, D. R., Maurer, E. P., Abatzoglou, J. T., & Hegewisch, K. C. (2015). Improved bias correction techniques for hydrological simulations of climate change. *Journal of Hydrometeorology*, *16*(6), 2421–2442. https://doi.org/10.1175/JHM-D-14-0236.1

Poméon, T., Diekkrüger, B., Springer, A., Kusche, J., & Eicker, A. (2018). Multi-Objective Validation of SWAT for Sparsely-Gauged West African River Basins—A Remote Sensing Approach Thomas. *Water*, *10*. https://doi.org/10.3390/w10040451

Poméon, T., Jackisch, D., & Diekkrüger, B. (2017). Evaluating the performance of remotely sensed and reanalysed precipitation data over West Africa using HBV light. *Journal of Hydrology*, *547*, 222–235. https://doi.org/10.1016/j.jhydrol.2017.01.055

Potapov, P., Hansen, M. C., Pickens, A., Hernandez-serna, A., Tyukavina, A., Turubanova, S., Zalles, V., Li, X., Khan, A., Stolle, F., Harris, N., Song, X.-P., Baggett, A., Kommareddy, I., & Kommareddy, A. (2022). The Global 2000-2020 Land Cover and Land Use Change Dataset Derived From the Landsat Archive : First Results. *Frontiers in Remote Sensing*, *3*, 1–22. https://doi.org/10.3389/frsen.2022.856903

Putra, I. D. G. A., Rosid, M. S., Sopaheluwakan, A., & Sianturi, Y. C. U. (2020). The CMIP5 projection of extreme climate indices in Indonesia using simple quantile mapping method. In A. N. I. Wardana, S. Purwono, & P. H. Liem (Eds.), *AIP Conference Proceedings* (Vol. 2223, Issue 1). AIP Publishing. https://doi.org/10.1063/5.0000849

Raju, K. S., & Kumar, D. N. (2015). Ranking general circulation models for India using TOPSIS. *Journal of Water and Climate Change*, *6*(2), 288–299. https://doi.org/10.2166/wcc.2014.074

Refaey, M. A., Hassan, M., Mostafa, H., & Aboelkhear, M. (2019). Multi Criterion Decision Making Techniques for Ranking Regional climate models Over Wadi El-Natrun Catchment. *Australian Journal of Basic and Applied Sciences*, *13*(5), 85–96. https://doi.org/10.22587/ajbas.2019.13.5.9

Romilly, T. G., & Gebremichael, M. (2011). Evaluation of satellite rainfall estimates over Ethiopian river basins. *Hydrology and Earth System Sciences*, *15*(5), 1505–1514. https://doi.org/10.5194/hess-15-1505-2011

Rosenzweig, C., Casassa, G., Karoly, D. J., Imeson, A., Liu, C., Menzel, A., Rawlins, S., Root, T. L.,

Seguin, B., & Tryjanowski, P. (2007). Assessment of observed changes and responses in natural and managed systems. In M. L. Parry, O. F. Canziani, J. P. Palutikof, P. J. van der Linden, & C. E. Hanson (Eds.), *Climate Change 2007: Impacts, Adaptation and Vulnerability. Contribution of Working Group II to the Fourth Assessment Report of the Intergovernmental Panel on Climate Change.* (pp. 79–131). Cambridge University Press.

Sarr, M. A., Seidou, O., Tramblay, Y., & El Adlouni, S. (2015). Comparison of downscaling methods for mean and extreme precipitation in Senegal. *Journal of Hydrology: Regional Studies*, *4*(August), 369–385. https://doi.org/10.1016/j.ejrh.2015.06.005

Sawunyama, T., & Hughes, D. A. (2010). Using satellite-based rainfall data to support the implementation of environmental water requirements in South Africa. *Water SA*, *36*(4), 379–385. https://doi.org/10.4314/wsa.v36i4.58401

Schneider, U., Finger, P., Meyer-Christoffer, A., Ziese, M., & Becker, A. (2018). *Global Precipitation Analysis Products of the GPCC*.

Schuol, J, & Abbaspour, K. C. (2006). Calibration and uncertainty issues of a hydrological model (SWAT) applied to West Africa. *Advances in Geosciences*, *9*, 137–143. https://doi.org/10.5194/adgeo-9-137-2006

Schuol, Jürgen, Abbaspour, K. C., Srinivasan, R., & Yang, H. (2008). Estimation of freshwater availability in the West African sub-continent using the SWAT hydrologic model. *Journal of Hydrology*, *352*, 30–49. https://doi.org/10.1016/j.jhydrol.2007.12.025

Schuol, Jürgen, Abbaspour, K. C., Yang, H., Srinivasan, R., & Zehnder, A. J. B. (2008). Modeling blue and green water availability in Africa. *Water Resources Research*, *44*, 1–18. https://doi.org/10.1029/2007WR006609

Searcy, J. (1959). Flow-Duration Curves. In W. J. HICKEL (Ed.), *Manual of hydrology: Part 2. Low-flow techniques*. UNITED STATES GOVERNMENT PRINTING OFFICE. https://doi.org/10.3133/wsp1542A

Seibert, J. (2000). Multi-criteria calibration of a conceptual runoff model using a genetic algorithm. *Hydrology and Earth System Sciences*, *4*(2), 215–224. https://doi.org/10.5194/hess-4-215-2000

Seibert, J., & Beven, K. J. (2009). Gauging the ungauged basin: How many discharge measurements are needed? *Hydrology and Earth System Sciences*, *13*(6), 883–892. https://doi.org/10.5194/hess-13-883-2009

Seibert, J., & Vis, M. J. P. (2012). Teaching hydrological modeling with a user-friendly catchment-runoff-model software package. *Hydrology and Earth System Sciences*, *16*(9), 3315–3325. https://doi.org/10.5194/hess-16-3315-2012

Senent-Aparicio, J., Pérez-Sánchez, J., Carrillo-García, J., & Soto, J. (2017). Using SWAT and fuzzy TOPSIS to assess the impact of climate change in the headwaters of the Segura River Basin (SE Spain). *Water (Switzerland)*, *9*(2). https://doi.org/10.3390/w9020149

Seneviratne, S. I., Zhang, X., Adnan, M., Badi, W., Dereczynski, C., Luca, A. Di, Ghosh, S.,

Iskandar, I., Kossin, J., Lewis, S., Otto, F., Pinto, I., Satoh, M., Vicente-Serrano, S. M., Wehner, M., & Zhou, B. (2021). Weather and climate extreme events in a changing climate. In V. Masson-Delmotte, P. Zhai, A. Pirani, S. L. Connors, C. Péan, S. Berger, N. Caud, Y. Chen, L. Goldfarb, M. I. Gomis, M. Huang, K. Leitzell, E. Lonnoy, J. B. R. Matthews, T. K. Maycock, T. Waterfield, O. Yelekçi, R. Yu, & B. Zhou (Eds.), *Climate Change 2021: The Physical Science Basis. Contribution of Working Group I to the Sixth Assessment Report of the Intergovernmental Panel on Climate Change* (pp. 1513–1766). Cambridge University Press. https://doi.org/10.1017/9781009157896.013

SFG. (2013). *Water Cooperation for a Secure World: Focus on the Middle East*. https://www.strategicforesight.com/publication_pdf/20795water-cooperature-sm.pdf

SFG. (2015). *Water Cooperation Quotient*.

SFG. (2017). *Water Cooperation Quotient*.

Shiklomanov, I. (1993). World fresh water resources. In P. H. Gleick (Ed.), *Water in Crisis: A Guide to the World's Fresh Water Resources* (pp. 13–24). Oxford University Press.

Shiru, M. S., Shahid, S., Chung, E. S., Alias, N., & Scherer, L. (2019). A MCDM-based framework for selection of general circulation models and projection of spatio-temporal rainfall changes: A case study of Nigeria. *Atmospheric Research*, *225*(December 2018), 1–16. https://doi.org/10.1016/j.atmosres.2019.03.033

Shiwakoti, S. (2017). Hydrological modeling and climate change impact assessment using HBV Light Model: A case study of Karnali River Basin. *XVI World Water Congress*.

Sillmann, J., Stjern, C. W., Myhre, G., Samset, B. H., Hodnebrog, Ø., Andrews, T., Boucher, O., Faluvegi, G., Forster, P., Kasoar, M. R., Kharin, V. V, Kirkevåg, A., Lamarque, J., Olivié, D. J. L., Richardson, T. B., Shindell, D., & Takemura, T. (2019). Extreme wet and dry conditions affected differently by greenhouse gases and aerosols. *Npj Climate and Atmospheric Science*, *June*, 1–7. https://doi.org/10.1038/s41612-019-0079-3

Sitch, S., Brovkin, V., von Bloh, W., van Vuuren, D., Eickhout, B., & Ganopolski, A. (2005). Impacts of future land cover changes on atmospheric CO2 and climate. *Global Biogeochemical Cycles*, *19*(2), 1–15. https://doi.org/10.1029/2004GB002311

Sofia, G., Roder, G., Fonta, G. D., & Tarolli, P. (2017). Flood dynamics in urbanised landscapes : 100 years of climate and humans ' interaction. *Scientific Reports*, *7*, 1–12. https://doi.org/10.1038/srep40527

Sofiati, I., & Nurlatifah, A. (2019). The prediction of rainfall events using WRF (weather research and forecasting) model with ensemble technique. *International Conference Series: Earth and Environmental Science*, *374*, 12036. https://doi.org/10.1088/1755-1315/374/1/012036

Song, J., Her, Y., Shin, S., Cho, J., Paudel, R., Khare, Y., Obeysekera, J., & Martinez, C. J. (2020). Evaluating the performance of climate models in reproducing the hydrological characteristics of rainfall events. *Hydrological Sciences Journal*, *65*(9), 1490–1511. https://doi.org/10.1080/02626667.2020.1750616

Soriano, E., Mediero, L., & Garijo, C. (2019). Selection of bias correction methods to assess the impact of climate change on flood frequency curves. *Water (Switzerland)*, *11*(11), 2266–2281. https://doi.org/10.3390/w11112266

Stampoulis, D., & Anagnostou, E. (2012). Evaluation of global satellite rainfall products over Continental Europe. *Journal of Hydrometeorology*, *13*(2), 588–603. https://doi.org/10.1175/JHM-D-11-086.1

Stanski, H. R., Wilson, L. J., & Burrows, W. R. (1989). Survey of common verification methods in Meteorology. In *MSRB 89-5*. https://www.cawcr.gov.au/projects/verification/Stanski_et_al/Stanski_et_al.html

Stanzel, P., Kling, H., & Bauer, H. (2018). Climate change impact on West African rivers under an ensemble of CORDEX climate projections. *Climate Services*, *11*(July 2017), 36–48. https://doi.org/10.1016/j.cliser.2018.05.003

Sun, Q., Miao, C., Duan, Q., Ashouri, H., Sorooshian, S., & Hsu, K.-L. (2017). A Review of Global Precipitation Data Sets: Data Sources, Estimation, and Intercomparisons. *Reviews of Geophysics*, *56*(1). https://doi.org/10.1002/2017RG000574

Tabari, H. (2020). Climate change impact on flood and extreme precipitation increases with water availability. *Scientific Reports*, *10*, 1–10. https://doi.org/10.1038/s41598-020-70816-2

Tabari, H., Hosseinzadehtalaei, P., Aghakouchak, A., & Willems, P. (2019). Latitudinal heterogeneity and hotspots of uncertainty in projected extreme precipitation Latitudinal. *Environmental Research Letters*, *14*, 1–10. https://doi.org/10.1088/1748-9326/ab55fd

Tarnavsky, E., Grimes, D., Maidment, R., Black, E., Allan, R. P., Stringer, M., Chadwick, R., & Kayitakire, F. (2014). Extension of the TAMSAT Satellite-Based Rainfall Monitoring over Africa and from 1983 to Present. *Journal of Applied Meteorology and Climatology*, *53*, 2805–2822. https://doi.org/10.1175/JAMC-D-14-0016.1

Taylor, K. E. (2001). Summarizing multiple aspects of model performance in a single diagram. *Journal of Geophysical Research: Atmospheres*, *106*(D7), 7183–7192. https://doi.org/10.1029/2000JD900719

Teutschbein, C., & Seibert, J. (2012). Bias correction of regional climate model simulations for hydrological climate-change impact studies: Review and evaluation of different methods. *Journal of Hydrology*, *456–457*, 12–29. https://doi.org/10.1016/j.jhydrol.2012.05.052

Theil, H. (1950). A rank-invariant method of linear and polynomial regression analysis. I, II, III I, II, III. *Proceedings van de Koninklijke Nederlandse Akademie van Wetenschappen 53*, 398–392, 521–525, 1397–1412. https://www.eea.europa.eu/data-and-maps/indicators/oxygen-consuming-substances-in-rivers/theil-h-1950

Thiam, S., Salas, E. A. L., Houngue, N. R., Almoradie, D. A. S., Verleysdonk, S., Adounkpe, J. G., & Komi, K. (2022). Modelling Land Use and Land Cover in the Transboundary Mono River Catchment of Togo and Benin Using Markov Chain and Stakeholder's Perspectives. *Sustainability*, *14*(4160). https://doi.org/https://doi.org/10.3390/su14074160

Togo. (2020). *Établissement de rapports sur l'indicateur mondial 6.5.2 des ODD*. https://unece.org/sites/default/files/2021-11/Togo_2ndReporting_SDG652_2020_web.pdf

Togo Government. (2018). *Plan national de développement 2018 - 2022*. https://www.togofirst.com/media/attachments/2019/04/02/-pnd-2018-2022.pdf

Trisos, C. H., Adelekan, I. O., Totin, E., Ayanlade, A., Efitre, J., Gemeda, A., Kalaba, K., Lennard, C., Masao, C., Mgaya, Y., Ngaruiya, G., Olago, D., Simpson, N. P., & Zakieldeen, S. (2022). Africa. In H.-O. Pörtner, D. C. Roberts, M. Tignor, E. S. Poloczanska, K. Mintenbeck, A. Alegría, M. Craig, S. Langsdorf, S. Löschke, V. Möller, A. Okem, & B. Rama (Eds.), *Climate Change 2022: Impacts, Adaptation and Vulnerability. Contribution of Working Group II to the Sixth Assessment Report of the Intergovernmental Panel on Climate Change* (pp. 1285–1455). Cambridge University Press. https://doi.org/10.1017/9781009325844.011.1286

U. Charlene Gaba, O. (2015). An Ensemble Approach Modelling to Assess Water Resources in the Mékrou Basin, Benin. *Hydrology*, *3*(2), 22. https://doi.org/10.11648/j.hyd.20150302.11

UN-Water. (2018). *Progress on transboundary water cooperation 2018: global baseline for SDG indicator 6.5.2*. UN and UNESCO. https://unece.org/DAM/env/water/publications/WAT_57/ECE_MP.WAT_57.pdf

UN-Water. (2021). *Progress on Transboundary Water Cooperation: Global status of SDG indicator 6.5.2 and acceleration needs*. UN and UNESCO. https://unece.org/sites/default/files/2021-12/SDG652_2021_2nd_Progress_Report_ENG_web.pdf

UN. (2021). *The United Nations World Water Development Report 2021: Valuing Water*. UNESCO. https://doi.org/10.4324/9780429453571-2

UNDP. (1994). *Human Development Report 1994*. Oxford University Press. https://doi.org/10.1163/9789004481206_047

UNDP. (2010). *Evaluation des dommages, pertes et besoins de reconstruction Post catastrophes des inondations de 2010 au Togo*. https://www.gfdrr.org/sites/default/files/publication/pda-2010-togo-fr.pdf

UNECE. (2015a). *Policy Guidance Note on the Benefits of Transboundary Water Cooperation: Identification, Assessment and Communication*. United Nations. https://www.unece.org/fileadmin/DAM/env/water/publications/WAT_Benefits_of_Transboundary_Cooperation/ECE_MP.WAT_47_PolicyGuidanceNote_BenefitsCooperation_1522750_E_pdf_web.pdf

UNECE. (2015b). *Water and climate change adaptation in transboundary basins: Lessons learned and good practices*. United Nations. http://www.unece.org

UNFCC. (2011). *Climate change and freshwater resources: a synthesis of adaptation actions undertaken by Nairobi work programme partner organisations*. https://unfccc.int/resource/docs/publications/11_nwp_clim_freshwater_en.pdf

Veldkamp, T. I. E., Zhao, F., Ward, P. J., De Moel, H., Aerts, J. C. J. H., Schmied, H. M., Portmann,

F. T., Masaki, Y., Pokhrel, Y., Liu, X., Satoh, Y., Gerten, D., Gosling, S. N., Zaherpour, J., & Wada, Y. (2018). Human impact parameterizations in global hydrological models improve estimates of monthly discharges and hydrological extremes: A multi-model validation study. *Environmental Research Letters*, *13*. https://doi.org/10.1088/1748-9326/aab96f

Vivekananda, J. (2022). Why Climate Change Matters for Human Security. In *Reimagining the Human-Environment Relationship*. International Development Research Centre (IDRC). https://collections.unu.edu/eserv/UNU:8836/UNUUNEP_Vivekananda_RHER.pdf

Vogel, M. R., & Fennessey, N. M. (1994). Flow-duration curves. New interpretation and confidence intervals. *Journal of Water Resources Planning and Management*, *120*(4), 485–504. https://sites.tufts.edu/richardvogel/files/2019/04/flowDuration1.pdf

von Mises, R. (1936). La distribution de la plus grande de n valeurs. *Rev. Math. Union Interbalcanique*, *1*, 141–160.

Wang, L., Ranasinghe, R., Maskey, S., van Gelder, P. H. A. J. M., & Vrijling, J. K. (2015). Comparison of empirical statistical methods for downscaling daily climate projections from CMIP5 GCMs: A case study of the Huai River Basin, China. *International Journal of Climatology*, *36*(1), 145–164. https://doi.org/10.1002/joc.4334

WB, & UNDP. (2011). *Inondations au Bénin: Rapport d'évaluation des besoins post catastrophe*. https://www.gfdrr.org/sites/default/files/publication/pda-2011-benin-fr.pdf

Wetzel, M., Schudel, L., Almoradie, A., Komi, K., Adounkpè, J., Walz, Y., & Hagenlocher, M. (2022). Assessing Flood Risk Dynamics in Data-Scarce Environments — Experiences From Combining Impact Chains With Bayesian Network Analysis in the Lower Mono River. *Frontiers in Water*, *4*(March), 1–16. https://doi.org/10.3389/frwa.2022.837688

WMO. (2012). *Standardized Precipitation Index User Guide* (M. Svoboda, M. Hayes, & D. Wood (eds.); Vol. 1090).

WMO. (2019). *Guidance on Environmental Flows. Integrating E-flow Science with Fluvial Geomorphology to Maintain Ecosystem Services* (Issue 1235). World Meteorological Organization (WMO).

Xia, X., Liu, Y., Jing, W., & Yao, L. (2021). Assessment of Four Satellite-Based Precipitation Products over the Pearl River Basin, China. *IEEE Access*, *9*. https://doi.org/10.1109/ACCESS.2021.3095239

Yéo, W. E., Goula, B. T. A., Diekkrüger, B., & Afouda, A. (2016). Vulnerability and adaptation to climate change in the Comoe River Basin (West Africa). *SpringerPlus*, *5*. https://doi.org/10.1186/s40064-016-2491-z

Yilmaz, B., & Harmancioglu, N. B. (2010). Multi-criteria decision making for water resource management: A case study of the Gediz River Basin, Turkey. *Water SA*, *36*(5), 563–576. https://doi.org/10.4314/wsa.v36i5.61990

Yip, S., Ferro, C. A. T., Stephenson, D. B., & Hawkins, E. (2011). A Simple, coherent framework for partitioning uncertainty in climate predictions. *Journal of Climate*, *24*(17), 4634–4643.

https://doi.org/10.1175/2011JCLI4085.1

Zeyaeyan, S., Fattahi, E., Ranjbar, A., & Vazifedoust, M. (2017). Classification of rainfall warnings based on the TOPSIS method. *Climate*, *5*(2). https://doi.org/10.3390/cli5020033

Ziese, M., Rauthe-Schöch, A., Becker, A., Finger, P., Meyer-Christoffer, A., & Schneider, U. (2018). *GPCC Full Data Daily Version.2018 at 1.0°: Daily Land-Surface Precipitation from Rain-Gauges built on GTS-based and Historic Data*. GPCC Full Data Daily Version 2018. https://doi.org/10.5676/DWD_GPCC/FD_D_V2018_100

8. Appendices

8.1. Appendix I. TOPSIS ranking scores for rainfall

Station	CNRM-CCLM4	ICHEC-CCLM4	MOHC-CCLM4	MPI-CCLM4	ICHEC-RACMO22T	MOHC-RACMO22T	CCCma-RCA4	CNRM-RCA4	CSIRO-RCA4	IPSL-RCA4	MIROC-RCA4	MOHC-RCA4	MPI-RCA4	ICHEC-REMO	MPI-REMO
Abomey	0.03	0.84	0.83	0.87	0.87	0.13	0.10	0.76	0.25	0.16	0.88	0.94	0.94	0.84	0.27
Adeta	0.12	0.87	0.84	0.84	0.83	0.11	0.10	0.11	0.22	0.08	0.25	0.28	0.89	0.87	0.22
Afagnan	0.01	0.10	0.11	0.11	0.11	0.08	0.06	0.06	0.11	0.07	0.14	0.16	0.17	0.11	0.90
Agouna	0.03	0.51	0.52	0.93	0.92	0.49	0.06	0.11	0.16	0.09	0.52	0.21	0.53	0.88	0.18
Akaba	0.36	0.87	0.61	0.62	0.62	0.08	0.32	0.13	0.20	0.11	0.39	0.21	0.64	0.64	0.34
Aklakou	0.10	0.16	0.18	0.18	0.17	0.16	0.16	0.16	0.21	0.18	0.24	0.26	0.27	0.18	0.81
Amou-Oblo	0.18	0.49	0.74	0.76	0.53	0.49	0.12	0.18	0.22	0.16	0.26	0.55	0.48	0.55	0.47
Aneho-Glidji	0.11	0.20	0.19	0.23	0.77	0.23	0.21	0.18	0.27	0.25	0.29	0.34	0.35	0.66	0.96
Anie-Mono	0.26	0.91	0.60	0.93	0.30	0.45	0.46	0.53	0.33	0.19	0.59	0.59	0.94	0.35	0.52
Aplahoue	0.02	0.80	0.83	0.85	0.89	0.12	0.10	0.14	0.22	0.15	0.87	0.96	0.94	0.82	0.25
Atakpame	0.10	0.91	0.53	0.53	0.90	0.49	0.10	0.13	0.19	0.49	0.53	0.53	0.54	0.90	0.23
Athieme	0.03	0.14	0.14	0.87	0.91	0.13	0.13	0.79	0.18	0.14	0.20	0.25	0.25	0.83	0.18
Bante	0.47	0.85	0.92	0.91	0.53	0.49	0.46	0.17	0.23	0.09	0.54	0.53	0.93	0.53	0.53
Bassila	0.34	0.84	0.91	0.90	0.90	0.33	0.33	0.12	0.21	0.09	0.39	0.41	0.94	0.86	0.40
Blitta	0.37	0.89	0.81	0.83	0.67	0.61	0.33	0.34	0.19	0.07	0.37	0.41	0.87	0.94	0.34
Bohicon	0.02	0.52	0.51	0.52	0.84	0.10	0.09	0.49	0.18	0.11	0.52	0.54	0.54	0.84	0.21
Bopa	0.02	0.16	0.17	0.18	0.89	0.12	0.11	0.10	0.19	0.14	0.91	0.25	0.25	0.83	0.20
Dogbo	0.03	0.11	0.10	0.11	0.11	0.08	0.07	0.06	0.12	0.07	0.95	0.16	0.16	0.12	0.12
Grand-Popo	0.05	0.09	0.10	0.12	0.17	0.16	0.14	0.11	0.17	0.15	0.18	0.22	0.22	0.10	0.91
Kara	0.38	0.89	0.89	0.90	0.41	0.29	0.30	0.38	0.32	0.30	0.46	0.40	0.92	0.46	0.65
Kougnohou	0.19	0.82	0.63	0.65	0.53	0.31	0.30	0.31	0.24	0.18	0.33	0.38	0.67	0.77	0.27
Kpewa-Aledjo	0.31	0.90	0.75	0.91	0.66	0.29	0.28	0.30	0.23	0.29	0.36	0.35	0.92	0.78	0.54
Lokossa	0.02	0.17	0.89	0.86	0.82	0.79	0.17	0.12	0.23	0.17	0.22	0.27	0.30	0.80	0.25
Lonkly	0.03	0.84	0.87	0.87	0.86	0.11	0.08	0.14	0.19	0.10	0.24	0.26	0.95	0.21	0.21
Malfacassa	0.35	0.66	0.68	0.91	0.68	0.34	0.33	0.34	0.20	0.34	0.40	0.22	0.94	0.67	0.38
Nangbeto	0.05	0.86	0.93	0.90	0.79	0.15	0.11	0.06	0.26	0.07	0.80	0.89	0.31	0.84	0.29
Niaouli	0.03	0.12	0.12	0.13	0.94	0.10	0.09	0.07	0.15	0.11	0.16	0.20	0.20	0.87	0.15
Notse	0.08	0.88	0.18	0.92	0.15	0.09	0.07	0.10	0.16	0.07	0.19	0.22	0.98	0.16	0.18
Penesoulou	0.27	0.90	0.76	0.76	0.53	0.27	0.26	0.28	0.17	0.25	0.31	0.30	0.53	0.52	0.32
Savalou	0.07	0.87	0.52	0.92	0.52	0.49	0.09	0.09	0.17	0.08	0.50	0.52	0.53	0.88	0.18

Sokode	0.28	0.91	0.53	0.93	0.92	0.28	0.28	0.28	0.19	0.10	0.32	0.33	0.75	0.75	0.33
Sotouboua	0.13	0.93	0.59	0.59	0.43	0.22	0.22	0.22	0.16	0.06	0.25	0.28	0.78	0.62	0.23
Tabligbo	0.01	0.17	0.18	0.89	0.83	0.12	0.12	0.10	0.19	0.14	0.19	0.24	0.25	0.81	0.23
Tchamba	0.29	0.91	0.74	0.90	0.32	0.27	0.26	0.26	0.30	0.07	0.33	0.32	0.75	0.53	0.50
Tchetti	0.04	0.84	0.88	0.90	0.85	0.79	0.08	0.14	0.19	0.10	0.86	0.24	0.93	0.83	0.22
Toffo	0.04	0.17	0.13	0.16	0.90	0.08	0.06	0.10	0.15	0.11	0.19	0.22	0.21	0.88	0.89
Wahala	0.11	0.87	0.24	0.91	0.89	0.11	0.09	0.13	0.21	0.11	0.23	0.27	0.97	0.88	0.24
Yegue	0.34	0.66	0.68	0.91	0.40	0.63	0.33	0.35	0.19	0.10	0.40	0.40	0.93	0.67	0.40

8.2. Appendix II. Topsis ranking scores for temperature

Station	CNRM-CCLM4	ICHEC-CCLM4	MOHC-CCLM4	MPI-CCLM4	ICHEC-RACMO22T	MOHC-RACMO22T	CCCma-RCA4	CNRM-RCA4	CSIRO-RCA4	IPSL-RCA4	MIROC-RCA4	MOHC-RCA4	MPI-RCA4	ICHEC-REMO	MPI-REMO
Abomey	0.34	0.53	0.80	0.83	0.75	0.37	0.43	0.39	0.53	0.46	0.08	0.21	0.76	0.62	0.76
Adeta	0.23	0.75	0.67	0.63	0.56	0.31	0.46	0.26	0.43	0.31	0.00	0.18	0.89	0.46	0.64
Afagnan	0.38	0.49	0.75	0.84	0.75	0.35	0.41	0.42	0.56	0.48	0.00	0.22	0.67	0.67	0.82
Agouna	0.29	0.24	0.89	0.74	0.76	0.47	0.38	0.38	0.62	0.47	0.20	0.33	0.47	0.57	1.00
Akaba	0.52	0.22	0.58	0.31	0.30	0.21	0.24	0.66	0.83	0.72	0.48	0.56	0.27	0.18	0.74
Aklakou	0.44	0.31	0.67	0.72	0.50	0.50	0.53	0.51	0.65	0.56	0.03	0.29	0.42	0.53	0.94
AmouOblo	0.46	0.34	0.68	0.41	0.39	0.09	0.18	0.59	0.79	0.67	0.37	0.48	0.41	0.23	0.86
AnehoGlidji	0.44	0.31	0.67	0.72	0.50	0.50	0.53	0.51	0.65	0.56	0.03	0.29	0.42	0.53	0.94
AnieMono	0.41	0.14	0.69	0.49	0.50	0.38	0.30	0.55	0.70	0.60	0.38	0.45	0.27	0.38	0.86
Aplahoue	0.34	0.58	0.77	0.83	0.75	0.37	0.44	0.40	0.54	0.46	0.08	0.21	0.82	0.63	0.76
Atakpame	0.31	0.21	0.75	0.64	0.63	0.39	0.31	0.43	0.62	0.50	0.21	0.33	0.41	0.49	0.89
Athieme	0.38	0.49	0.75	0.84	0.75	0.35	0.41	0.42	0.56	0.48	0.00	0.22	0.67	0.67	0.82
Bante	0.40	0.29	0.56	0.65	0.53	0.41	0.40	0.46	0.67	0.52	0.12	0.42	0.45	0.51	0.51
Bassila	0.45	0.28	0.55	0.63	0.48	0.32	0.33	0.51	0.68	0.56	0.23	0.53	0.43	0.49	0.49
Blitta	0.52	0.34	0.45	0.43	0.34	0.31	0.37	0.58	0.76	0.67	0.25	0.56	0.39	0.28	0.38
Bohicon	0.34	0.53	0.80	0.83	0.75	0.37	0.43	0.39	0.53	0.46	0.08	0.21	0.76	0.62	0.76
Bopa	0.38	0.49	0.75	0.84	0.75	0.35	0.41	0.42	0.56	0.48	0.00	0.22	0.67	0.67	0.82
DogboTota	0.38	0.49	0.75	0.84	0.75	0.35	0.41	0.42	0.56	0.48	0.00	0.22	0.67	0.67	0.82
GrandPopo	0.59	0.53	0.65	0.62	0.43	0.12	0.17	0.62	0.68	0.68	0.37	0.62	0.56	0.47	0.46
Kara	0.59	0.53	0.65	0.62	0.43	0.12	0.17	0.62	0.68	0.68	0.37	0.62	0.56	0.47	0.46
Kougnohou	0.46	0.34	0.68	0.41	0.39	0.09	0.18	0.59	0.79	0.67	0.37	0.48	0.41	0.23	0.86
KpewaAledjo	0.50	0.33	0.54	0.58	0.39	0.11	0.16	0.60	0.64	0.64	0.36	0.68	0.45	0.39	0.42
Lokossa	0.38	0.49	0.75	0.84	0.75	0.35	0.41	0.42	0.56	0.48	0.00	0.22	0.67	0.67	0.82

Lonkly	0.34	0.58	0.77	0.83	0.75	0.37	0.44	0.40	0.54	0.46	0.08	0.21	0.82	0.63	0.76
Malfacassa	0.40	0.23	0.54	0.60	0.44	0.25	0.25	0.52	0.57	0.55	0.24	0.60	0.43	0.42	0.44
Nangbeto	0.31	0.21	0.75	0.64	0.63	0.39	0.31	0.43	0.62	0.50	0.21	0.33	0.41	0.49	0.89
Niaouli	0.38	0.49	0.78	0.85	0.75	0.32	0.39	0.42	0.57	0.48	0.00	0.22	0.69	0.67	0.82
Notse	0.24	0.66	0.80	0.89	0.80	0.44	0.54	0.28	0.45	0.33	0.00	0.18	0.94	0.68	0.80
Penesoulou	0.50	0.29	0.57	0.61	0.45	0.21	0.24	0.57	0.66	0.62	0.32	0.59	0.44	0.47	0.48
Savalou	0.31	0.17	0.82	0.60	0.63	0.39	0.33	0.45	0.65	0.51	0.26	0.34	0.34	0.49	0.97
Sokode	0.49	0.27	0.50	0.55	0.39	0.27	0.29	0.55	0.66	0.61	0.25	0.57	0.40	0.39	0.42
Sotouboua	0.52	0.34	0.45	0.43	0.34	0.31	0.37	0.58	0.76	0.67	0.25	0.56	0.39	0.28	0.38
Tabligbo	0.38	0.51	0.75	0.85	0.75	0.35	0.43	0.42	0.57	0.49	0.00	0.22	0.73	0.68	0.77
Tchamba	0.50	0.33	0.54	0.58	0.39	0.11	0.16	0.60	0.64	0.64	0.36	0.68	0.45	0.39	0.42
Tchetti	0.29	0.24	0.89	0.74	0.76	0.47	0.38	0.38	0.62	0.47	0.20	0.33	0.47	0.57	1.00
Toffo	0.34	0.53	0.80	0.83	0.75	0.37	0.43	0.39	0.53	0.46	0.08	0.21	0.76	0.62	0.76
Wahala	0.24	0.33	0.89	0.88	0.86	0.47	0.33	0.30	0.60	0.38	0.18	0.39	0.57	0.70	1.00
Yegue	0.44	0.25	0.50	0.68	0.53	0.41	0.38	0.51	0.68	0.59	0.16	0.48	0.44	0.48	0.43

9. Publications

Houngue, N. R., Almoradie, A. D. S., & Evers, M. (2022). A Multi Criteria Decision Analysis Approach for Regional Climate Model Selection and Future Climate Assessment in the Mono River Basin, Benin and Togo. *Atmosphere*, 13, 1–19. https://doi.org/10.3390/atmos13091471 Academic

Thiam, S., Salas, E. A. L., **Houngue, N. R.**, Almoradie, D. A. S., Verleysdonk, S., Adounkpe, J. G., & Komi, K. (2022). Modelling Land Use and Land Cover in the Transboundary Mono River Catchment of Togo and Benin Using Markov Chain and Stakeholder's Perspectives. *Sustainability*, 14. https://doi.org/https://doi.org/10.3390/su14074160

Houngue, C.F.C., **Houngue, N.R.** (2022): Study of temperature control system of a solar-heated anaerobic digester in Cotonou, Benin Republic, using hardware in the Loop simulation. *Journal of Applied Sciences and Environmental Management*, 26(1). https://doi.org/10.4314/jasem.v26i1.21

Hounguè, N. R., Ogbu, K. N., Almoradie, A. D. S., & Evers, M. (2021). Evaluation of the performance of remotely sensed rainfall datasets for flood simulation in the transboundary Mono River catchment, Togo and Benin. *Journal of Hydrology: Regional Studies*, 36. https://doi.org/10.1016/j.ejrh.2021.100875

Ogbu, K. N., **Hounguè, N. R.**, Gbode, I. E., & Tischbein, B. (2020). Performance Evaluation of Satellite-Based Rainfall Productsover Nigeria. *Climate*, 8. https://doi.org/10.3390/cli8100103

Lawin, A. E., Hounguè, R., M'Po, Y. N. T., **Hounguè, N. R.**, Attogouinon, A., & Afouda, A. A. (2019). Mid-century climate change impacts on Ouémé River discharge at Bonou Outlet (Benin). *Hydrology*, *6*(72). https://doi.org/10.3390/hydrology6030072

Lawin, E., **Hounguè, N. R.**, Biaou, C. A., & Badou, D. F. (2019). Statistical analysis of recent and future rainfall and temperature variability in the Mono River watershed (Benin, Togo). *Climate*, *7*(8). https://doi.org/10.3390/cli7010008

10. Conference contributions

Houngue, N.R. (2021). Climate change and hydrologic studies in a data scarce area: Case of the Mono River basin in west Africa. Symposium for Research and Capacity Development in West Africa - WASCAL and German Partners, University of Wurzburg, September 22 - 23 September 2021, Würzburg, Germany.

Houngue, N.R., Ogbu, K., Almoradie, A., and Evers, M. (2021). Evaluation of the Performance of Remotely Sensed Rainfall Datasets for Flood Monitoring in the Transboundary Mono River Catchment, Togo and Benin, EGU General Assembly 2021, online, 19–30 Apr 2021, EGU21-11176, https://doi.org/10.5194/egusphere-egu21-11176.

Houngue, N.R., Evers, M., and Almoradie, A. (2020): Impacts of Climate and Land Use Change in the Management of a Transboundary Basin- Case Study of Mono River catchment, EGU General Assembly 2020, Online, 4–8 May 2020, EGU2020-1145, https://doi.org/10.5194/egusphere-egu2020-1145.